Functional Polymers from Macrolactones

By

Zeliha Ates, M.Sc.

A Thesis Presented at Dublin City University for the Degree of Doctor of Philosophy

DCU

Supervisor

Dr. Andreas Heise

School of Chemical Sciences

PhD   **July 2014**

DECLARATION

I hereby certify that this material, which I now submit for assessment on the programme of study leading to the award of Doctor of Philosophy is entirely my own work, that I have exercised reasonable care to ensure that the work is original, and does not to the best of my knowledge breach any law of copyright, and has not been taken from the work of others save and to the extent that such work has been cited and acknowledged within the text of my work.

Signed : _____

  Zeliha Ates

ID No : 59103132

Date :

Annem, babam ve kardeşime...

Acknowledgments

This is a long story which really doesn't start with the phrase of once upon a time…It is not a fairy tale but surely it is a long story in a short time… This story is about a scientific as well as social growth with different rhythms of life. There are many people who made it possible and more colourful till I reach this point. I am gratefully thankful to each of the characters in my story for making it more meaningful and worth to have such memories. Here are the main characters of my story…

Firstly, I would like to express my gratitude to Dr. Andreas Heise for being an extraordinary supervisor and more being a mentor. Thanks for his unlimited patient, encouragements, trust and understanding. Also I am glad that he gave freedom of finding my polymeric way during my studies which motivate me for being confident. Surely, I cannot forget that his friendly manner all the time made this scientific trip much easier.

Next, I would like to thank to all of the technical staff in the School of Chemistry; Veronica, John, Ambrose, Brendan, Vincent, Damien, Mary, and Niamh. Without their help and support, it wouldn't be easy to work in the lab or deal with problems of any instrument. Thanks greatly to all of them for making many things simple with their helps.

Next, a big thank you goes to past and former members of PRG; Antonis, Jaco, Fabrice, Tushar, Mark, Timo, Marcello, Ida, Claudia, Paul, Jin. First of all, thanks for making the lab more enjoyable to work and being more than colleagues. PRG parties, lunch times, conferences, trips, coffee times...The list of memories to be remembered is surely long but I will not be that much sentimental. All of those was fun and will be missed.

Gracious thanks to Fabrice and Ian for valuable chemistry discussion times for making all bonds and angles clear all the time.

Another big thank you goes to my Dubliner Turkish delights, Elif, Ozlem, and Tugce. First of all, thanks for being so patience with this crazy girl and sharing my happy and sad moments. Thanks for not letting me be home sick at all! I am grateful that you all

cheer me up whenever I needed and make me feel your support all the time. And with memories worth to remember with its own taste; sweet, bitter, crazy and funny! Fasil nights, hiking adventures, museums, whole day cooking therapies, history, photo shooting, girls nights, gym sessions, discovery of Irish land. Certainly, it is already all missed…

Next big thank you goes to my past and former housemates; Svenja, Ram, Monika, Declan, Dirk, and Giusy. The house wouldn't be like home without any of you. First of all, thanks for all you sharing the life with me either happy or sad and being patient with my water/fire Zelis mood! Cooking times, crazy baking sessions, relaxing winey Friday evenings, trips, night outs, arty farty cinema sessions, last minute ideas, shopping times, Howth, festivals, and many other memories will be missed. I will definitely not forget the moment of counting stars in Doolin!

I would also like to thank my friends Melanie, Maria, Sebnem, Pinar, and Basak for putting different colours to my story and boosting my energy as well. Particularly, thanks to Maria for crazy hug and chocolate sessions especially during my writing times it helped a lot as the evidence showed 20 second hug is vital.

At last but not the least…without her none of this would be possible! Thanks for encouraging me to be the author of this story mum. I am grateful to feel you just beside me wherever I am without any time limit. Thanks for believing me in any condition more than me! I am also gratefully thanked to my dad for his unlimited supports and raising me up with the will of doing everything with my best. And thanks to my dearest brother for being next to me whenever I need support and help in my life.

As a final point, I am grateful to meet with all of the characters in my amazingly fantastic story. With all of you, this story has a unique rhythm with lots of colors in it which makes it priceless.

Once upon a time when I was Dubliner…..

Zeliha
Dublin, 2014

Table of Contents

List of Figures

List of Tables

Abstract

The presented work is focused on the design of (bio)functional materials from naturally occurring macrolactones. Enzymatic ring opening polymerization of such monomers affords aliphatic polyesters with promising material properties including biocompatibility, biodegradation and good mechanical properties. A drawback of these, as well as most aliphatic polyesters, is the lack of functionality, which is a potential hurdle to open biomedical applications in which the materials play a more active and possibly dynamic role. The primary aim of this thesis is the development of a methodology to introduce various functional groups to linear unsaturated poly(globalide) by utilizing thiol-ene coupling reactions as a post-polymerization modification. Secondly, this methodology should allow the design of three-dimensional materials, which can be bioconjugated. This includes for instance functional cross-linked films produced by thiol-ene coupling reactions and subsequent thiol-ene functionalization and well as exploring surface initiated ARGET-ATRP in order to increase the density of surface functional groups. Beyond the development of chemical routes it is the aim of the thesis to provide a first proof of concept for the feasibility of the developed approaches to design advanced biomaterials by investigating the conjugation with biomolecules. Moreover, first evidence for the processibility into the more complex three-dimensional materials such as scaffolds and particles is provided.

Abbreviations

12MCA	12-Mercaptodecanoic acid
4VP	4-Vinylpyridine
ADMET	Acyclic Diene Metathesis
AIBN	Azobisisobutyronitrile
Am	Ambrettolide
ARGET-ATRP	Activator ReGenerated by Electron Transfer ATRP
ATR-IR	Attenuated total reflectance infrared spectroscopy
ATRP	Atom Transfer Radical Polymerization
B3MP	Butyl-3-mercapto propionate
BAET	2-(boc-amino) ethanethiol
CALB	Candida antarctica lipase B
CBS	Sodium carbonate buffer
C_{gel}	Concentration of gel for synthesizing PCL–PHB scaffolds (%)
Chb	Chitobiase
c-ROP	Catalytic ROP
CRP	Controlled radical polymerization
CTAs	Chain transfer agents
CuAAC	Copper(I)-catalyzed azide-alkyne cycloaddition

DBU	1,8-Diazabicyclo[5.4.0]undec-7- ene
DCM	Dichloromethane
DCP	Dicumyl peroxide
DDL	12-Dodecanolide
DEA	2-(diethylamino)ethyl methacrylate
DMAEMA	2-(dimethylamino)- ethyl methacrylate
DMAP	4-Dimethylyaminopyridine
DMF	Dimethylformamide
DPP	Diphenyl phosphate
DSC	Differential scanning calorimetry
DsRed	Coral-derived red fluorescent protein
EBiB	Ethyl 2-bromoisobutyrate
EDC	1-Ethyl-3-(3-dimethylaminopropyl) carbodiimide hydrochloride
eGFP	Enhanced Green Fluorescent Protein
EGMP	Ethylene glycol bis(3-mercapto propionate)
EMC	Enzyme-monomer complex
e-ROP	Enzymatic ROP
FDA	Food and Drug Administration
FITC	Fluorescein isothiocyanate
FTIR	Fourier transform infrared spectroscopy

FT-Raman	Fourier transform Raman spectroscopy
GI	Globalide
GMA	Glycidyl methacrylate
GMH	Glucose monohydrate
GPC	Gel permeation chromatography
HB	Hyperbranched
HDL	16-Hexadecanolide
HDPE	High-density polyethylene
HiC	Humicola insolens
HLB	Hydrophile-lipophile balance
LA	$_L$-Lactide
LCST	The lower critical solution temperature
LDPE	Low density polyethylene
Me$_6$TREN	(-)-sparteine, tris[2-(dimethylamine)ethyl]amine
MH	6-Mercapto 1-hexanol
ML	Macrolactone
MMA	Methyl methacrylate
Mn	Number average molecular weight
mSBF	Modified simulated body fluid
MTBD	7-methyl-1,5,7-triazabicyclo[4.4.0]dec-5-ene
MW	Molecular weight

Mw	Weight average molecular weight
nACA	n-Acetyl cysteamine
NaMA	Sodium methacrylate
NaSS	Sodium 4-styrenesulfonate
NCA	*N*-carboxy anhydrides
NHCs	N-heterocyclic carbenes
NIPAM	N-isopropylacrylamide
NMP	Nitroxide mediated polymerization
NMR	Nuclear magnetic resonance
Novozyme 435	CALB immobilized on macroporous acrylic resin
NZ435	Novozyme 435
O/W	Oil in water
PAA	Poly(acrylic acid)
PBS	Phosphate buffer solution
PCL	Poly(ε-Caprolactone)
PDEAEMA	Poly[(2-(diethylamino)ethyl methacrylate]
PDI	Polydispersity index
PDL	Pentadecalactone (15-pentadecanolide)
PDLLA	Poly(D,L-lactide)
PE	Polyethylene

PEG	Poly(ethylene glycol)
PEGDT	Poly (ethylene glycol) dithiol
PGA	Poly(glycolide)
PGI	Poly(globalide)
PGMA	Poly(glycidyl methacrylate)
PGMET	Poly(ethylene glycol) monoethyl etherthiol
PgVL	α-Propargyl-d-valerolactone
PHB	Poly(β-hydroxybutyrate)
PLA	Poly(lactic acid)
PLG	Poly(d,l-lactide-*co*-glycolide)
PLGA	Poly(lactic-co-glycolic acid)
PML	Poly(macrolactone)
PMMA	Poly(methyacrylic acid)
PNIPAM	Poly(N-isopropylacrylamide)
PNP-GlcNAc	4-Nitrophenyl N-acetyl-β-D-glucosaminide
poly(DEA)	Poly(2-(diethylamino)ethyl methacrylate)
Poly(HEMA)	Poly(2-hydroxyethyl methacrylate)
polyHIPE	Polymerized high internal phase emulsion
PP	Poly(propylene)
PPDL	Poly(pentadecalactone)
PPL	Porcine pancreatic lipase

P*t*BA	Poly(*tert*-butylacrylate)
PVA	Poly(vinyl alcohol)
RAFT	Reversible addition fragmentation chain transfer
RCM	Ring-closing metathesis
ROMP	Ring-opening metathesis polymerization
ROP	Ring Opening Polymerization
RP	Rapid prototyping
RT	Room temperature
SAM	Self-assembly monolayer
SEM	Scanning electron microscope
SI	Sacrificial initiator
SI-ARGET-ATRP	Surface initiated ARGET-ATRP
SI-CRP	Surface-initiated controlled radical polymerizations
SI-FRP	Surface-initiated free radical polymerization
SIP	Surface initiated polymerization
$Sn(Oct_2)$	Tin(II) 2-ethylhexanoate
St	Styrene
*t*BA	*tert*-Butyl acrylate
TBD	1,5,7-Triazabicyclo[4.4.0]dec-5-ene
T_g	Glass transition temperature

TG	1-Thioglycerol
TGA	Thermal gravimetric analysis
THF	Tetrahydofuran
T_m	Melting temperature
TPMA	Tris(2-pyridylmethyl)amine
UDL	11-Undecanolide
UV	Ultraviolet
XPS	X-ray photoelectron spectroscopy
ε-CL	ε-Caprolactone

General Introduction

1.1 Renewable materials

A wide range of industrial materials such as solvents, fuels, synthetic fibers, and chemical products are being manufactured from petroleum resources. The high consumption of petroleum and fossil resources is encouraging current and future chemists to orient their research towards designing safer chemicals, products, and processes from renewable feedstock with an increased awareness of environmental and industrial impact[1,2]. When looking into biomass components, it is possible to identify a range of chemical structures that can be transformed into families of useful building blocks, intermediates and products[1]. Of course, the final economical benefit of a particular synthetic route or family of products will depend on the feedstock and processing costs, the current market volumes and prices, and the possibility of creating new market opportunities.

Polymeric materials synthesized from renewable monomers have already gained an established position among synthetic materials, both in academia and in industry. Owing to a growing concern about the depletion of the fossil fuel stocks and the accompanying price fluctuations, a large drive has been created for finding suitable alternatives. Biomass components such as oils, proteins, carbohydrates can be subjected to several transformations to yield renewable chemical building blocks. According to their natural molecular biomass origins, renewable monomers can be divided as: (i) oxygen-rich monomers namely carboxylic acids, polyols, dianhydroalditols, and furans, (ii) hydrocarbon-rich monomers including vegetable oils, fatty acids, terpenes, terpenoids and resin acids, (iii) hydro-carbonmonomers such as bio-ethene, bio-propene, bio-isoprene and bio-butene, and (iv) non-hydrocarbon monomers namely carbon dioxide and carbon monoxide[3]. Bio-based monomers proved to be very well suited as alternatives for some fossil derived building blocks and materials and some of these monomers have been intensively investigated by research groups[4–6]. Bio-based aliphatic and aromatic monomers are used to synthesize polyesters with different properties and end-uses. Aliphatic polyesters represent one of the most significant groups of polyesters from renewable resources such as vegetable oils, cutin, sugar, and polycarboxylic acid[7].

Long-chain fatty acids derived from plant oils are, for example, a promising class of renewable monomers for the synthesis of aliphatic polyesters[8]. Such hydrophobic and semicrystalline polyesters have polyethylene (PE) like structures but unlike PE have ester groups separated by generally 13 to 17 methylene units[9]. Several methodologies have been reported to synthesize such polymers by ring-opening metathesis polymerization (ROMP), polycondensation of fatty acid-derived diols and diesters, and thiol-ene reactions[10,11]. Alternatively, ring opening polymerization of lactones can be employed to obtain such aliphatic polyesters[12–14]. Ring opening polymerization (ROP) of lactones can be achieved either catalytically or enzymatically which will be discussed in section 1.2.1 and 1.2.2.

1.2 Ring opening polymerization (ROP)

Aliphatic polyesters occupy an important position in polymer science resulting from their remarkable properties such as good mechanical properties, hydrolyzability and biocompatibility. These properties lead them to take an important place as biomaterials in biomedical applications. Artificial skin, bone screws, and implants are just a few examples that can be listed for such medical applications[15,16]. Generally, the ring-opening polymerization of lactones is carried out in bulk or solution (Tetrahydrofuran (THF), toluene etc.), emulsion or dispersion[17]. The temperature range for bulk polymerization is usually 100-150 °C while lower temperatures are used for solution polymerization in order to minimize the inter- and intra-molecular transesterification reactions (as well as being dictated by the solvent boiling point). Most of the lactones polymerize in the presence of catalysts or initiators whereas a few can polymerize spontaneously upon heating or standing. A very broad range of initiators and catalysts are reported in the literature to polymerize lactones. The type of initiator determines the mechanism of polymerization, which is mainly cationic, anionic, coordination-insertion, organocatalytic and enzymatic polymerization[18].

Anionic ring-opening polymerization of lactones occurs by the nucleophilic attack of a negatively charged initiator on the carbonyl carbon or on the carbon atom adjacent to the acyl-oxygen. The propagating species is negatively charged and counter-balanced with a positive ion. The nature of the ionic propagating chain end and the solvent decides the

reacting complex being either ionic or almost covalent. The effective initiators are alkali metals, alkali metal oxides, or alkali metal naphthalenide complexes with crown ether. The mechanism of the polymerization, either living or non-living, depends on the reaction conditions and type of initiator[18,19]. On the other hand, cationic ROP of lactones has been known for a long time but not widely used owing to its poor control over molecular parameters. The cationic ring-opening polymerization involves the formation of a positively charged species with a subsequent attack by a monomer. The attack results in a ring-opening of positively charged species through an S_N2-type mechanism. The cationic polymerization is difficult to control and often affords low molecular weight polymers[18,19].

| Glycolide | Lactide | δ-valerolactone | 3(s)-isopropylmorpholine-2,5-dione |

| 12-dodecanolide | Pentadecalactone | Ambrettolide | α-methylenemacrolide |
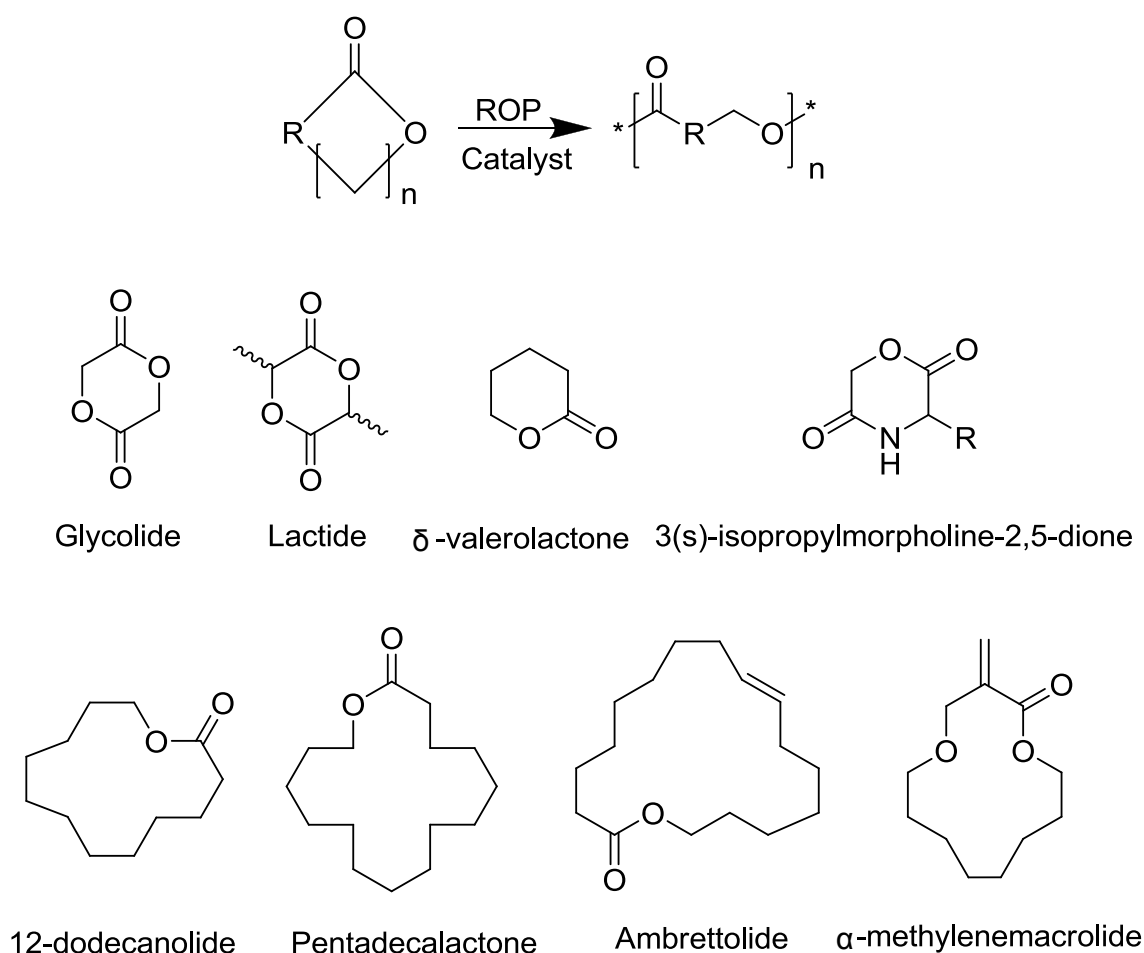
Figure 1.1: Ring-opening polymerization for the preparation of polyesters and several examples of cyclic monomers.

1.2.1 Catalytic Ring-opening polymerization

In order to obtain better control of the polymerization, anionic initiators were replaced with less reactive and more selective organometallic derivatives. In coordination-insertion ROP, propagation proceeds through the coordination of the monomer to the active species and then insertion of the monomer into the metal-oxygen bond by rearrangement of electrons. The growing chain remains attached to the metal through an alkoxide bond during the propagation and termination results in a hydroxyl end group by hydrolysis. The most widely used initiators are various aluminum, tin alkoxides, and carboxylates. Such initiators with bulky coordinated groups are capable of producing stereoregular polymers with narrow PDI (Poly dispersity index) and controlled molecular weight as well as defined end groups[18,19]. In particular, tin(II) bis(2-ethyl-hexanoate), tin(II) octoate, has been shown to be a highly active catalyst for the ROP of cyclic esters. Tin(II) octoate has been successfully applied as catalyst for the ROP of different ring-size lactones in bulk and in solution[17].

The catalytic ROP (c-ROP) of lactones offers potential to control the molecular weight, polydispersity and the structure of resulting polymer. It also opens opportunities to polymerize lactones having some functionalities while several functional groups could coordinate with the metal of the catalyst and interfere with the polymerization[20]. The driving force behind the c-ROP of lactones is the release of ring strain in the transition from cyclic ester to the polyester chain. The reactivity of lactones in c-ROP decreases as the ring strain decreases, i.e. with increasing lactone ring size.

Lithium compounds are efficient catalysts for ROPs and the activity of these compounds varies with the type of the coordination sites and reaction conditions. The catalytic activity of lithium catalysts has been analyzed for the ROP of different cyclic monomers such as caprolactone, lactide, cyclic carbonate, and employed for the synthesis of block and graft polymers[21]. Typically lactide and ε-caprolactone monomers were screened in c-ROP for which higher yields and molecular weights were obtained in comparison to macrolactones. On the other hand, aluminum salen complexes show good catalytic

activity in the c-ROP of lactones and the c-ROP of large ring size lactones afforded high molecular weight polyester[22,23]. Recently, Bouyahyi and Duchateau reported metal-catalyzed ROP of pentadecalactone (PDL) and copolymerization with ε-caprolactone (ε-CL)[24]. High molecular weight poly(pentadecalactone) (PPDL) with Mn up to 130 000 g/mol was produced as well as block copolymers and gradually randomized copolymers with different thermal properties.

One major drawback of using these catalysts is the increasing environmental concerns. Toxicity of metal catalyst limits the usage of such materials for biomedical applications. For example, tin(II) bis(2-ethyl-hexanoate) is widely used as catalyst for ring opening polymerization (ROP) of lactones[25,26]. In practice, the complete removal of the organometallic compounds can be challenging and economically unfeasible. Traditional synthesis often also relies on protection/or deprotection steps to obtain desired products. The use of organic catalysts or enzymes is a non-toxic alternative for ROP. Both have gained significant attention recently and for example enzymatic catalysis is also employed in this work for the ROP of macrolactones in order to synthesize polyesters for possible biomedical applications by a green route.

1.2.1.1 Organocatalytic ROP

A powerful alternative to traditional metal-based catalyst is organic catalysts for ROP. 4-Dimethylyaminopyridine (DMAP) for the ring opening polymerization of lactide has been first reported by Nederberg et al.[27]. Furthermore, N-heterocyclic carbenes (NHCs), bifunctional thiourea-amine catalyst (TU/A), (-)-sparteine, tris[2-(dimethylamine)ethyl]amine (Me$_6$TREN), 1,8-diazabicyclo[5.4.0]undec-7- ene (DBU), 7-methyl-1,5,7-triazabicyclo[4.4.0]dec-5-ene (MTBD), 1,5,7-triazabicyclo[4.4.0]dec-5-ene (TBD), and diphenyl phosphate (DPP) were reported by several groups[28–33]. Most of the organic catalysts are straightforward to use and only require dry conditions to achieve control over the molecular weight and high level of end-group fidelity. In many cases, water is able to act as a competitive initiator resulting in loss of end group control and lower molecular weights. Such catalysis having high polymerization rates at ambient

temperatures allows the ROP of monomers with low ring strain to afford higher monomer conversions.

1.2.2 Enzymatic Ring-opening polymerization

Enzymes catalyze metabolic reactions via biosynthetic routes in living cells. Enzymes can catalyze the synthesis of natural macromolecules such as proteins, polysaccharides, polyesters etc. Natural polymer synthesis occurs *in vivo* by enzyme catalyzed addition of activated monomers in the cell by a complex metabolic process under mild conditions of temperature and pressure in an aqueous medium. Natural and non-natural polymers produced via enzymatic catalysis are nowadays explored as a green strategy for designing useful materials for technical as well as biomedical applications[34–36]. Enzymatic reactions in polymer synthesis proceed with high control of chemoselectivity, regioselectivity and enantioselectivity making protection chemistry obsolete in some cases. Moreover, these reactions take place under mild conditions without using toxic reagents thus contributing to sustainable production. If both an enzyme catalyst and a renewable monomer is used this can be considered green polymer chemistry.

In vitro enzymatic catalysis using lipases was first reported in the 1930s for the organic synthesis of esters in organic media[37]. Numerous studies were reported about ring-opening polymerization catalyzed by enzymes, mostly lipases, highlighting several advantages whilst producing high molecular weight polyesters. Enzymes have high enantio- and regioselectivity, and the ability to be used in bulk reaction media while offering promising substrate conversion efficiency due to their high selectivity and catalyst recyclability. ROP of lactones with different ring size, lactides and cyclic carbonates producing polyesters and polycarbonates through lipase catalysis have been studied intensively. For example, Kobayashi and co-workers reported several studies on e-ROP of lactones (e.g. ε-CL) under varying reaction parameters[38–40]. Kumar and Gross subsequently reported that poly(ε-CL) with a higher molecular weight was obtained in high yield when toluene was used as a solvent[41]. On the other hand, the polycondensation of hydroxy acids, diacids or polyanhydrides with diols can also be lipase catalyzed as an eco-friendly lipase catalyzed polymerization[42–45].

Meanwhile, numerous studies were performed to introduce new enzymes which are able to initiate ROP and polycondensations. For example, Cutinases are extracellular fungal enzymes whose natural function is catalyzing the hydrolysis of ester bonds in cutin, a lipid-polyester found in the cuticle of higher plants[46]. A cutinase from Humicola insolens (HiC) has been found to have the unusual characteristic of catalyzing polyester synthesis[46,47]. Monomer conversion follows first order kinetics and chain transfer to monomer does not occur while temperature has no noticeable effect on molecular weight with comparison to other reported enzymes.
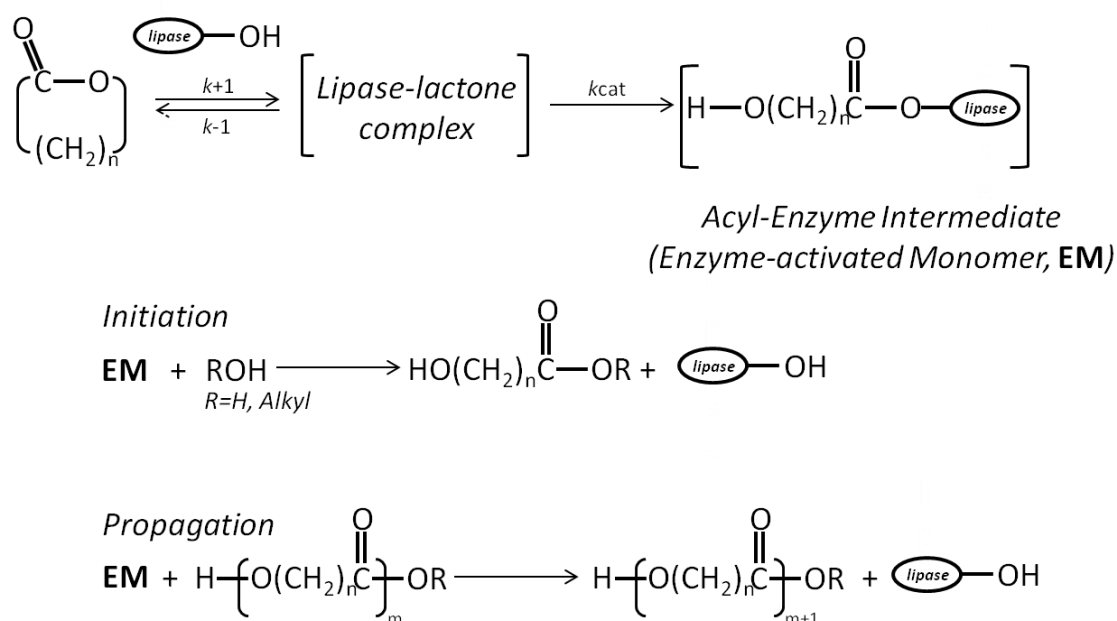
Figure 1.2: General mechanism of lipase-catalyzed ROP of lactones[45].

The proposed mechanism of enzymatic ROP of lactones involves the formation of an enzyme-monomer complex (EMC) between the catalytic site of the lipase (serine residue) and the lactone. The EMC formation step is believed to be the rate-determining step of the overall polymerization[45]. The initiation step consists of a nucleophilic attack of a nucleophile such as water or alcohol onto the acyl carbon of the intermediate to form ω-hydroxy carboxylic acid (propagating species). In the propagation step, the nucleophilic attack of the terminal hydroxyl group of a propagating chain on EMC leads

to the formation of a one unit extended polymer chain. Therefore, the polymerization proceeds through an `activated monomer mechanism` (Figure 1.2).

MacDonald et al. reported that the initiation step is faster than the propagation step, hence, the propagation step determines the overall rate of polymerization[48]. On the other hand, different nucleophiles (water, butanol and butyl amine) were explored to figure out their effects on chain initiation and propagation for ring opening polymerization of CL by Gross et al[49]. They reported the monomer conversion followed first-order law and was independent of the type and concentration of nucleophile for ROP of CL in the presence of porcine pancreatic lipase (PPL) as catalyst. Initiation was reported to be rapid relative to chain growth. Moreover, it is reported by several studies that kinetics of e-ROP follows Michaelis-Menten as well as 1st order kinetics[39,50].

1.3 Macrolactones

Interest in macrocyclic lactones has been increasing since the isolation of exaltolide 1 by Kerschbaum in 1927[51]. Macrocyclic lactones, 14- to 19-membered, can be extracted from natural sources including the angelica plant root (Angelica archangelica)[52,53]. These natural lactones have long been used in different chemical industries in fragrances and pharmaceuticals and more recently have also been investigated as monomers to afford diverse functional polymers. For example, pentadecalactone, naturally-occuring scent molecule of humans as well as other mammals, is a male pheromone which is produced by apocrine glands of the male armpit[54]. PDL is a perfume and fragrance ingredient added to cosmetics and beauty product having a sweet, powdery, and woody smell[55]. It is FDA approved for use as an indirect food additive.

Due to the increasing demand for macrolactones in industry, various approaches were devised for their synthesis[53]. The lactonization of seco-acids appears to be one of the most used methodologies to obtain macrocyclic lactones even though many other efficient macrocyclization techniques were reported such as intramolecular cross-coupling, ring-closing metathesis (RCM), and Nozaki-Hiyama-Kishi reaction[51]. The activation of either alcohol or the carboxylic acid terminal group is essential owing to the

entropic and enthalpic factors. The entropic factor is dominant for medium ring lactones due to the enthalpic factor from strain energy in the ring being formed. On the other hand, the enthalpic factor decreases while the entropic factor increases as the rings formed are almost strain free for the intramolecular reaction in large ring lactones[51].

1.4 Enzymatic ROP of macrolactones

ROP of macrolactones (MLs) leads to processable functional polymers where the ring opening reactivity of lactones of various ring sizes are completely different in chemical and enzymatic polymerizations. As non-strained monomers their reactivity decreases with increasing ring-size in the chemically catalyzed reaction, while macrolides (macrolactones) are readily recognized by lipases owing to their hydrophobic nature and molecular shape compared to the small ring lactones such as ε-caprolactone and δ-valerolactone. Such non-strained monomers, 11-undecanolide (12-membered, UDL), 12-dodecanolide (13-membered, DDL), 15-pentadecanolide (16-membered, PDL) and 16-hexadecanolide (17-membered, HDL), might have even higher or comparable polymerization rates in comparison to δ-valerolactone and ε-caprolactone[40,56,57].

Several groups have reported the polymerization of macrolactones via catalytic as well as enzymatic methods[41,56,58–60]. It is worth discussing PPDL as an example, one of the mostly studied poly(macrolactone)s. It is reported that PDL and other macrolides behave differently from smaller lactones concerning their polymerization behavior[61]. Duda et al. used zinc octoate/butyl alcohol for the ROP and reported low reactivity of the catalyst towards PDL which results in low monomer conversion after long reaction times at high temperatures (26% after 7 days at 100°C) as well as low molecular weight of 1,350 g/mol[56]. Recently, Duchateau and co-workers reported for the first time a highly efficient c-ROP of PDL and several other macrolactones such as ambrettolide and their copolymers by using various aluminum salen complexes[22,23]. The c-ROP rates were reported to be first order affording PPDL with Mn of over 150 000 g/mol.

One of the first systematic studies on the lipase catalyzed ROP of PDL has been reported by Gross and coworkers[62]. PPDL with weight average molecular weights (M_w) ranging

from 25 000 to 481 000 g/mol were obtained by methodical variation of reaction time and water content. Lipase catalyzed polymerization of lactones with different ring sizes has also been reported by other groups. Kobayashi et al. published on the ring opening polymerization of lactones catalyzed by lipases[63]. Several subsequent studies by them investigated the effect of reaction parameters on the polymerization such as different type of lipases, different ring size lactones, as well as temperature. Comparison of the kinetics of chemical polymerization and enzymatic polymerization of lactones for medium and large ring sizes, 6-, 7-, 9-, 12-, 13, 16, and 17-membered lactones, was done by the initiation with zinc octoate/butyl alcohol and with lipase pseudomonas fluorescense/octyl alcohol system[56]. As the enzyme origin directly affects the polymerization characteristics of lactones with different ring size many researchers explore various enzymes in the polymerization of different ring size lactones[64,65]. 11-Undecanolide (12-membered, UDL), 12-dodecanolide (13-membered, DDL), 15-pentadecanolide (16-membered, PDL) and 16-hexadecanolide (17-membered, HDL) were subjected to lipase catalysed polymerization by using lipases from different origins[39]. For the polymerization of DDL, lipases CC (from C. cylindracea), PC (from P. cepacia), PF (Pseudomonas fluorescens lipase) and PPL showed high catalytic reactivity and the activity order was as follows: lipase PC> lipase PF> lipase CC>PPL. Moreover, various enzymes, immobilized and non-immobilized, as well as the influence of water content of the reaction media for the ROP of PDL were investigated by Bisht et al.[14]. Resulting conversion values were reported to be almost identical for immobilized and non-immobilized enzymes[14] while immobilized enzymes offer the practical advantage of easy removal from reaction media.

On the other hand, the majority of reported polymerization reactions have employed Lipase B from *Candida Antarctica*. Polymerizations of macrocylic esters up to 84-ring atoms containing in-chain functional moieties were, for example, catalyzed by *Candida Antarctica* lipase B (CALB)[66]. Novozyme 435, CALB immobilized on macroporous acrylic resin, was used to conduct ROP in bulk and solution[14,41]. Novozyme 435-catalysed copolymerizations of ω-pentadecalactone/ε-caprolactone was also investigated[41]. Despite the large difference in the reactivity ratios of ω-pentadecalactone (reactivity rate of polymerization; r_1=1.742) and ε-caprolactone (r_2=0.135) , the isolated

copolymers had repeat unit sequence distributions that approximated that of random copolymers as a result of Novozyme 435 transesterification reactions between chains[41].

Moreover, kinetic studies of Novozyme-435 catalyzed ROP of lactones with different ring sizes (6- to 13- and the 16-membered ring) were achieved by Palmans and coworkers[61]. Several factors affecting the rate of lipase catalyzed ROP such as temperature, solvent, concentration, choice of initiator and the water content of the enzyme were studied. The authors state that the differences in the polymerization rates cannot only be related to physical properties such as the dipole moment of the monomer. Initial rate constants of Novozyme-435 catalyzed polymerization of 10-decanolactone, 11-undecanolactone and 12-dodecanolactone were found to be 0.1, 0.38 and 4.9 h^{-1} while all having dipole moments of around 1.9D. On the other hand, the Micheales-Menten contstants, K_m and V_{max} can be used for the understanding of this relation where K_m was relatively independent of the ring size while V_{max} did not show any noticeable trend. Several factors such as basicity and dipole moment of the lactone and steric interactions with surrounding amino acid residues in the active site may contribute to the reactivity of lactones[61,67].

1.5 Materials from Poly(macrolactones)

The diversity in polymer synthesis and properties offers the opportunity to tailor hybrid materials for wide range of biomedical applications. In order to qualify for these applications high entry barriers in terms of product safety and properties have to be overcome. Biocompatibility is one of the primary requirements that all materials have to meet for applications in the body. The need for biodegradability, on the other hand, depends on specific application. While some applications require the ability of degradation *in vivo* at a certain rate, for example, in drug delivery devices or scaffolds, other materials may need to be non-degradable e.g. implants.

Poly(ϵ-CL), poly(lactides), poly(glycolides) and copolymers[16,68–72] of those are typical degradable materials from aliphatic polyesters. Recently, macrolactones such as globalide (Gl, unsaturated 16-membered lactone), ambrettolide (Am, unsaturated 17-

membered lactone), hexadecalactone (HDL, saturated 17-membered lactone) and pentadecalactone) (PDL, 16-membered lactone) were investigated by several groups in order to position these polymers among other biomaterials to identify promising applications[62,73,74]
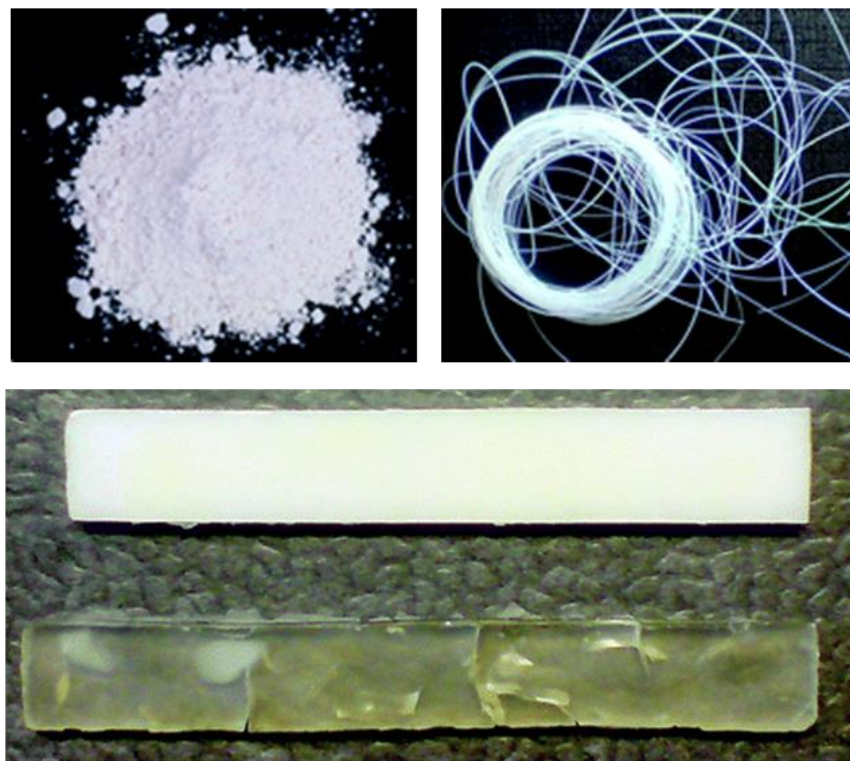
Figure 1.3: PPDL powder and examples of PPDL fibers from the melt by Ram extrusion[59]. PAm plate before curing (top) and after curing (bottom) with DCP[73].

PPDL, one of the most investigated poly(macrolactone)s, is an aliphatic polyester having the properties of low density polyethylene (PE) (LDPE) resulting from its high crystallinity of the methylene units[75]. It has a melting point (T_m) around 100 °C and a glass transition temperature (T_g) of -27°C whereas LDPE has T_m of 97-117°C and T_g of -25°C. Due to the presence of ester bonds in the polymer backbone it has the potential of being (bio)degradable.

As for PE, the long linear aliphatic carbon chain of PPDL is responsible for its high crystallinity giving rise to the expectation of good fiber properties from these materials (Figure 1.3). Mechanically strong fibers can be obtained where the lateral interactions

between the polymers chains in the fibers is highest and thus a high orientation of the chains in crystallites is advantageous as in the case of PE. In this respect, the molecular weight of the polymer should be as high as possible for maximal lateral chain interactions and for a limiting number of chain ends. Additionally, short plasticizing polymer chains should be absent as they reduce the mechanical properties of the bulk material. For example, high molecular weight (143,000 g/mol) PPDL was melt processed into fibers which were further elongated to about 9-10 times their original length[59]. Analysis of the fibers revealed differences in crystal orientation as a function of the processing conditions where a high strength of up to 0.74 GPa was observed for the fiber with the highest crystal orientation. However, as the degree of orientation increases, the elongation at break decreases. The effect of PPDL molecular weight on its mechanical, thermal and rheological properties was also reported in comparison with linear high-density polyethylene (HDPE)[62]. As PPDL Mw is increased above 18.9×10^4, the entanglement network strength is enhanced and strain-hardening takes place at high strains. Samples prepared by press-molding (130 °C) with high Mw resulted in tough properties with elongation at break about 650% and tensile strength about 60.8 MPa comparable to linear HDPE. Moreover, Young`s modulus, melting enthalpy and crystallinity as a function of molecular weight show similar trends as the elongation at break.

Polymers from PDL, hexadecaloctone as well as their unsaturated analogues ambrettolide and globalide have been investigated for their degradation and thermal properties by van der Meulen et al.[73]. It was found that PPDL is neither enzymatically nor hydrolytically degradable in buffer solutions resulting from its high crystallinity and hydrophobicity. Nevertheless, MTT assay for metabolic cell activity of a 3T3 mouse fibroblast cell line showed no toxicity for all polymers. Moreover, thermal cross-linking in the presence of dicumyl peroxide (DCP) and thiol-ene cross-linking was used to obtain transparent (fully amorphous) films from unsaturated PMLs (Figure 1.3)[73]. Cross-linked semicrystalline PPDL films were also prepared earlier from thiol-ene functionalised PPDL and multifunctional ene-groups by Malmstrom and co workers[76]. The network properties were dependent on the efficiency of thiol-ene couplings as the final network were still bearing crystallinity.

Thermoset properties of Gl/ε-CL copolymers were investigated by Claudino et al.[77]. Thermoset syntheses were conducted via photoinduced thiol-ene reactions in the melt. The addition of ε-CL resulted in the increase of the chain mobility while decreasing the density of functional groups. Organic acid catalyzed polymerization of PDL, Gl and Am was also investigated in bulk and in aqueous miniemulsion in order to obtain polyester latexes[74]. Strong acids enhanced the polymerization and latexes were produced by thermal cross-linking of copolymers from miniemulsion of Am and Gl with low molecular weight (1500 g/mol).

Due to the increasing demand for such polymers from natural raw materials as well as for their unique properties, macrolactones were explored for the design of functional materials in this thesis.

1.6 Surface functionalisation

Polymers take part in various biomedical applications such as tissue engineering, medical devices and drug delivery systems[70,78–82]. Using polymers in such applications may require certain properties like biocompatibility, or certain surface properties like wettability. The surface properties of materials play an essential role in determining the overall biocompatibility of the materials as the surface of the material is in direct contact with the biological environment[83]. A choice of surface modification studies has been reported using methods such as wet chemical modification, plasma treatment, UV irradiation, chemical grafting, and incorporating protein[84].

The classical approach, wet chemical surface modification, affords generative functional groups on the surface by treatment with liquid reagents such as acid solutions[85]. For example, chromic acid and potassium permanganate in sulfuric acid have been used to introduce oxygen-containing reactive functionalities to PE and poly(propylene) (PP)[86,87]. On the other hand, exposing polymer surfaces to UV light can generate reactive sites which can be converted into functional groups upon exposure to gas or can be used for UV-induced graft polymerization. The depth of the surface reactivity can be tailored by varying the wavelength. UV irradiation can also be used to initiate radical graft

polymerization as well as thiol-ene coupling reactions[88]. Additionally, solvent-free surface modification of polymers can be achieved by plasma treatment. The type of the functionality can vary according to the selected plasma gas (Ar, N_2, H_2O, and NH_3); for example oxygen-containing functional groups can be introduced onto PCL surfaces via oxygen plasma treatment[89].

1.6.1 Surface initiated polymerization

Surface initiated polymerization (SIP) is a very attractive route to tailor the chemical and physical properties of a substrate[90–93]. The coating with certain functional properties has been essential to design, develop and manufacture hybrid materials for industrial applications. Surface functionalisation with polymer brushes via controlled radical polymerization (CRP) allows obtaining thicker coatings which can overcome chemical and mechanical instability. Two common methodologies, `grafting from` and `grafting to`, are mainly used to introduce polymer brushes on a range of surfaces[94]. Polymers with reactive groups or segments can be prepared according to the desired properties and attached onto surface by `grafting onto` technique. The more efficient `grafting from` methodology requires the introduction of functional initiators onto the surface to grow functional brushes. Dense brushes possessing different morphology, thickness and composition can be synthesized by proper choice of the initiating system, temperature, monomer and concentration.

The generation of polymer brushes can be achieved via a large variety of synthetic routes through the `grafting from` technique with excellent control such as ring opening polymerizations (ROP), cationic/anionic polymerizations, atom transfer radical polymerization (ATRP), nitroxide mediated polymerizations (NMP) and polymerizations via reversible addition fragmentation chain transfer (RAFT)[95–98].
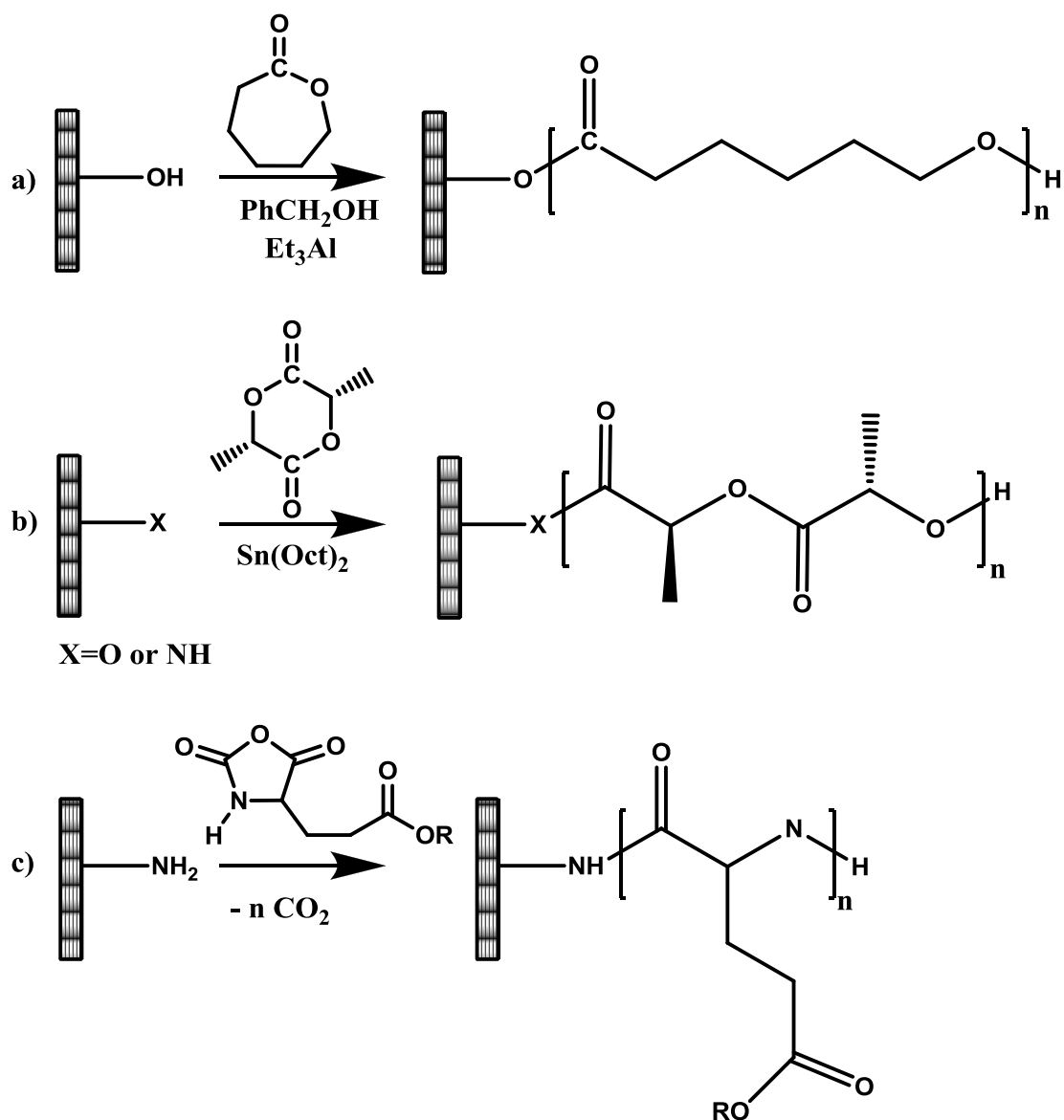
Figure 1.4: SI-ring opening polymerization of (a) ε-caprolactone, (b) lactide and (c) glutamate from a flat surface[99].

A limited number of studies have reported surface-initiated ROP of cyclic monomers such as ε-caprolactone, $_L$-lactide (LA). The surface-initiated polymerization of LA from Au and Si/SiO2 surfaces was demonstrated using catalytic tin(II)octoate $(Sn(Oct)_2)$[100]. The polymerization of $_L$-Lactide was initiated through a self-assembly monolayer (SAM) of thiol terminated by hydroxyl groups deposited on gold and SAM of silane terminated by amine groups on silicon substrates. In one example also enzyme catalysed synthesis of PCL from a gold surface was reported by Yoon et al.[93]. The self-assembly of 1-

mercapto-undec-11-tri(ethylene glycol) let to the formation of hydroxyl functionalities onto the gold substrate. Subsequently, ROP of CL was catalyzed by Novozyme 435 in toluene at 55 °C and a postulated formation of PCL brushes by a chain growth from hydroxyl group decorated substrate surface. Moreover, amine functionalised silicon wafers and quartz slides were decorated through *N*-carboxy anhydrides (NCA) of γ-benzyl and γ-methyl ∟-glutamates that undergo ROP in the presence of amine groups (Figure 1.4)[99,101–103].

Controlled Radical Polymerization
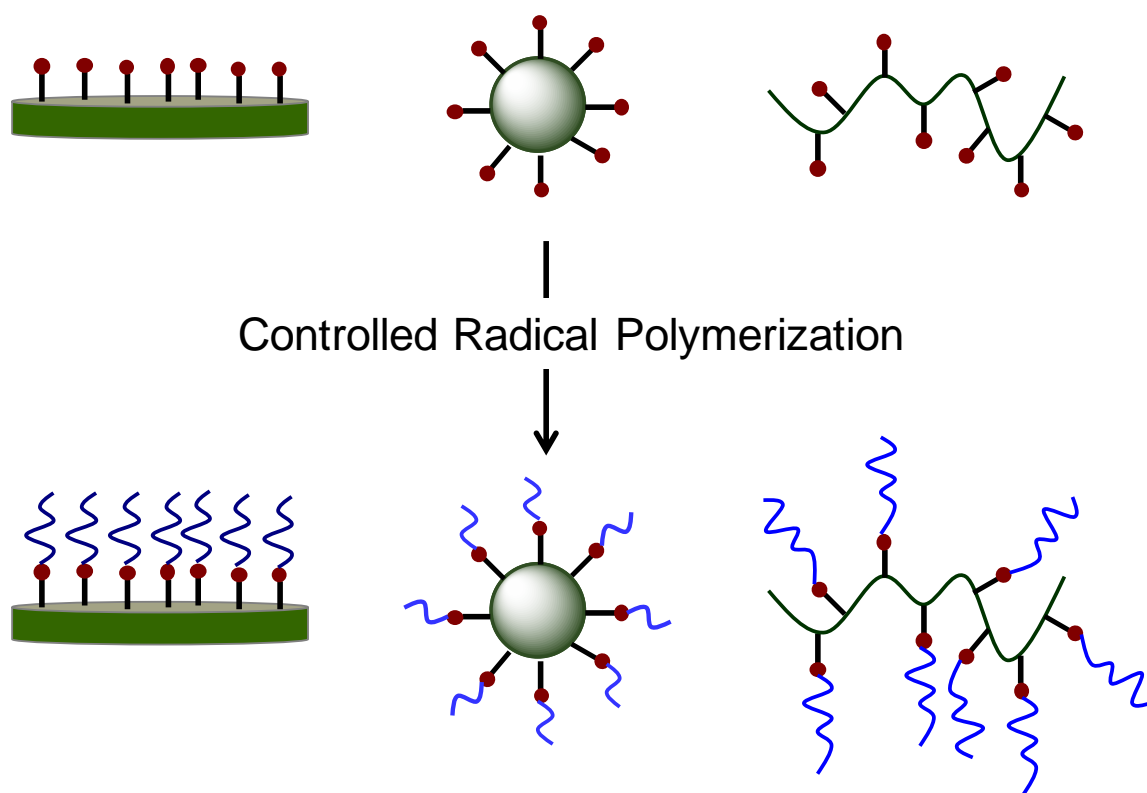
Figure 1.5: Polymer brushes can be synthesized by controlled radical polymerisation using a 'grafting from' technique from various functional substrates such as flat surfaces, particles and polymers[104].

Surface-initiated controlled radical polymerizations (SI-CRP) are particularly versatile as they allow preparation of different brush architectures with block or random copolymer brushes, cross-linked polymer brushes, hyperbranched polymer brushes, standard binary mixed polymer brushes, free-standing polymer brushes, molecular weight gradient polymer brushes, chemical composition gradient polymer brushes, and grafting density

gradient brushes[98]. Consequently these techniques have been used to produce polymer brushes from a variety of surfaces including silica, gold, polymers, cellulose and others[92,97,105–108].
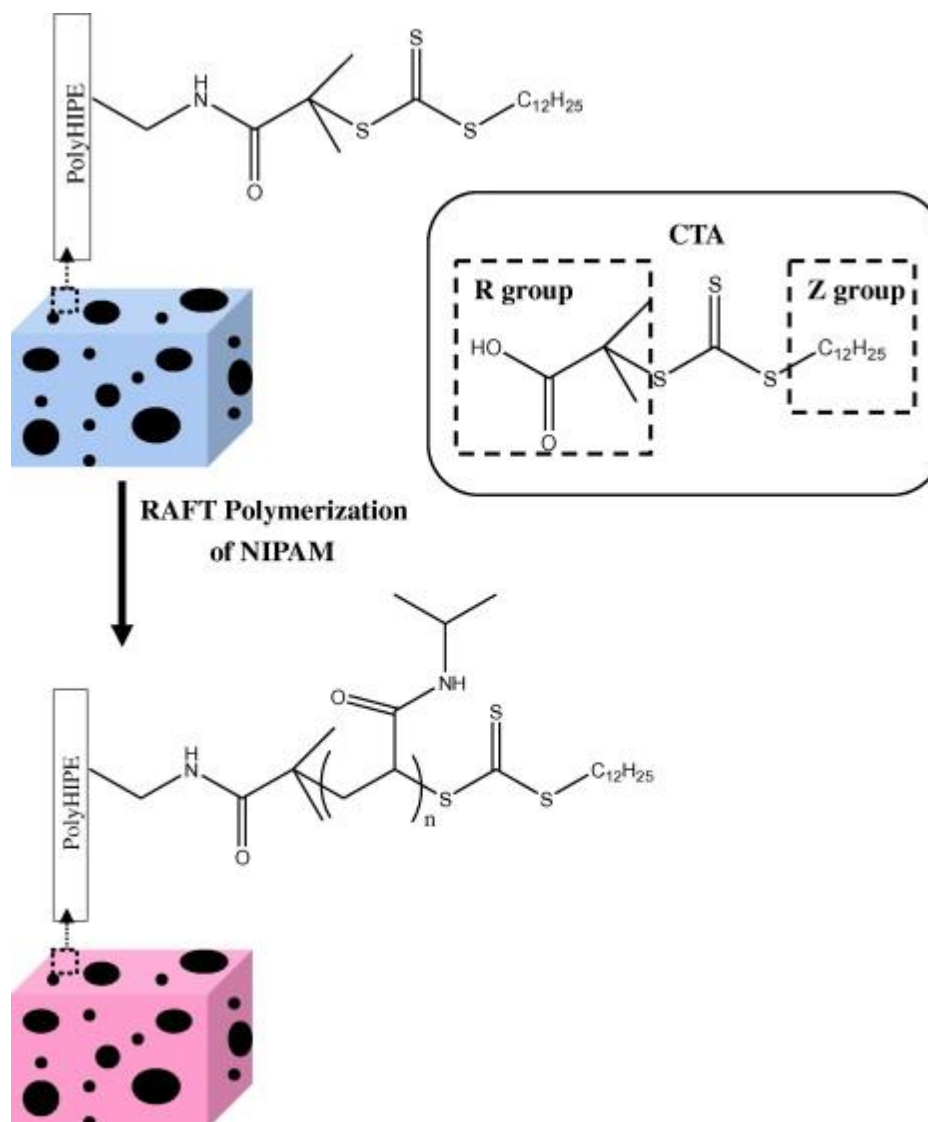
Figure 1.6: RAFT polymerization of NIPAM from a chain transfer agent (CTA) decorated surface of a porous polymer[109].

Nitroxide mediated polymerization (NMP) works through a reversible deactivation process by coupling an active chain-end radical with a nitroxide leaving group. NMP of styrene via a `grafting from` approach was initially reported by Husseman et al.[110]. The formation of polystyrene brushes through nitroxide moieties were performed onto silicon

wafers after introduction of active alkoxyamine in the presence of triethylamine catalyst.Surface modification of silicon wafers was also reported by surface-initiated free radical polymerization (SI-FRP), reverse ATRP, and RAFT techniques through ester-free initiators[111]. On the other hand, RAFT polymerization can afford surface polymer brushes by a series of reversible addition-fragmentation steps based on the transfer moiety and dormant species[108]. The functionalisation of the substrate with RAFT agents can be a challenging step and often several modification steps might be required. Moreover, different substrates were also decorated via RAFT technique e.g. amino functionalized macroporous monoliths from polymerized high internal phase emulsion (polyHIPE)[109]. The wettability of monolithic materials was increased by a dense coating of PNIPAM which was growth from chain transfer agents (CTAs) decorated porous surfaces (Figure 1.6).

1.7 Surface initiated ATRP

Initially reported by Matyjaszewski and Sawamoto, Atom Transfer Radical Polymerization (ATRP) is an efficient technique to design a variety of controlled structures[112,113]. The principal of ATRP relies on a redox reaction between a solubilized transition metal and alkyl halide to generate an equilibrium between propagating radicals and dormant polymer chains. A repetitive atom-transfer process is reversibly formed between a macromolecular alkyl halide P_n-X and a redox-active transition-metal complex Cu^I-X/ligand in which $P_n{}^*$ radicals propagate (k_p; rate constant of propagation). Termination (k_t; rate constant of termination) also occurs by coupling and disproportionation. The relative rates of the k_{act} and k_{deact} control the equilibrium while the termination is suppressed by the low instantaneous radical concentration.

$$P_n\text{-}X \;+\; M_t^{\,n}/L \;\underset{k_{deact}}{\overset{k_{act}}{\rightleftharpoons}}\; P_n^{\,*} \;+\; X\text{-}M_t^{\,n+1}/L$$

$$k_p \quad \text{Monomer}$$

$$k_t$$

$$P_n\text{-}P_m \,/\, P_n \,\&\, P_m$$
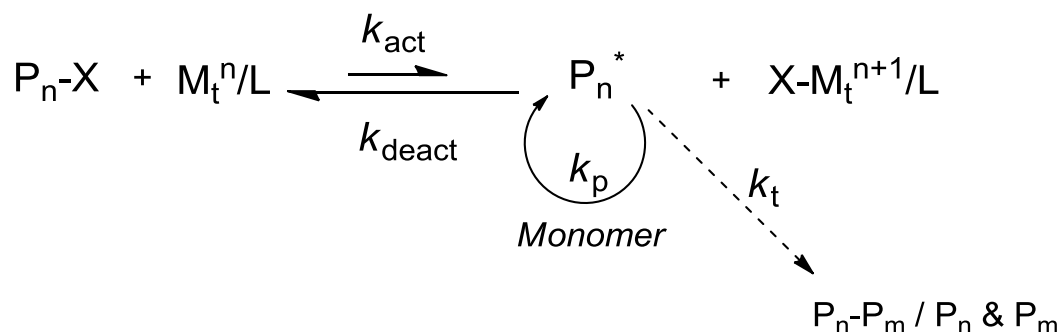
Figure 1.7: The general scheme for the mechanism of ATRP[114].

Cu(I) is the most commonly used ATRP catalyst although a variety of transition metal catalysts is available. This catalyst can be used for the polymerization of polar/non-polar monomers, charged/neutral monomers, hydrophilic/hydrophobic monomers and the reaction can be performed in bulk, organic solvent or water[115]. Moreover, alkyl halide containing initiator allows the introduction of end group functionality where the polymer contains functionality at one end and a halogen at the other end. Functional groups can be obtained by using either substitution reactions, electrophilic or radical addition reactions of halogen end groups. The same synthetic route offers opportunities to synthesize polymers from di- or multifunctional initiators as well as hyperbranched polymers. Various functional monomers (e.g. substituted styrenes, (meth)acrylates, 4-vinylpyridine, and (met)acrylamides) can be used to conduct (co)polymerisation via ATRP in a controlled manner resulting in well-defined polymers with a good control over polydispersity and molecular weight[114,116,117].

ATRP has extensively been reported to create functional polymer brushes with control over the polymer architecture and molecular weight. ATRP appears as a very robust technique in comparison to other controlled/living polymerization techniques for the synthesis of polymer brushes[98,104,118]. One such class, stimuli-responsive molecular brushes, was reported comprehensively with different topologies and chemical compositions of side chains. A wide range of stimuli, such as temperature, pH, or light, have been employed to advance the properties of polymers[88,96,119–122]. For example, PCL-based membranes having both temperature and electrolyte responsive properties were reported by Cai et al.[123]. Diblock copolymers brushes of NIPAM with sulfur-sulfur

bridges were prepared by using a disulfide based ATRP initiator, which later could be cleaved to obtain thiol-terminated PNIPAM. Dual responsive (temperature and electrolyte) membranes, were produced via surface initiated ATRP of sodium 4-styrenesulfonate (NaSS). Moreover, dual responsive cellulose surfaces were also reported surface initiated ATRP. Thermo-responsive brushes of N-isopropylacrylamide (NIPAM), pH-responsive brushes of 4-vinlypyridine (4VP) and block copolymers of NIPAM and 4VP showed reversible response to both triggers while improving the wettability[124]. Qiu et al. later reported also dual-responsive cellulose membranes with the potential applications in water treatment and separation[125]. Simultaneous grafting of NIPAM and poly[(2-(diethylamino)ethyl methacrylate] (PDEAEMA) afforded reversible temperature- and pH-responsive surfaces while high grafting thickness and linear increase of brush thickness with reaction time reported.
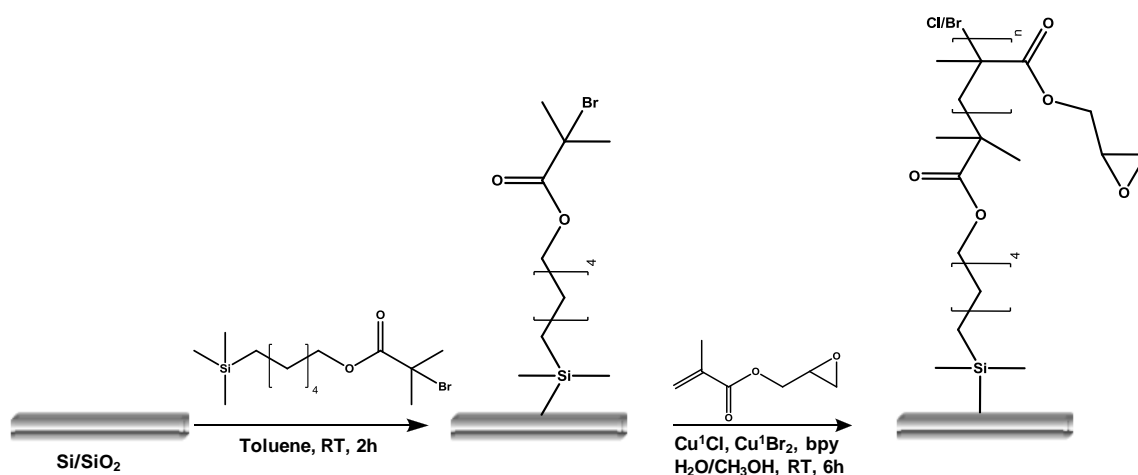
Figure 1.8: Functionalization of ATRP initiator-functionalized silicon wafers with SI-ATRP of PGMA[126].

On the other hand, graphene[127], silicon wafers[106], titanium or steel surfaces[128,129] were also modified via SIP methodologies. For example, silicon wafers were decorated with poly(glycidyl methacrylate) (PGMA) for the use of X-ray photoelectron spectroscopy (XPS) depth studies (Figure 1.8). The localization and spatial distribution of functional groups were investigated after the post-modification of PGMA brushes with bovine serum albumin[126]. Moreover, silicon based substrates were reported by SI-ATRP of

different monomers such as poly(2-hydroxyethyl methacrylate) (poly(HEMA))[130]. Hybrid surfaces were afforded through coupling with –NH$_2$ groups of collagen and poly(HEMA) brushes after ATRP onto hydrogen-terminated surfaces in water. Besides, Tugulu et al. reported the functionalisation of poly(HEMA) brushes with short-peptide ligands for the potential usage as blood-contacting biomaterials[131].

1.7.1 Surface initiated ARGET-ATRP

One drawback of classic ATRP is the relatively large amount of catalyst (typically 0.1-1 mol % relative to monomer) used to overcome the effect of termination reactions while increasing the concentration of persistent radicals. Resulting products may contain residual metal, which could limit their applicability for various biomedical and electronic applications. For that reason, more efficient and greener catalyst systems were developed to render ATRP more feasible metal sensitive applications
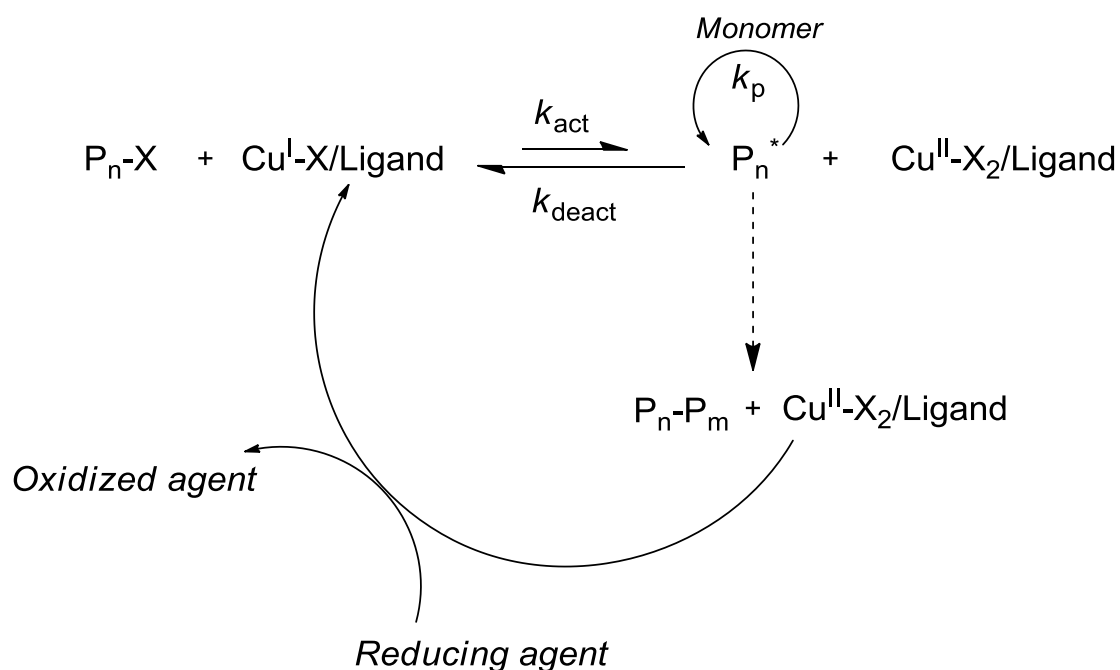
Figure 1.9: The general scheme for the mechanism of ARGET-ATRP[132].

Activators regenerated by electron transfer (ARGET)-ATRP is one development allowing to use a very small amount of active catalyst (typically ppm levels of copper

catalyst). In this process the deactivator Cu(II) is constantly converted into the polymerization activator Cu(I) via a redox reaction[94]. Environmentally friendly reducing agents (e.g. ascorbic acid, sugars, amines, tin(II)octoates) continuously regenerate the metal complex to the lower oxidation state. The large excess of reducing agent not only reduces Cu(II) to Cu(I) but also acts as oxygen and radical scavenger[132]. This offers the opportunity to conduct ARGET-ATRP in the presence of limited amount of air (i.e. oxygen) while classic ATRP needs to be carried under oxygen free environment as required in any radical polymerization technique[94].

Owing to the mentioned advantageous of this methodology, a wide range of polymeric systems with different properties were designed while having good control over their molecular architectures. For example, a systematic study concerning the optimization of reducing agent and catalyst concentration afforded disulfide functionalized polymers with control over the chain length[116]. A range of monomers were studied which represent acrylates, methacrylates, styrenics, PEG mimics and cationic classes of monomers. Batch polymerization of selected monomers by ARGET-ATRP resulted in thiol-terminated chains having the potential of conjugation to other molecules such as proteins or drugs. Like with normal ATRP, stimuli responsive properties can be tailored by ARGET-ATRP allowing to create dual responsive systems[133]. Moreover, polymers with different architectures can be synthesized such as star polymers[134].

ARGET-ATRP has also been explored for the synthesis of surface polymer brushes. For example, surface initiated polymerization of sodium methacrylate (NaMA) and 2-(dimethylamino)ethyl methacrylate (DMAEMA) was reported by following ARGET-ATRP methodology onto silica surfaces. The responses of polyampholytic block copolymer brushes were reported to be identical to homopolymers by the change of pH[135]. Similarly, silica particles were decorated with poly(2-(diethylamino)ethyl methacrylate) (poly(DEA)) brushes in order to use the intrinsic reducing ability of the tertiary amines groups of DEA. The pH-response of the brush modified particles was reported to show highly reversible response when pH changed between 4 and 7 (Figure 1.10)[96]. Moreover, PAA coated polyHIPE (polymerized high internal phase emulsion) via SI-ARGET-ATRP is worth mentioning in terms of using this technique for

functionalisation of porous substrates. These materials hold potential for bioseperation applications as proved by the covalent attachment of enhanced green fluorescent protein (eGFP) and coral-derived red fluorescent protein (DsRed)[95].
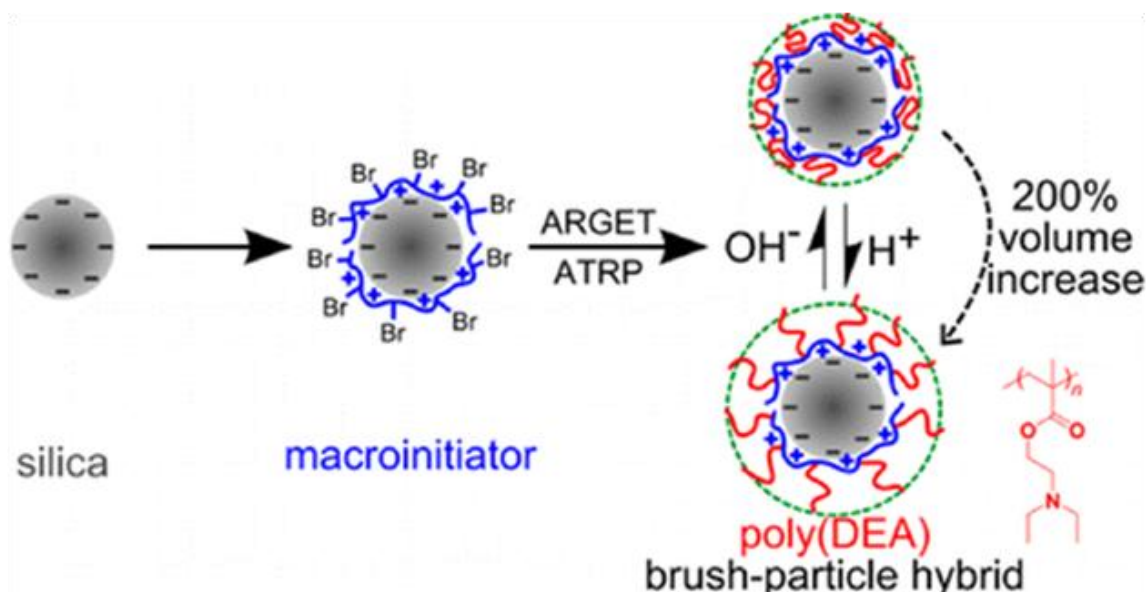
Figure 1.10: pH-Responsive brush decorated silica hybrids prepared via surface-initiated ARGET ATRP[96].

For practical purposes sacrificial initiator (SI) is often added to the surface grafting polymerization. It provides benefits in both synthesis and especially characterization of polymer brushes on the flat surfaces. In such systems, sufficient concentration of persistent radicals is generated by the termination of radicals formed in solution. Additionally, monomer conversion, molecular weight and polydispersity of the grafted brushes can be determined from the free polymer obtained in the presence of SI polymerization using techniques such as ^{1}H NMR or GPC assuming a correlation between the surface and the solution process. For example, kinetics of the grafting methyl methacrylate (MMA), styrene (St), and glycidyl methacrylate (GMA) from cellulose via ARGET-ATRP were monitored through free polymers obtained in the presence of sacrificial initiator (Figure 1.11)[117]. Recently, Hansson et al. used the free polymers formed from `grafting from` methodology as the prepolymer for the `grafting

25

to` methodology for the systematic comparison of the two grafting approaches[136]. The `grafting from` approach provided more control over the distribution and the amount of polymer for cellulose substrates.
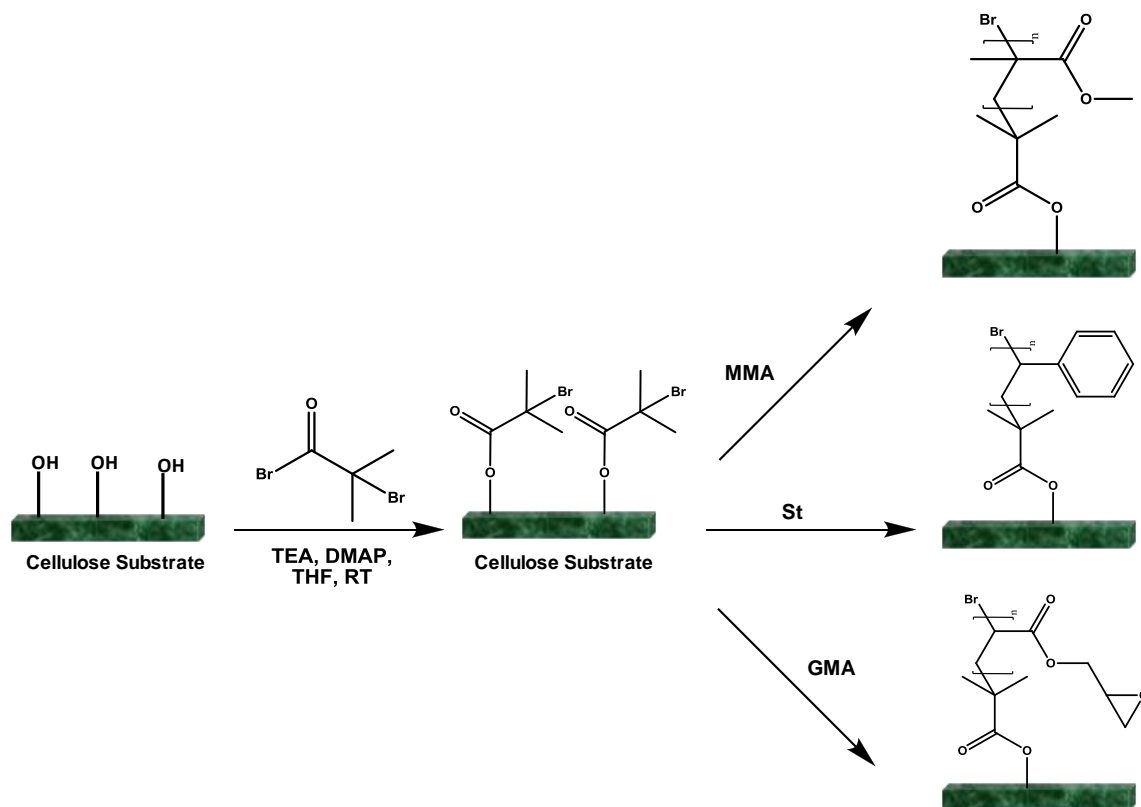
Figure 1.11: ARGET ATRP of MMA, St and GMA from a cellulose substrate[117].

1.8 Thiol-ene reactions

A thiol-ene reaction is the addition of a thiol compound to a double bond. Thiol-ene reactions are a simple and adaptable methodology to prepare polymer networks using combinations of multifunctional alkenes and thiols[137]. Thiol-ene chemistry owns several advantageous such as ease of preparation, resistance to oxygen inhibition, processing without solvent and fast curing[137,138]. Generally, thiol-ene reactions have been conducted under radical conditions which proceed through a typical chain process with initiation, propagation and termination steps. It is often induced photochemically causing the formation of a thiyl radical in the initiation step from a thiol in the presence of

photoinitiator (Figure 1.12). This is followed by the direct addition of the thiyl radical to the C=C bond yielding an intermediate carbon-centered radical followed by chain transfer to a second molecule of thiol to give the thiol-ene addition product. Anti-Markovnikov orientation results in the simultaneous generation of a new thiyl radical. Lastly, termination reactions occurs through typical radical-radical coupling reactions[138].
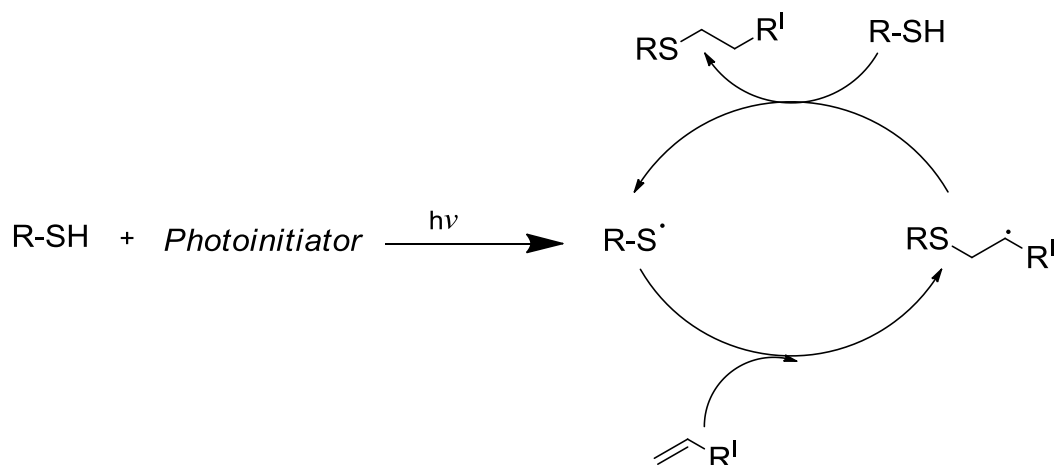
Figure 1.12: Mechanism of photoinduced free-radical thiol–ene coupling[138].

Due to the listed advantageous, this reaction can easily be used in applications like surface grafting, film patterning, thermoplastics and degradable materials[139–142]. Besides such applications, the radical mediated thiol-ene reactions were reported as a convenient tool for the post-polymerization modification of well-defined polymers[143].
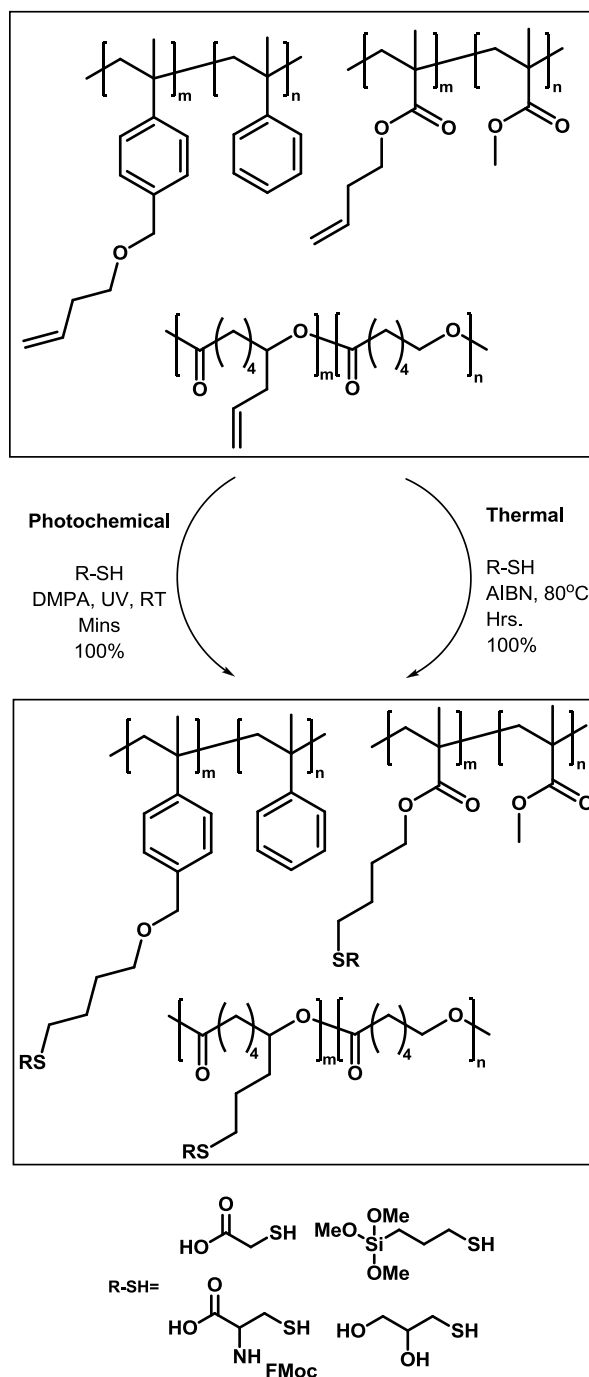
Figure 1.13: Post-polymerization modification of polymers bearing alkene groups via thiol-ene addition either through photochemical or thermal initiation[143].

Either a radical source or UV irradiation can be used to initiate the anti-Markovnikov addition of thiol to alkenes. An example worth to mention was reported by Hawker and

co-workers, i.e. the efficiency and orthogonality of both photochemically and thermally initiated thiol-ene coupling reactions were investigated with single or multiple alkene functionalized copolymers synthesized by controlled polymerization techniques (Figure 1.13)[144]. A complete double bond conversion was reported by using both methodologies while shorter reaction time and milder conditions as well as higher tolerance to functional groups were observed in the case of photoinitiator used methodologies. Moreover, orthogonal thiol-ene reactions were reported for the synthesis of highly functional aliphatic polyesters[145]. The ROP of alkene- and alkyne-substituted lactones were catalyzed by 1,5,7-triazabicyclo[4.4.0]dec-5-ene (TBD) yielding low PDI aliphatic polyersters. Thiol-ene (as well as azide-alkyne) click chemistry was used for the post-polymerization modification of copolymers as well as for cross-linking to afford polyesters nanoparticles with alkene functionality (Figure 1.14). Additional functionalisation were conducted by thiol-ene reactions[145].
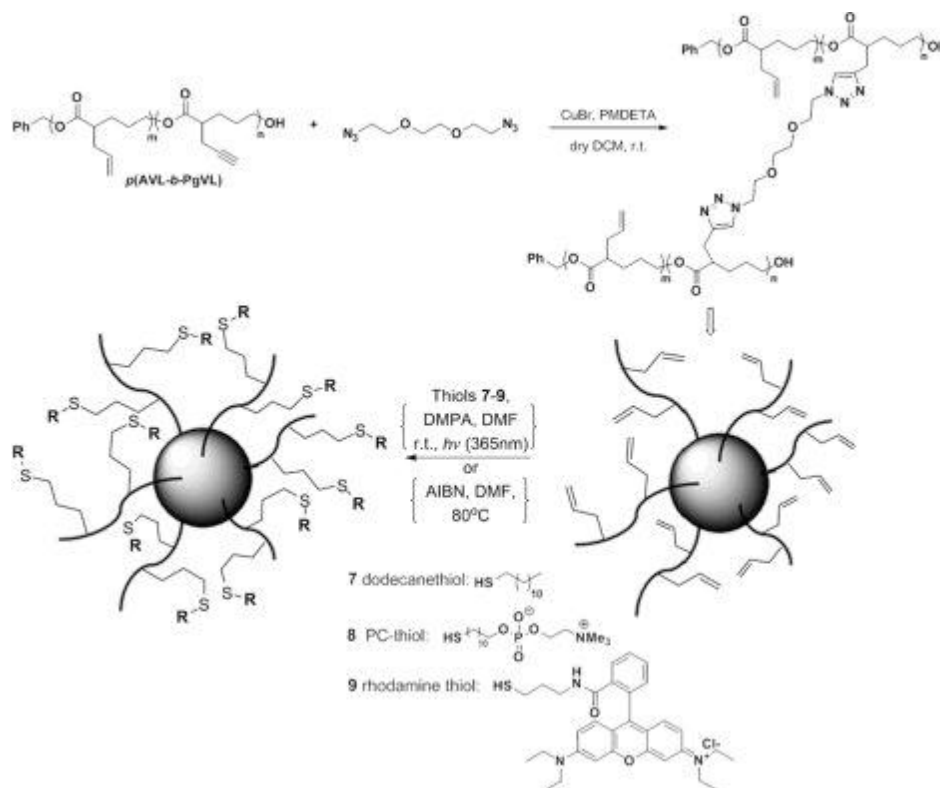
Figure 1.14: Cross-linked nanoparticles obtained by CuAAC of *p*(AVL-*b*-PgVL) (5) with 1,8-diazido-3,6-dioxaoctane and subsequent thiol-ene reactions[145].

Moreover, the radical thiol-ene reactions were used as pre-treatment for the synthesis of plant oil and fatty acid derived polymers[11,146]. Samuelsson et al. investigated the effect of the thiol structure on the reaction rate and found that both the structure of the thiols and the unsaturations in fatty acids greatly affect the addition of thiol[147]. In addition, mercapto acetates showed higher reaction rates than mercapto propionates. Roper et al. also reported that the structure-reactivity relationship for alkenes are significantly affected by the ene accessibility and location, substitution, and conformation[148]. Moreover, detailed kinetic studies were reported in order to establish a direct relationship between alkene structure and reactivity by using thiol-ene photo-additions of two mono-/tri-functional thiol monomers bearing a propionate ester moiety and $_D$-limonene, a naturally occurring diolefinic substrate presents as fragrance in the peel of oranges and essential oils of citrus fruit (Figure 1.15)[149]. The thiol-ene coupling at the *exo*-olefinic bond was found to be faster (6.5 times) than at the endocyclic unsaturation under solution conditions. Moreover, the radical addition of 2-mercaptoethanol onto oleic acid was reported under mild conditions via UV irradiation at room temperature without photoinitiator. As the content of polyunsaturated fatty chains was higher, the rate of thiol-ene reaction was lower. Bulk reactions afforded better yields in the case of maximum UV intensity were applied[150]. The same group later reported thiol-ene coupling of fatty acids to synthesize a wide range of both ester- and amide- containing pseudo-telechelic diols[151]. Moreover, different forms of cellulose, one of the most abundant renewable polymers, were also modified through different routes involving thiol-ene coupling reactions[152].
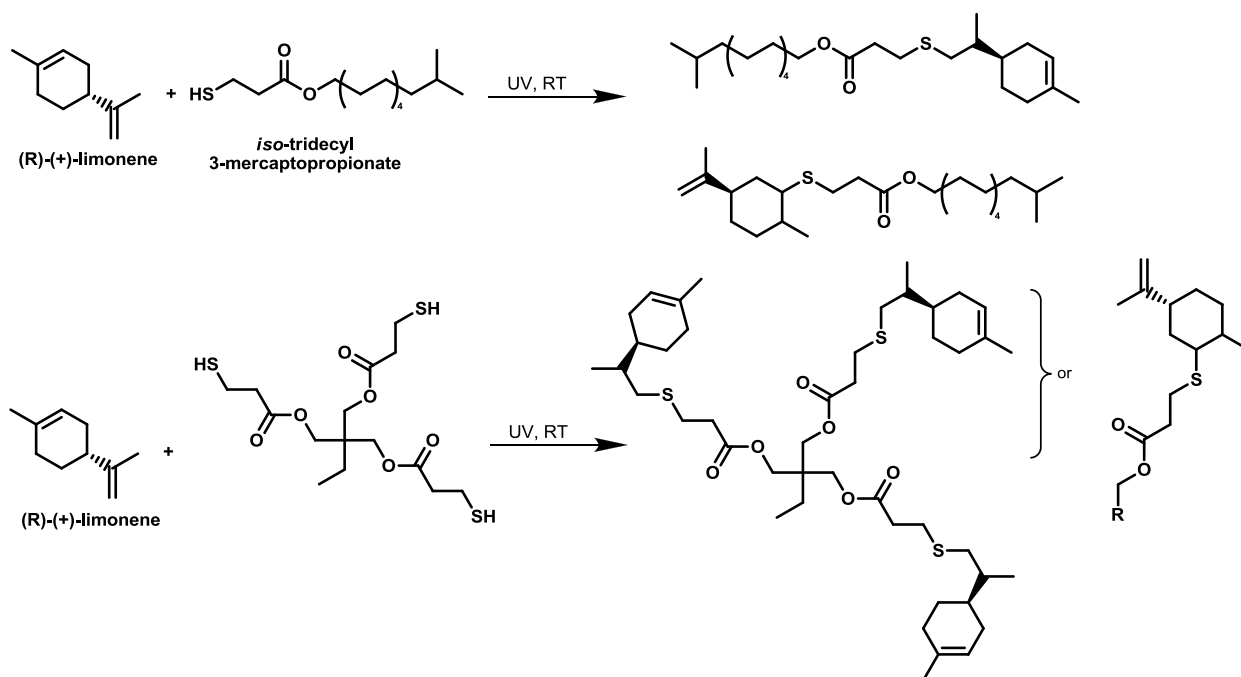
Figure 1.15: Selective thiol–ene coupling between (R)-(+)-limonene and mono- or tri-functional thiol compounds[149].

Thiol and acrylate functionality bearing polymers have the potential of creating polymer networks via free radical or thiol-ene based approaches. For example, coatings or adhesives can be prepared by thiol-ene chemistry[148]. Allyl ether functionalized hyperbranched (HB) polyesters were used to obtain highly cross-linked films by using multi-thiol compounds via UV-curing[153,154]. Based on the thermal and physical properties, thiol-ene cross-linked hyperbranched molecules can be used instead of dendrimers for thermoset applications without any significant difference[154]. Moreover, ester and ether based hydrogels were obtained by varying the chain length of PEG and crosslinker showed different hydrolytic stability with a variety of T_g. Likewise, a systematic study of photoinduced thiol-ene cross-linking of copolymers from lactones was reported[77]. Thermal and visco-elastic properties of reported networks prove the potential of such coatings from renewable materials. Another example of renewable materials, polysaccharides were also modified by a combination of organocatalysis and thiol-ene reactions under environmentally friendly conditions (Figure 1.16)[155].
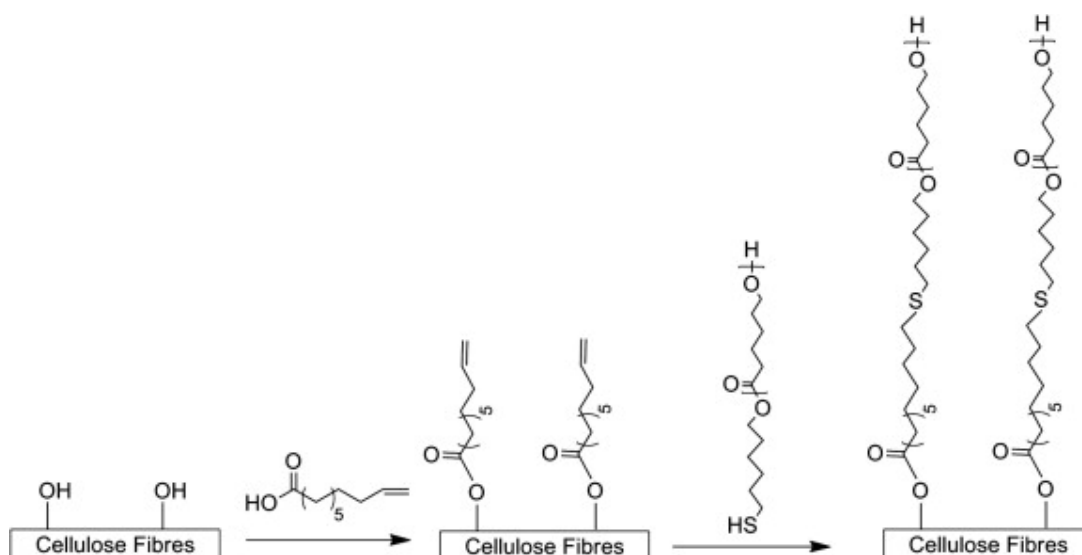
Figure 1.16: Grafting-to via thiol-ene chemistry of PCL onto cellulose[155,156]

The potential of thiol-ene coupling reactions has been increasingly recognized for the synthesis of functional materials as well as being a very versatile methodology for functionalisation and cross-linking. Particularly, a range of different functional groups can be introduced for the application driven design of novel functional materials. Resulting from such advantageous, thiol-ene coupling reactions were used to obtain cross-linked PML films and for the functionalisation of these films in this thesis.

1.9 References

1. A. Corma, S. Iborra, and A. Velty, *Chem. Rev.*, 2007, **107**, 2411–2502.

2. R. Mülhaupt, *Macromol. Chem. Phys.*, 2013, **214**, 159–174.

3. K. Yao and C. Tang, *Macromolecules*, 2013, **46**, 1689–1712.

4. P. A. Wilbon, F. Chu, and C. Tang, *Macromol. Rapid Commun.*, 2013, **34**, 32–43.

5. M. Firdaus and M. A. R. Meier, *Green Chem.*, 2013, **15**, 370–380.

6. T. Witt and S. Mecking, *Green Chem.*, 2013, **15**, 2361–2364.

7. C. Vilela, A. F. Sousa, A. C. Fonseca, A. C. Serra, J. F. J. Coelho, C. S. R. Freire, and A. J. D. Silvestre, *Polym. Chem.*, 2014, **5**, 3119–3141.

8. U. Biermann, U. Bornscheuer, M. A. R. Meier, J. O. Metzger, and H. J. Schäfer, *Angew. Chem. Int. Ed. Engl.*, 2011, **50**, 3854–3871.

9. D. Quinzler and S. Mecking, *Angew. Chem. Int. Ed. Engl.*, 2010, **49**, 4306–4308.

10. H. Mutlu and M. A. R. Meier, *J. Polym. Sci. Part A Polym. Chem.*, 2010, **48**, 5899–5906.

11. O. Türünç and M. A. R. Meier, *Macromol. Rapid Commun.*, 2010, **31**, 1822–1826.

12. M. Bouyahyi, M. P. F. Pepels, A. Heise, and R. Duchateau, *Macromolecules*, 2012, **45**, 3356–3366.

13. R. Slivniak and A. J. Domb, *Biomacromolecules*, 2005, **6**, 1679–1688.

14. K. S. Bisht, L. A. Henderson, R. A. Gross, D. L. Kaplan, and G. Swift, *Macromolecules*, 1997, **30**, 2705–2711.

15. B. D. Ulery, L. S. Nair, and C. T. Laurencin, *J. Polym. Sci. B. Polym. Phys.*, 2011, **49**, 832–864.

16. H. Seyednejad, A. H. Ghassemi, C. F. van Nostrum, T. Vermonden, and W. E. Hennink, *J. Control. Release*, 2011, **152**, 168–176.

17. A.-C. Albertsson and I. K. Varma, *Biomacromolecules*, 2003, **4**, 1466–1486.

18. A. Albertsson and I. K. Varma, in *Advances in Polymer Science*, Springer, 2002, vol. 157, pp. 1–40.

19. A.-C. Albertsson, Ed., *Advances in Polymer Science*, Springer, 2001.

20. S. El Habnouni, V. Darcos, and J. Coudane, *Macromol. Rapid Commun.*, 2009, **30**, 165–169.

21. A. K. Sutar, T. Maharana, S. Dutta, C.-T. Chen, and C.-C. Lin, *Chem. Soc. Rev.*, 2010, **39**, 1724–1746.

22. I. van der Meulen, E. Gubbels, S. Huijser, R. Sablong, C. E. Koning, A. Heise, and R. Duchateau, *Macromolecules*, 2011, **44**, 4301–4305.

23. M. P. F. Pepels, M. Bouyahyi, A. Heise, and R. Duchateau, *Macromolecules*, 2013, **46**, 4324–4334.

24. M. Bouyahyi and R. Duchateau, *Macromolecules*, 2014, **47**, 517–524.

25. T. Chen, Z. Qin, Y. Qi, T. Deng, X. Ge, J. Wang, and X. Hou, *Polym. Chem.*, 2011, **2**, 1190–1194.

26. P. Olsén, T. Borke, K. Odelius, and A.-C. Albertsson, *Biomacromolecules*, 2013, **14**, 2883–2890.

27. F. Nederberg, E. F. Connor, M. Möller, T. Glauser, and J. L. Hedrick, *Angew. Chem. Int. Ed. Engl.*, 2001, **40**, 2712–2715.

28. A. P. Dove, *ACS Macro Lett.*, 2012, **1**, 1409–1412.

29. A. P. Dove, R. C. Pratt, B. G. G. Lohmeijer, D. A. Culkin, E. C. Hagberg, G. W. Nyce, R. M. Waymouth, and J. L. Hedrick, *Polymer (Guildf).*, 2006, **47**, 4018–4025.

30. F. Jing and M. a Hillmyer, *J. Am. Chem. Soc.*, 2008, **130**, 13826–13827.

31. D. J. Coady, A. C. Engler, H. W. Horn, K. M. Bajjuri, K. Fukushima, G. O. Jones, A. Nelson, J. E. Rice, and J. L. Hedrick, *ACS Macro Lett.*, 2012, **1**, 19–22.

32. R. C. Pratt, B. G. G. Lohmeijer, D. a Long, R. M. Waymouth, and J. L. Hedrick, *J. Am. Chem. Soc.*, 2006, **128**, 4556–4557.

33. B. G. G. Lohmeijer, R. C. Pratt, F. Leibfarth, J. W. Logan, D. A. Long, A. P. Dove, F. Nederberg, J. Choi, C. Wade, R. M. Waymouth, J. L. Hedrick, R. V August, V. Re, M. Recei, and V. September, 2006, 8574–8583.

34. S. Kobayashi and A. Makino, *Chem. Rev.*, 2009, **109**, 5288–5353.

35. D. J. A. Cameron and M. P. Shaver, *Chem. Soc. Rev.*, 2011, **40**, 1761–1776.

36. S. B. I. Endo, S. E. W. Hu, B. M. J. Nielsen, G. S. G. T. Tsao, R. U. A. Zeng, and J. Z. W. Zhou, *Advances in Biochemical Engineering / Biotechnology*, 2011.

37. B. Ernest and A. Sym, *Biochem J.*, 1930, **24**, 1265–1281.

38. H. Uyama, K. Takeya, and S. Kobayashi, *Macromolecules*, 1996, 7046–7050.

39. S. Namekawa, S. Suda, H. Uyama, and S. Kobayashi, *Int. J. Biol. Macromol.*, 1999, **25**, 145–151.

40. S. Kobayashi, K. Takeya, S. Sudu, and H. Uyama, *Macromol. Chem. Phys.*, 1998, **736**, 1729–1736.

41.   A. Kumar, B. Kalra, A. Dekhterman, and R. A. Gross, *Macromolecules*, 2000, 6303–6309.

42.   M. J.-L. Tschan, E. Brulé, P. Haquette, and C. M. Thomas, *Polym. Chem.*, 2012, **3**, 836–851.

43.   M. Eriksson, K. Hult, E. Malmström, M. Johansson, S. M. Trey, and M. Martinelle, *Polym. Chem.*, 2011, **2**, 714–719.

44.   S. Namekawa, H. Uyama, and S. Kobayashi, *Biomacromolecules*, 2000, **1**, 335–338.

45.   S. Kobayashi, *Macromol. Rapid Commun.*, 2009, **30**, 237–266.

46.   M. Hunsen, A. Abul, W. Xie, and R. Gross, *Biomacromolecules*, 2008, **9**, 518–522.

47.   M. Hunsen, A. Azim, H. Mang, S. R. Wallner, A. Ronkvist, W. Xie, and R. A. Gross, *Macromolecules*, 2007, 148–150.

48.   R. T. MacDonald, S. K. Pulapura, Y. Y. Svirkin, R. A. Gross, D. L. Kaplan, J. Akkara, G. Swift, and S. Wolk, *Macromolecules*, 1995, **28**, 73–78.

49.   L. A. Henderson, Y. Y. Svirkin, R. A. Gross, D. L. Kaplan, and G. Swift, *Macromolecules*, 1996, **29**, 7759–7766.

50.   M. Matsumoto, D. Odachi, and K. Kondo, *Biochem. Eng. J.*, 1999, **4**, 73–76.

51.   A. Parenty, X. Moreau, G. Niel, and J.-M. Campagne, *Chem. Rev.*, 2013, **113**, 1–40.

52.   P. Kraft, J. A. Bajgrowicz, C. Denis, and G. Fra, *Angew. Chem. Int. Ed. Engl.*, 2000, **39**, 2980–3010.

53.   A. S. Williams, *Synthesis (Stuttg).*, 1999, 1707–1723.

54.   http://www.truthinaging.com/ingredients/pentadecal,.(23/01/2014)

55.   http://everything2.com/title/human+male+attractant+scent+chemical,. (23/01/2014)

56.   A. Duda, A. Kowalski, S. Penczek, H. Uyama, and S. Kobayashi, *Macromolecules*, 2002, **35**, 4266–4270.

57.   S. Namekawa and K. S. Uyama, Hiroshi, *Proc. Japan Acad.*, 1998, **74**, 65–68.

58.   I. van der Meulen and Y. Li, *Biomacromolecules*, 2011, **12**, 837–843.

59.   M. de Geus, I. van der Meulen, B. Goderis, K. van Hecke, M. Dorschu, H. van der Werff, C. E. Koning, and A. Heise, *Polym. Chem.*, 2010, **1**, 525–533.

60.   H. Uyama, H. Kikuchi, K. Takqa, and S. Kobayashi, *Acta Polym.*, 1996, **47**, 357–360.

61.   L. Van Der Mee, F. Helmich, R. De Bruijn, J. A. J. M. Vekemans, A. R. A. Palmans, and E. W. Meijer, *Macromolecules*, 2006, **39**, 5021–5027.

62.   J. Cai, C. Liu, M. Cai, J. Zhu, F. Zuo, B. S. Hsiao, and R. A. Gross, *Polymer.*, 2010, **51**, 1088–1099.

63.   H. Uyama and S. Kobayashi, *Chem. Lett.*, 1993, 1149–1150.

64.   I. K. Varma, A.-C. Albertsson, R. Rajkhowa, and R. K. Srivastava, *Prog. Polym. Sci.*, 2005, **30**, 949–981.

65.   S. Kobayashi, *Proc. Japan Acad. Ser. B*, 2010, **86**, 338–365.

66.   B. Manzini, P. Hodge, and A. Ben-Haida, *Polym. Chem.*, 2010, **1**, 339–436.

67.   M. A. J. Veld, A. R. A. Palmans, and E. W. Meijer, *J. Polym. Sci. Part A Polym. Chem.*, 2007, **45**, 5968–5978.

68.   K. Nakane, C. Tamaki, Y. Hata, T. Ogihara, and N. Ogata, *J. Appl. Polym. Sci.*, 2008, **108**, 2139–2143.

69.   W. Amass, A. Amass, and B. Tighe, *Polym. Int.*, 1998, **47**, 89–144.

70.   J. V Seppälä, A. O. Helminen, and H. Korhonen, *Macromol. Biosci.*, 2004, **4**, 208–217.

71.   P. Mainil-Varlet, C. Hauke, V. Maquet, G. Printzen, S. Arens, T. Schaffner, R. Jérme, S. Perren, and U. Schlegel, *J. Biomed. Mater. Res.*, 2001, **54**, 335–343.

72.   M. Vert, *Biomacromolecules*, 2005, **6**, 538–546.

73.   I. van der Meulen, M. de Geus, H. Antheunis, R. Deumens, E. A. J. Joosten, C. E. Koning, and A. Heise, *Biomacromolecules*, 2008, **9**, 3404–3410.

74.   A. Pascual, J. R. Leiza, and D. Mecerreyes, *Eur. Polym. J.*, 2013, **49**, 1601–1609.

75.   M. L. Focarete, M. Scandola, A. Kumar, and R. A. Gross, *J. Polym. Sci. B. Polym. Phys.*, 2001, 1721–1729.

76.   N. Simpson, M. Takwa, K. Hult, M. Johansson, M. Martinelle, and E. Malmström, *Macromolecules*, 2008, **41**, 3613–3619.

77. M. Claudino, I. van der Meulen, S. Trey, M. Jonsson, A. Heise, and M. Johansson, *J. Polym. Sci. Part A Polym. Chem.*, 2012, **50**, 16–24.

78. R. Ravichandran, S. Sundarrajan, J. R. Venugopal, S. Mukherjee, and S. Ramakrishna, *Macromol. Biosci.*, 2012, **12**, 286–311.

79. M. Sokolsky-Papkov, K. Agashi, A. Olaye, K. Shakesheff, and A. J. Domb, *Adv. Drug Deliv. Rev.*, 2007, **59**, 187–206.

80. K. Saralidze, L. H. Koole, and M. L. W. Knetsch, *Materials (Basel).*, 2010, **3**, 3537–3564.

81. P. Plikk, S. Målberg, and A.-C. Albertsson, *Biomacromolecules*, 2009, **10**, 1259–1264.

82. R. Jain, N. H. Shah, A. W. Malick, and C. T. Rhodes, *Drug Dev. Ind. Pharm.*, 1998, **24**, 703–727.

83. Y. Jiao and F. Cui, *Biomed. Mater.*, 2007, **2**, 24–37.

84. J. M. Goddard and J. H. Hotchkiss, *Prog. Polym. Sci.*, 2007, **32**, 698–725.

85. A. Cammarano, G. Luca, and E. Amendola, *Cent. Eur. J. Chem.*, 2012, **11**, 35–45.

86. J.-S. Kong, D.-J. Lee, and H.-D. Kim, *J. Appl. Polym. Sci.*, 2001, **82**, 1677–1690.

87. G. Tao, A. Gong, J. Lu, H.-J. Sue, and D. E. Bergbreiter, *Macromolecules*, 2001, **34**, 7672–7679.

88. D. He, H. Susanto, and M. Ulbricht, *Prog. Polym. Sci.*, 2009, **34**, 62–98.

89. S. Yoshida, K. Hagiwara, T. Hasebe, and A. Hotta, *Surf. Coatings Technol.*, 2013, **233**, 99–107.

90. C. M. Hui, J. Pietrasik, M. Schmitt, C. Mahoney, J. Choi, M. R. Bockstaller, and K. Matyjaszewski, *Chem. Mater.*, 2013, **26**, 745–762.

91. F. J. Xu, Z. H. Wang, and W. T. Yang, *Biomaterials*, 2010, **31**, 3139–3147.

92. J. C. Tuberquia, N. Nizamidin, R. R. Harl, J. Albert, J. Hunter, B. R. Rogers, and G. K. Jennings, *J. Am. Chem. Soc.*, 2010, **132**, 5725–5734.

93. K. R. Yoon, K.-B. Lee, Y. S. Chi, W. S. Yun, S.-W. Joo, and I. S. Choi, *Adv. Mater.*, 2003, **15**, 2063–2066.

94. K. Matyjaszewski, H. Dong, W. Jakubowski, J. Pietrasik, and A. Kusumo, *Langmuir*, 2007, **23**, 4528–4531.

95. F. Audouin, R. Larragy, M. Fox, B. O'Connor, and A. Heise, *Biomacromolecules*, 2012, **13**, 3787–3794.

96. B. T. Cheesman, J. D. Willott, G. B. Webber, S. Edmondson, and E. J. Wanless, *ACS Macro Lett.*, 2012, **1**, 1161–1165.

97. S. Hansson, E. Ostmark, A. Carlmark, and E. Malmström, *ACS Appl. Mater. Interfaces*, 2009, **1**, 2651–2659.

98. R. Barbey, L. Lavanant, D. Paripovic, N. Schüwer, C. Sugnaux, S. Tugulu, and H.-A. Klok, *Chem. Rev.*, 2009, **109**, 5437–5527.

99. A. Olivier, F. Meyer, J.-M. Raquez, P. Damman, and P. Dubois, *Prog. Polym. Sci.*, 2012, **37**, 157–181.

100. I. S. Choi and R. Langer, *Macromol. Symp.*, 2001, **34**, 5361–5363.

101. E. J. Vorenkamp, V. Erb, M. Stamm, and A. J. Schouten, *Langmuir*, 2001, **17**, 6477–6484.

102. K. R. Yoon, K.-B. Lee, Y. S. Chi, W. S. Yun, S.-W. Joo, and I. S. Choi, *Adv. Mater.*, 2003, **15**, 2063–2066.

103. R. H. Wieringa, E. A. Siesling, P. F. M. Geurts, P. J. Werkman, E. J. M. Vorenkamp, V. E. Stamm, and A. J. Schouten, *Langmuir*, 2001, **17**, 6477–6484.

104. J. Pyun, T. Kowalewski, and K. Matyjaszewski, *Macromol. Rapid Commun.*, 2003, **24**, 1043–1059.

105. A. M. Shanmugharaj, W. S. Choi, and S. H. Ryu, *J. Polym. Sci. Part A Polym. Chem.*, 2010, **48**, 5092–5099.

106. Y. Liu, V. Klep, B. Zdyrko, and I. Luzinov, *Langmuir*, 2004, **20**, 6710–6718.

107. A. Carlmark and E. E. Malmström, *Biomacromolecules*, 2003, **4**, 1740–1745.

108. M. Baum and W. J. Brittain, *Macromolecules*, 2002, **35**, 610–615.

109. F. Audouin and A. Heise, *Eur. Polym. J.*, 2013, **49**, 1073–1079.

110. M. Husseman, E. E. Malmström, M. Mcnamara, M. Mate, D. Mecerreyes, D. G. Benoit, J. L. Hedrick, P. Mansky, E. Huang, T. P. Russell, and C. J. Hawker, *Macromolecules*, 1999, **32**, 1424–1431.

111. E. D. Bain, K. Dawes, A. O. Evren, X. Hu, C. B. Gorman, S. Jir, and J. Genzer, *Macromolecules*, 2012, **45**, 3802–3815.

112. M. Kato, M. Kamigaito, M. Sawamoto, and T. Higashimura, *Macromolecules*, 1996, **28**, 1721–1723.

113. J. Wang and K. Matyjaszewski, *J. Am. Chem. Soc.*, 1995, **117**, 5614–5615.

114. V. Coessens, T. Pintauer, and K. Matyjaszewski, *Prog. Polym. Sci.*, 2001, **26**, 337–377.

115. N. Ayres, *Polym. Rev.*, 2011, **51**, 138–162.

116. D. J. Siegwart, M. Leiendecker, R. Langer, and D. G. Anderson, *Macromolecules*, 2012, **45**, 1254–1261.

117. S. Hansson, E. Ostmark, A. Carlmark, and E. Malmström, *ACS Appl. Mater. Interfaces*, 2009, **1**, 2651–2659.

118. S. Edmondson, V. L. Osborne, and W. T. S. Huck, *Chem. Soc. Rev.*, 2004, **33**, 14–22.

119. S. Yamamoto, J. Pietrasik, and K. Matyjaszewski, *Macromolecules*, 2008, **41**, 7013–7020.

120. C. Weber, R. Hoogenboom, and U. S. Schubert, *Prog. Polym. Sci.*, 2012, **37**, 686–714.

121. S. S. Balamurugan, G. B. Bantchev, Y. Yang, and R. L. McCarley, *Angew. Chem. Int. Ed. Engl.*, 2005, **44**, 4872–4876.

122. H. Lee, J. Pietrasik, S. S. Sheiko, and K. Matyjaszewski, *Prog. Polym. Sci.*, 2010, **35**, 24–44.

123. T. Cai, M. Li, K.-G. Neoh, and E.-T. Kang, *J. Mater. Chem.*, 2012, **22**, 16248–16258.

124. J. Lindqvist, D. Nyström, E. Ostmark, P. Antoni, A. Carlmark, M. Johansson, A. Hult, and E. Malmström, *Biomacromolecules*, 2008, **9**, 2139–2145.

125. X. Qiu, X. Ren, and S. Hu, *Carbohydr. Polym.*, 2013, **92**, 1887–1895.

126. R. Barbey, V. Laporte, S. Alnabulsi, and H. Klok, *Macromolecules*, 2013, **46**, 6151–6158.

127. D. Wang, G. Ye, X. Wang, and X. Wang, *Adv. Mater.*, 2011, **23**, 1122–1125.

128. F. Zhang, Z. L. Shi, P. H. Chua, E. T. Kang, and K. G. Neoh, *Ind. Eng. Chem. Res.*, 2007, **46**, 9077–9086.

129. S. J. Yuan, F. J. Xu, S. O. Pehkonen, Y. P. Ting, K. G. Neoh, and E. T. Kang, *Biotechnol. Bioeng.*, 2009, **103**, 268–281.

130. F. J. Xu, S. P. Zhong, Y. W. Tong, E. T. Kang, and K. G. Neoh, *Tissue Eng.*, 2005, **11**, 3–9.

131. S. Tugulu, P. Silacci, N. Stergiopulos, and H.-A. Klok, *Biomaterials*, 2007, **28**, 2536–2546.

132. W. Jakubowski and K. Matyjaszewski, *Angew. Chemie*, 2006, **45**, 4482–4486.

133. Y. Q. Yang, X. D. Guo, W. J. Lin, L. J. Zhang, C. Y. Zhang, and Y. Qian, *Soft Matter*, 2012, **8**, 454–464.

134. J. Burdyńska, H. Y. Cho, L. Mueller, and K. Matyjaszewski, *Macromolecules*, 2010, **43**, 9227–9229.

135. Y. K. Jhon, S. Arifuzzaman, A. E. Özçam, D. J. Kiserow, and J. Genzer, *Langmuir*, 2012, **28**, 872–882.

136. S. Hansson, V. Trouillet, T. Tischer, A. S. Goldmann, A. Carlmark, C. Barner-Kowollik, and E. Malmström, *Biomacromolecules*, 2013, 64–74.

137. C. E. Hoyle, T. Y. Lee, and T. Roper, *J. Polym. Sci. Part A Polym. Chem.*, 2004, **42**, 5301–5338.

138. A. B. Lowe, *Polym. Chem.*, 2010, **1**, 17–36.

139. P. van de Wetering, A. T. Metters, R. G. Schoenmakers, and J. A. Hubbell, *J. Control. Release*, 2005, **102**, 619–627.

140. V. S. Khire, Y. Yi, N. A. Clark, and C. N. Bowman, *Adv. Mater.*, 2008, **20**, 3308–3313.

141. V. S. Khire, A. W. Harant, A. W. Watkins, K. S. Anseth, and C. N. Bowman, *Macromolecules*, 2006, **39**, 5081–5086.

142. A. W. Harant, V. S. Khire, M. S. Thibodaux, and C. N. Bowman, *Macromolecules*, 2006, **39**, 1461–1466.

143. K. A. Günay, P. Theato, and H.-A. Klok, *J. Polym. Sci. Part A Polym. Chem.*, 2013, **51**, 1–28.

144. L. M. Campos, K. L. Killops, R. Sakai, J. M. J. Paulusse, D. Damiron, E. Drockenmuller, B. W. Messmore, C. J. Hawker, and C. B. Lyon, *Macromolecules*, 2008, **41**, 7063–7070.

145. A. L. Silvers, C.-C. Chang, and T. Emrick, *J. Polym. Sci. Part A Polym. Chem.*, 2012, **50**, 3517–3529.

146. O. Türünç and M. A. R. Meier, *Eur. J. Lipid Sci. Technol.*, 2013, **115**, 41–54.

147. J. Samuelsson, M. Jonsson, T. Brinck, and M. Johansson, *J. Polym. Sci. Part A Polym. Chem.*, 2004, **42**, 6346–6352.

148. T. M. Roper, C. A. Guymon, E. S. Jonsson, and C. E. Hoyle, *J. Polym. Sci. Part A Polym. Chem.*, 2004, **42**, 6283–6298.

149. M. Claudino, M. Jonsson, and M. Johansson, *RSC Adv.*, 2013, **3**, 11021–11034.

150. M. Desroches, S. Caillol, V. Lapinte, R. Auvergne, and B. Boutevin, *Macromol. Symp.*, 2011, **44**, 2489–2500.

151. M. Desroches, S. Caillol, R. Auvergne, B. Boutevin, and G. David, *Polym. Chem.*, 2012, **3**, 450–457.

152. Y. Habibi, *Chem. Soc. Rev.*, 2014, **43**, 1519–1542.

153. C. Nilsson, E. V. A. Malmström, M. Johansson, and S. M. Trey, *J. Polym. Sci. Part A Polym. Chem.*, 2008, **47**, 589–601.

154. S. M. Trey, C. Nilsson, E. Malmström, and M. Johansson, *Prog. Org. Coatings*, 2010, **68**, 151–158.

155. G.-L. Zhao, J. Hafrén, L. Deiana, and A. Córdova, *Macromol. Rapid Commun.*, 2010, **31**, 740–744.

156. A. Carlmark, E. Larsson, and E. Malmström, *Eur. Polym. J.*, 2012, **48**, 1646–1659.

Side-chain Functionalisation of Unsaturated Polyesters

Abstract

A novel method for the modification of poly(globalide), produced by enzymatic ring opening polymerization, is proposed by utilising thiol-ene coupling reactions as the post-polymerization modification of unsaturated polyesters. Various thiol compounds bearing different functional groups were studied with varying the reaction conditons to allow the control over the functionalization. This methodology may offer a chemically simplistic route to the (bio)functionalisation of polyesters resulting from the functionalities introduced via thiol-ene reactions.

2.1 Introduction

Aliphatic polyesters have received significant recent attention owing to their use in a number of biomedical applications, with key research focussed particularly on their use as degradable drug delivery vehicles and in tissue engineering[1]. Notable advantageous material properties include excellent biodegradability, biocompatibility, and nontoxicity. In addition, the production of biocompatible degradation products renders the application of polyesters as biomaterials suitably appropriate. Aliphatic polyesters can be prepared by either a step-growth polycondensation process or the ring-opening polymerisation (ROP) of cyclic esters (lactones)[2]. The popularity of the latter methodology stems from the fact that it produces polyesters with a high degree of control, with respect to molecular weight, polydispersity and end-group fidelity, under relatively mild reaction conditions. A wide range of catalytic systems have been reported for the ROP of cyclic esters including organometallic, organic, and enzyme catalysts[3–6].

Despite the suitability of incorporating polyesters into biomaterials, their use in highly sophisticated biomedical applications is hindered by the difficulty of polyester side-chain functionalisation. Material modification to allow specific interactions within biological systems significantly enhances biomaterial performance, potentially offering the material a dynamic role in its application[7–9]. Functionalization of polyesters was reported by various methodologies including functionalization prior to polymerization and post-polymerization functionalization. Mostly, ε-CL derivatives were reported as functionalized polyesters by ROP. Halogen-bearing CL monomers are the most frequently used ones in ROP which consist of activation of monomer and then sustitution reaction[10]. Enzymatic ROP is also reported to synthesize functionalized polyesters having the advantage of regioselectivity, which can eliminate protection/deprotection steps. An example worth mentioning is the synthesis of two novel monomers containing functional groups, ambrettolide epoxide and isopropyl aleuriteate[11]. Homopolymerization of those functionalized monomers as well as the copolymerization with ε-CL were catalyzed by NZ435.

However, as recently highlighted by Pounder and Dove, the introduction of functional groups throughout the polymer chain via ROP remains very challenging[12]. The chemical polymerisation process is non-selective and does not tolerate the presence of even the most simple functional groups, such as hydroxy or amines, without inevitably producing a cross-linked polymer. Despite this synthetic hindrance there are numerous examples of side chain functionalised linear polyesters produced from ROP which underlines the demand for these materials. However, most examples reported are produced via rigorous, often multi-step, synthetic procedures to derivatise lactone or lactide monomers[12–14]. An alternative synthetic approach is the derivatisation of suitable substituted aliphatic polyesters, in which a stable substituted lactone precursor is polymerized and the polymer subsequently modified selectively. The application of click chemistry has proved to be efficient in polymer chemistry where the click concept relies on the application of highly efficient reactions occuring stoichiometrically. Cu(I) cataylzed Huisgen-1,3-dipolar cycloaddition between an azide and a terminal alkyne is a well known example of such reactions[15,16]. Diels-Alder reactions[17], ring opening of epoxides by amines[18,19], reactions of amino-oxy compounds with aldehydes or ketones[20,21] and a range of thiol-ene reactions where a sulhydryl compound reacts with an alkene[22,23] (via either an anionic, Michael addition or radical mechanism) can be counted among the wide range of reactions. Successful examples of the Michael addition reactions of thiols on polymers from γ-acrylic-ε-caprolactone were reported to synthesize functional or amphilic PCL based polymers[24]. Moreover, α-chloro-ε-caprolactone was copolymerized with ω-CL and the pendant chlorides substituted by azide[25]. The azide functionalized polymers were then reacted by Huisgens cycloaddition reactions with alkyne functionalized reagents having ester, amine and ammonium groups, as well as with alkyne derivatized PEO chains. Similarly, α-propargyl-δ-valerolactone and ω-CL copolymers afforded aliphatic polyester with pendant acetylene groups. The subsequent grafting of azide terminated PEG and azide functionalized peptide to these polyesters was sucessful and the materials showed biocompatibility[26].

In this chapter, we propose the chemically straightforward modification of aliphatic

polyesters by utilising highly efficient and robust thiol-ene reactions on unsaturated polyesters obtained from ROP of the unsaturated macrolactone globalide (Gl). This reaction may be employed for the post-polymerisation modification to allow the introduction of numerous different chemical groups to polymeric backbones, thereby potentially enabling the formation of biofunctional materials through considered materials engineering[5,27]. A few recent publications describe thiol-ene reactions on fatty acid monomers, however to our knowledge this paper offers the primary example of the thiol-ene functionalisation of a fatty acid derived polymer[28–30].

2.2 Results and Discussion

We have previously reported the enzymatic synthesis of homopolymers from globalide, which is derived from hydroxy fatty acids and is proven to be non-toxic[30]. The ROP of globalide was carried out in solution with Novozyme 435 (*Candida Antarctica* Lipase B (CALB) immobilised on a macroporous resin) to a molecular weight of 16,000 g/mol and a typically broad polydispersity of 2.5 due to transesterification reactions.
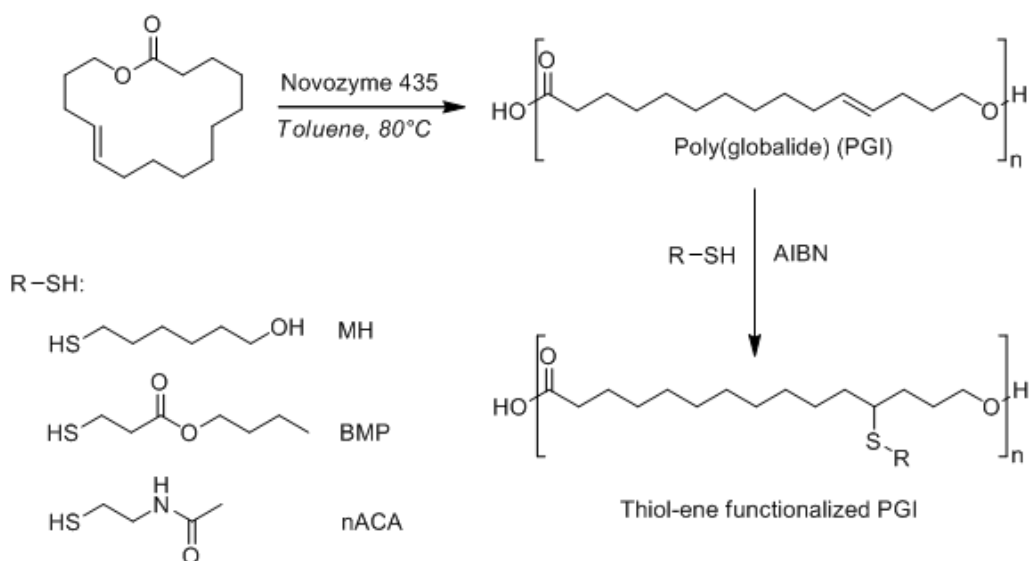
Figure 2.1 Polymerisation of globalide and thiol-ene reaction of poly(globalide) with 6-mercapto-1-hexanol (MH), butyl-3-mercapto propionate (B3MP) and N-acetylcysteamine (nACA). Globalide is a mixture of two constitutional isomers with the double bond at the 11 or 12 position. For reasons of clarity only one isomer is shown.

The thiol-ene functionalisation of polyglobalide (PGl) was undertaken by a thermally initiated reaction catalysed by AIBN in the bulk above the melting point of PGl or with a minimum amount of solvent when required to enable complete reactant miscibility. Initially butyl-3-mercapto propionate (B3MP) was chosen as a suitable model compound for this polymeric functionalisation owing to its thiol functionality.

Generally, internal double bonds as present in PGl and some fatty acids are less reactive than terminal ones due to the strically lower accesibility of internal double bonds. We therefore paid specific attention to the quantification of the thiol-ene reaction on the PGl by NMR spectroscopy. The ^{1}H NMR obtained for B3MP functionalised PGl reveals characteristic peaks corresponding to the repeat units of PGl and signals from the B3MP, which suggests a successful reaction. Significantly, the quantification of the thiol-ene coupling of B3MP to PGl revealed a reduction of the double bond peak at around 5.4 ppm in the spectra of the final product, indicating that the thiol-ene coupling efficiency was greater than 75 %.

The system proposed offers the opportunity to introduce a range of functionalities into the polyester backbone via the coupling of various thiol terminated linkers that also possess other chemical groups which offer potential for further chemical modification. 6-Mercapto-1-hexanol (MH) was selected as a suitable candidate for the introduction of a primary alcohol to the polymer via the methodology proposed. Upon formation, this alcohol-functionalised polyester may be further utilised for the introduction of carboxylic acid-terminated groups, such as amino acids, into the polyester via esterification as a method of biofunctionalisation.
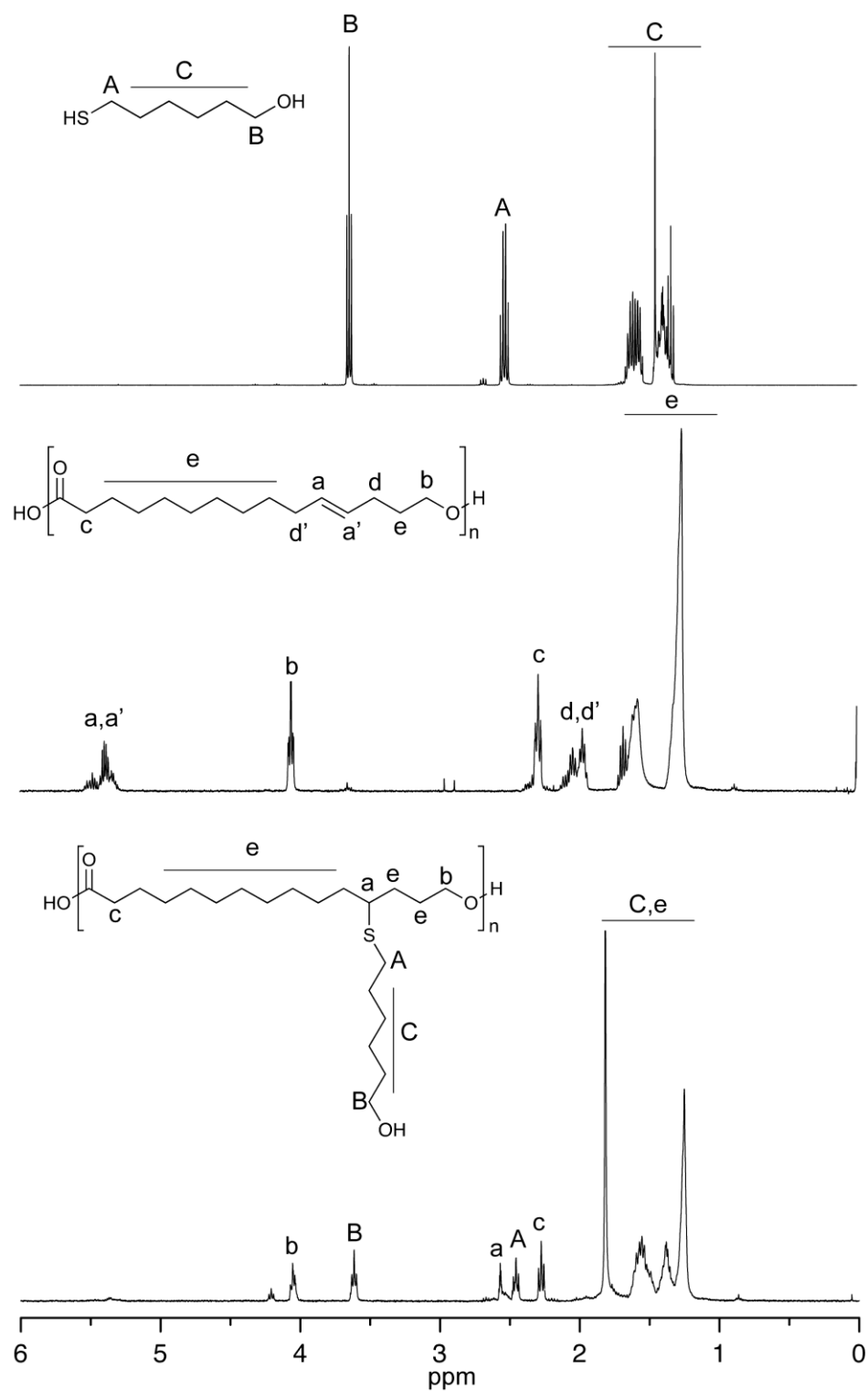
Figure 2.2: ^{1}H NMR spectra of 6-mercapto-1-hexanol (MH), poly(globalide) (PGl) and the thiol-ene coupling product from MH and PGl. Spectra recorded in CDCl$_3$ using a 400 MHz spectrometer. Globalide is a mixture of two constitutional isomers with the double bond at the 11 or 12 position.

The ^{1}H NMR spectra of MH, PGl and the product formed are given in Figure 2.2. Analogous to PGl functionalisation with B3MP, a reduction in the peak corresponding to the polyester double bond was observed. By comparing the integration of the peaks that correspond to the double bond in PGl at around 5.4 ppm (a, a') with the peaks representative of the methylene group adjacent to the hydroxyl terminal group (b), it was determined that the fraction of thiol-ene coupling was in excess of 95% which highlights the high efficiency of the thiol-ene reaction undertaken. Moreover, all characteristic peaks of both MH and PGl are present in the product spectrum. The peak of the methylene group adjacent to the thiol group at 2.6 ppm (A) shifted slightly upfield to 2.45 ppm after the thiol-ene reaction. Most importantly, the signal of the methylene group adjacent to the hydroxyl group of 6-mercapto-1-hexanol was still detected at 3.6 ppm as a triplet (B) confirming the hydroxy functionalisation of the polyester.
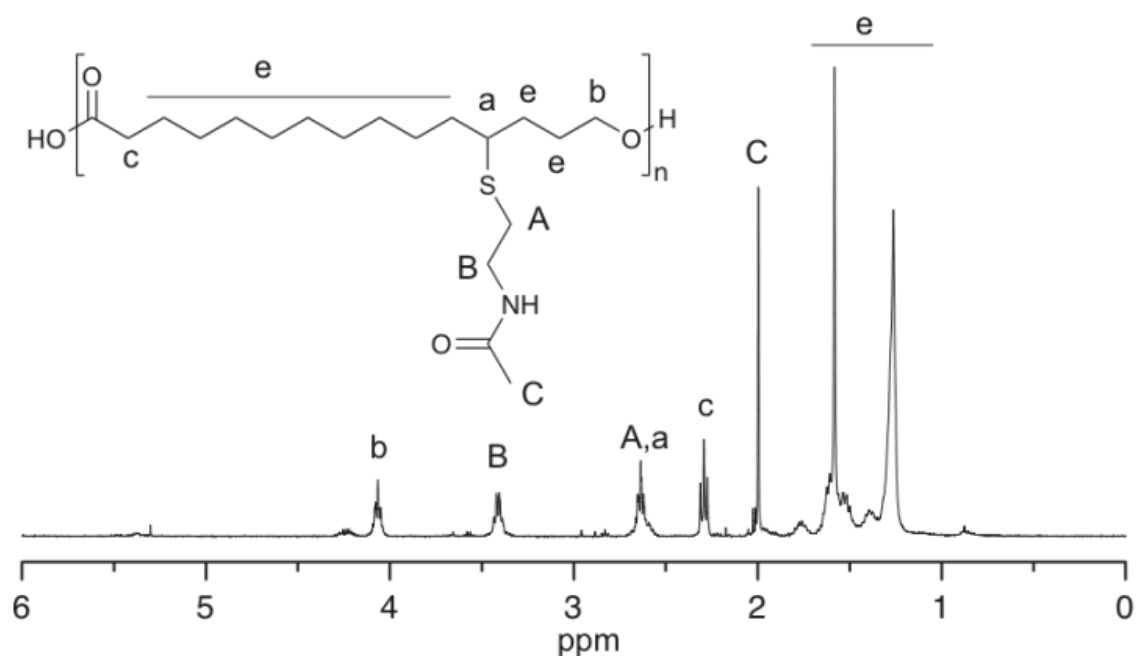
Figure 2.3: ^{1}H NMR spectra of N-acetylcysteamine (nACA) conjugated poly(globalide) (PGl-nACA). The spectrum was recorded in CDCl$_3$ using a 400 MHz spectrometer.

Amine functionality may be introduced into the polyester via the thiol-ene coupling of N-acetylcysteamine (nACA). Subsequent deacetylation would reveal free amine groups, affording a polyester to which direct protein modification is readily achievable. Analysis of the formed acetylated thiol-ene product by NMR (Figure 2.3) enabled the comparison of integrals corresponding to the double bond of PGl (5.4 ppm (a, a') with those representative of the amine proton (b). Optimal coupling conditions were found to give a reaction yield of ≥ 95% further highlighting the efficiency of the thiol-ene reaction.

Variation in the reaction conditions employed for the coupling of the three thiol-terminated side chains described to PGl had a marked effect on the coupling yield. Poor reactant miscibility dictated the necessary addition of THF to enhance thiol-ene reactions and consequent product formation for some reactions. However, excessive solvent addition reduces reactant concentrations to the detriment of the coupling yield (Table 2.2). The optimal reaction conditions found for the thiol-ene coupling of MH and nACA to PGl are given in Table 2.1. An excess of the thiol-bearing molecule was required for effective coupling due to the low reactivity of the PGl double bond. Further investigation into the coupling of nACA to PGl revealed that the initiator concentration also had a significant bearing on the reaction yield (Table 2.3). A 95% yield was recorded for the coupling of 6.6 mmol nACA to 0.01 mmol PGl (0.6 mmol double bonds) using 50 mg AIBN in contrast to a 60% yield when 10 mg AIBN was used.

Table 2.1 The optimal reaction conditions found for the thiol-ene coupling of three selected thiols to PGl. (Mn = 16,000 g/mol).

	Double Bond Concentration (mmol)[a]	Initiator Concentration (mg)	Solvent (THF)	Mn (g/mol)	Mw/Mn	Coupling Yield (%)
PGl-B3MP	0.6	10	None	15,900	3.2	75
PGl-MH	4.0	10	1 mL	26,000	2.2	≥ 95
PGl-nACA	6.6	50	1 mL	23,500	1.8	≥ 95

[a] The concentration of PGl double bonds was estimated from the molecular weight of the polymer as determined by GPC with poly(styrene) calibration. Due to the inherent error of this calculation only a relative comparison of the results can be made.

DSC analysis of the obtained thiol-ene functionalised polymers was performed to ascertain their thermal properties. PGl has a semi-crystalline morphology with a melting point of 48 °C. As the vast majority of double bonds present on the polyester backbone partake in the thiol-ene reaction, the crystalline structure of the polymer is disrupted resulting in an amorphous material as shown clearly in the DSC thermograms presented in Figure 2.4 (PGl, PGl-MH and PGl-nACA).
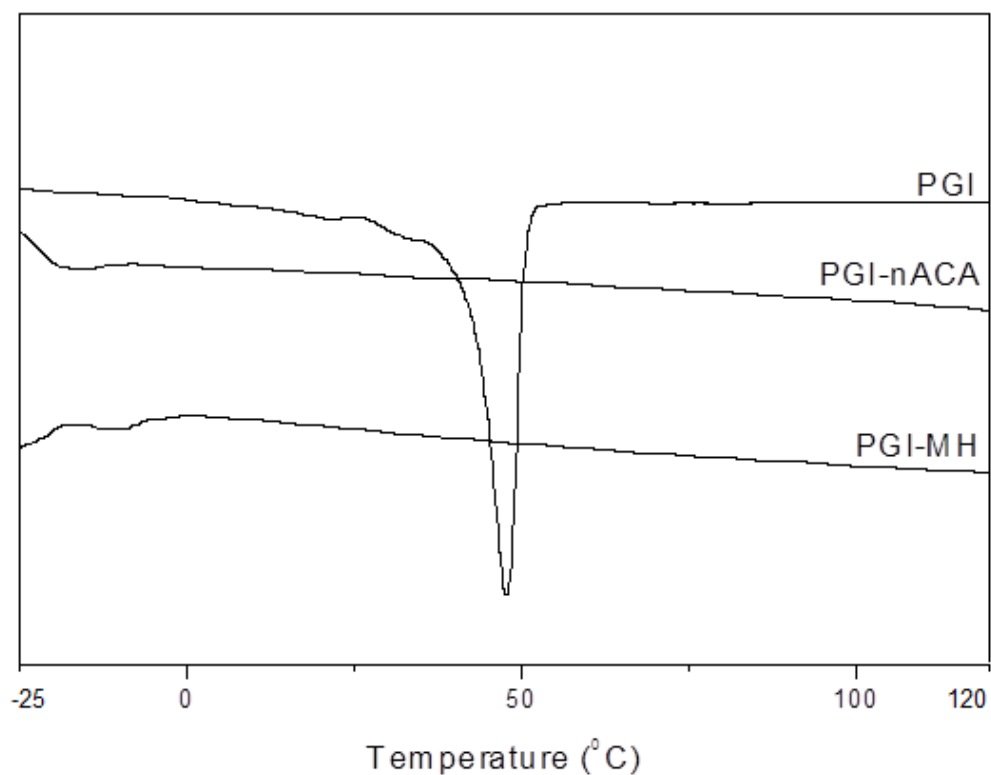
Figure 2.4: DSC thermograms (second heating cycle, heating rate of 10°C/min) of polyglobalide (PGl) and polyglobalide after thiol-ene coupling independently with 6-mercapto-1-hexanol (PGl-MH) and N-acetylcysteamine (PGl-nACA).

The molecular weights and polydispersities of PGl, PGl-B3MP, PGl-MH and PGl-nACA were determined by GPC. Analysis of the GPC data reveals a significant increase in the molecular weight and polydispersity of both PG-MH (26,000 g/mol) and PGl-nACA (23,500 g/mol) relative to unmodified PGl (16,000 g/mol) (Table 2.1). This increase in molecular weight corresponds well with the ^{1}H NMR data which suggested that in both instances a highly efficient thiol-ene coupling reaction occurred. A less significant change in Mn was observed for PGl-B3MP relative to unfunctionalised PGl, however the modified polymer possessed a greater polydispersity in comparison to PGl which made accurate molecular weight assignment difficult but suggests that PGl functionalisation has occurred. It also has to be noted that upon thiol-ene grafting a branched polymer is produced, which makes comparison of GPC results with the linear precursor is complex. Nevertheless, the shift in M_n, particularly in the formation of PGl-MH and PGl-nACA, validates this methodology for the functionalisation of PGl with three different thiol terminated linkers, offering a novel and chemically simplistic technique for polyester functionalisation.

2.3 Conclusions

The work detailed in this chapter offers a simple, single-step route for the synthesis of thiol-ene functionalised polyesters. Enzymatic ROP of polyglobalide offers a highly controlled mechanism to create linear polyesters possessing alkene functionality. Highly efficient thio-ene coupling reactions may be utilised to exploit this functionality to precisely introduce thiol terminated linkers pendant to the polyester backbone. The introduction of primary alcohol terminated 6-mercapto 1-hexanol and N-acetylcysteamine was demonstrated and both potentially enable further polymeric modification, via esterification or amidation of the deacytelated amine respectively, to introduce functional amino acid groups, amongst others, that possess a wide range of chemical and physical properties. This approach therefore readily enables the highly efficient and chemically simplistic biofunctionalisation of

a polyester compound to yield significant products of potential biomedical importance.

2.4 Experimental

2.4.1 Materials

Globalide was provided by Symrise. Novozyme 435 (*Candida Antarctica* Lipase B immobilised on cross-linked polyacrylate beads) was purchased from Novozymes A/S and dried over a molecular-sieve under vacuum. Butyl 3-mercapto propionate, 6-mercapto 1-hexanol, N-acetyl cysteamine, 1-thioglycerol, 2-(boc-amino) ethanthiol, 12-mercaptodecanoic acid and poly(ethylene glycol) monoethyl etherthiol were purchased from Sigma-Aldrich and used without further purification. Toluene was dried over aluminium oxide. All other reagents and solvents used were purchased from Sigma-Aldrich and used without further purification.

2.4.2 Methods

Gel Permeation Chromatography (GPC) measurements for all samples were performed using an Agilent 1200 series instrument equipped with GPC control software. All measurements were carried out using a Polymer Laboratories Gel 5 μm Mixed-C 300x7.5 mm column, at 40 °C. Tetrahydrofuran (THF) was used as the eluent at a flow rate of 1 mL/min. The molecular weights of all polymers were calculated based on polystyrene standards. ^{1}H NMR spectra was recorded using Bruker Avance 400 MHz spectrometer with CDCl$_3$ employed as the solvent in all experiments. Differential Scanning Calorimetry (DSC) measurements were performed on a TA Instruments Q200 DSC at a heating/cooling rate of 10 °C per minute.

2.4.3 Synthesis of Polyglobalide via Enzymatic Ring Opening Polymerization

Novozyme 435 (0.44 g) was dried in a Schlenk flask over a molecular-sieve at 40 °C in a vacuum oven overnight. Globalide (2.1 g) and dried toluene (2.0 g) were then added to reaction flask which was then purged with nitrogen gas before being heated in an oil bath set at 60 °C. After four hours, dichloromethane (DCM) was added to the reaction mixture to dissolve the product and inhibit enzyme activity. After the removal of Novozymes 435 by filtration, the product was isolated from the solution by precipitation in ice-cold methanol. The resultant polymer was dried overnight at room temperature under vacuum. Yield: 60%.

2.4.4 Synthesis of Thiol Functionalised Polymers

2.4.4.1 PGl-B3MP

Polyglobalide (0.1 g) and butyl 3-mercapto propionate (0.1 g) were weighed into a Schlenk flask and AIBN (10 mg) was added. The reaction flask was then purged with nitrogen gas. The reaction was started by immersing the reaction flask into an oil bath at 80 °C; solution agitation was provided by magnetic stirring. The reaction was allowed to run for 24 h. The products were dissolved in DCM and precipitated with ice-cold methanol. After decanting the solvent, traces of solvent was removed by rotary evaporation and products were dried overnight under vacuum at room temperature prior to further analysis. Yield of isolated polymer: 80%.

2.4.4.2 PGl-6MH

Table 2.2: The variation in thiol-ene coupling efficiency of MH to PGl in response to varied solvent concentrations.

	MW (g/mol)	Mw/Mn	Thiol-ene coupling (%)	Reaction Details[a]
PGl	1.6×10^4	2.5	-	-
PGl-MH1	2.08×10^4	2.2	≥95	*1 mL THF*
PGl-MH2	2.27×10^4	1.9	80-94	*Bulk*
PGl-MH3	2.49×10^4	3.7	47	*10 mL THF*

[a] Each thiol-ene coupling reaction conducted with *0.6 mmol PGl Double bonds* [b] and *4 mmol MH* in the presence of 10 mg AIBN.

[b] The concentration of PGl double bonds was estimated from the molecular weight of the polymer as determined by GPC with poly(styrene) calibration.

Polyglobalide (0.2 g) and 6-mercapto 1-hexanol (0.5 g) were weighed into a Schlenk flask in the presence of AIBN (10 mg). 1 mL of THF was added and the reaction flask was purged with nitrogen gas. The reaction commenced by immersing the reaction flask into an oil bath at 80 °C; solution agitation was provided by magnetic stirring. The reaction was allowed to run for 24 h. The products were dissolved in DCM and precipitated with ice-cold methanol. After decanting the solvent, traces of solvent was removed by rotary evaporation and products were dried overnight under vacuum at room temperature prior to further analysis. Yield of isolated polymer: 65%

2.4.4.3 PGl -nACA

Table 2.3: Experimental parameters were altered to determine a method for the optimal nACA functionalisation of PGl.

	MW (g/mol)	Mw/Mn	Thiol-ene coupling (%)	Reaction Details
PGl	1.6×10^4	2.5	-	-
PGl-nACA1	1.83×10^4	2.1	17	*0.6 mmol : 0.4mmol* [a] *Bulk Reaction* *10 mg AIBN*
PGl-nACA2	1.85×10^4	1.9	44	*0.6 mmol : 1.6 mmol* [a] *Bulk Reaction* *10 mg AIBN*
PGl-nACA3	1.28×10^4	2.4	55	*0.6 mmol: 1.6 mmol* [a] *1 mL THF* *10 mg AIBN*
PGl-nACA4	1.56×10^4	1.9	86	*0.6 mmol : 3.2 mmol* [a] *Bulk Reaction* *10 mg AIBN*
PGl-nACA5	2.19×10^4	1.7	73	*0.6 mmol : 6.6 mmol* [a] *Bulk Reaction* *10 mg AIBN*
PGl-nACA6	2.09×10^4	1.8	60	*0.6 mmol : 6.6 mmol* [a] *1 mL THF* *10 mg AIBN*
PGl-nACA7	2.35×10^4	1.8	≥ 95	*0.6 mmol : 6.6 mmol* [a] *1 mL THF* *50 mg AIBN*
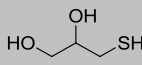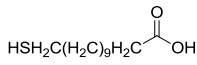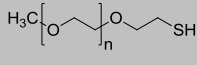
[a] The quantity of *PGl Double Bonds: nACA* used. The concentration of PGl double bonds was estimated from the molecular weight of the polymer as determined by GPC with poly(styrene) calibration.

Polyglobalide (0.2 g) and N-acetylcysteamine (0.78 g) were weighed into a Schlenk flask in the presence of AIBN (50 mg). 1 mL of THF was added and the reaction flask was purged with nitrogen gas. The reaction commenced by immersing the reaction flask into an oil bath at 80 °C; solution agitation was provided by magnetic stirring. The reaction was allowed to run for 24 h. The products were dissolved in DCM and precipitated with ice-cold methanol. After decanting the solvent, traces of solvent was

removed by rotary evaporation and products were dried overnight under vacuum at room temperature prior to further analysis. Yield of isolated polymer: 82%

2.4.4.4 Other thiol-ene functionalised polymers

Table 2.4: Experimental parameters of thiol compounds explored.

	Structure	Reaction Details	Thiol-ene coupling (%)
1-thioglycerol	HO, OH, SH	*0.6 mmol: 8.3 mmol* *PGl Double Bonds [a] :TG* *100 mg AIBN* *Bulk* *80 °C, 1 day*	18
12-mercaptodecanoic acid	HSH$_2$C(H$_2$C)$_9$H$_2$C—C(=O)OH	*1.2 mmol : 1.7 mmol* *PGl Double Bonds [a]:12MCA* *50 mg AIBN* *55 °C, 4 days*	12
Poly(ethylene glycol) monoethyl etherthiol	H$_3$C[O~~]$_n$O~~SH	*0.6 mmol: 0.25 mmol* *PGl Double Bonds[a]:PGMET(-SH)[b]* *100 mg AIBN* *2 mL THF* *55 °C, 4 day*	~2

[a] The concentration of PGl double bonds was estimated from the molecular weight of the polymer as determined by GPC with poly(styrene) calibration

[b] The concentration of -SH bonds was estimated from the molecular weight of the polymer given by the supplier.

In terms of obtaining a library of thiol-ene functionalized PGl, thiol-ene coupling of compounds in Table 2.4 was also explored. The ratio of thiol to double bond, reaction time, amount of solvent used were varied for each thiol compound to understand physical and chemical properties about each reaction. For example, the thiol-ene coupling of PGMET even after 4 days was not significant. This might be due to the low reactivity of thiol or the high molecular weight of PEG and needs to be further investigated. Other thiol compounds were poorly miscible with the polymer and produced low yields.

All of the reactions were terminated by the addition of DCM to the reaction mixture immersed in an ice bath. The products were precipitated with ice-cold methanol and the solvents gently removed by decantation. The obtained polymers were dissolved in DCM before being reprecipitated. This procedure was repeated a further two times. The final polymers were dried overnight under vacuum at room temperature prior to further analysis.

2.5 References

1.   A.-C. Albertsson and I. K. Varma, *Biomacromolecules*, 2003, **4**, 1466–1486.

2.   A. Albertsson and I. K. Varma, in *Advances in Polymer Science*, 2002, vol. 157, pp. 1–40.

3.   M. K. Kiesewetter, E. J. Shin, J. L. Hedrick, and R. M. Waymouth, *Macromolecules*, 2010, **43**, 2093–2107.

4.   O. Dechy-Cabaret, B. Martin-Vaca, and D. Bourissou, *Chem. Rev.*, 2004, **104**, 6147–6176.

5.   A. P. Dove, R. C. Pratt, B. G. G. Lohmeijer, D. A. Culkin, E. C. Hagberg, G. W. Nyce, R. M. Waymouth, and J. L. Hedrick, *Polymer*, 2006, **47**, 4018–4025.

6.   S. Kobayashi and A. Makino, *Chem. Rev.*, 2009, **109**, 5288–5353.

7.   Y. Ikada and H. Tsuji, *Macromol. Rapid Commun.*, 2000, **21**, 117–132.

8.   D. J. A. Cameron and M. P. Shaver, *Chem. Soc. Rev.*, 2011, **40**, 1761–1776.

9.   Y. Jiao and F. Cui, *Biomed. Mater.*, 2007, **2**, 24–37.

10.   S. El Habnouni, V. Darcos, and J. Coudane, *Macromol. Rapid Commun.*, 2009, **30**, 165–169.

11.   M. A. J. Veld, A. R. A. Palmans, and E. W. Meijer, *J. Polym. Sci. Part A Polym. Chem.*, 2007, **45**, 5968–5978.

12.   R. J. Pounder and A. P. Dove, *Polym. Chem.*, 2010, **1**, 260–271.

13.   C. K. Williams, *Chem. Soc. Rev.*, 2007, **36**, 1573–1580.

14. C. Jérôme and P. Lecomte, *Adv. Drug Deliv. Rev.*, 2008, **60**, 1056–1076.

15. H. C. Kolb, M. G. Finn, and K. B. Sharpless, *Angew. Chem. Int. Ed. Engl.*, 2001, **40**, 2004–2021.

16. H. Nandivada, X. Jiang, and J. Lahann, *Adv. Mater.*, 2007, **19**, 2197–2208.

17. C. R. Becer, R. Hoogenboom, and U. S. Schubert, *Angew. Chem. Int. Ed. Engl.*, 2009, **48**, 4900–4908.

18. S. Regati, Y. He, M. Thimmaiah, P. Li, S. Xiang, B. Chen, and J. C.-G. Zhao, *Chem. Commun. (Camb).*, 2013, **49**, 9836–9838.

19. A. Kamal, R. Ramu, M. A. Azhar, and G. B. R. Khanna, *Tetrahedron Lett.*, 2005, **46**, 2675–2677.

20. W. Wang, J. Wang, H. Li, and L. Liao, *Tetrahedron Lett.*, 2004, **45**, 7235–7238.

21. Y. Hayashi, J. Yamaguchi, K. Hibino, and M. Shoji, 2003, **44**, 8293–8296.

22. P. Lundberg, A. Bruin, J. W. Klijnstra, A. M. Nyström, M. Johansson, M. Malkoch, and A. Hult, *ACS Appl. Mater. Interfaces*, 2010, **2**, 903–912.

23. S. M. Trey, C. Nilsson, E. Malmström, and M. Johansson, *Prog. Org. Coatings*, 2010, **67**, 348–355.

24. J. Rieger, K. Van Butsele, P. Lecomte, C. Detrembleur, R. Jérôme, and C. Jérôme, *Chem. Commun.*, 2005, 274–276.

25. R. Riva, S. Schmeits, F. Stoffelbach, C. Jérôme, R. Jérôme, and P. Lecomte, *Chem. Commun.*, 2005, 5334–5336.

26. B. Parrish, R. B. Breitenkamp, and T. Emrick, *J. Am. Chem. Soc.*, 2005, **127**, 7404–7410.

27. A. Dondoni, *Angew. Chem. Int. Ed. Engl.*, 2008, **47**, 8995–8997.

28. O. Türünç and M. A. R. Meier, *Macromol. Rapid Commun.*, 2010, **31**, 1822–1826.

29. J. Samuelsson, M. Jonsson, T. Brinck, and M. Johansson, *J. Polym. Sci. Part A Polym. Chem.*, 2004, **42**, 6346–6352.

30. I. van der Meulen, M. de Geus, H. Antheunis, R. Deumens, E. A. J. Joosten, C. E. Koning, and A. Heise, *Biomacromolecules*, 2008, **9**, 3404–3410.

Functional Films from Unsaturated Poly(macrolactones)

Abstract

Macrolactones are naturally occurring materials, which can be polymerized to poly(macrolactones) with interesting properties. Here the prospect of functional films derived from the unsaturated macrolactone globalide was systematically investigated employing thiol-ene chemistry. The most feasible method involved the enzymatic polymerization of the monomer, followed by thiol-ene type cross-linking and surface functionalisation of the film. Evidence for the successful reactions was obtained from FTIR and FT Raman spectroscopy following the chemical modification of the polymer double bonds. Moreover, surface amine functionalisation was achieved by thio-ene grafting 2-(boc-amino) ethanthiol to the poly(globalide) surface and subsequent deprotection. The possibility of further conjugation was demonstrated by reaction of the surface amino groups with fluorescein isothiocyanate (FITC). The thus obtained films are bio-degradable providing an example of a renewable and degradable material platform with the potential of propertied enhancement for advanced application.

3.1 Introduction

Under the impression of depleting fossil reserves and associated price fluctuations, as well as environmental concerns, alternative feedstocks for the chemical industry are being sought[1,2]. Polymeric materials are no exception from this trend and polymers synthesized from renewable monomers have gained an established position among synthetic materials, both in academia and in industry[3]. Bio-based monomers, for example from biomass have been intensively investigated by many research groups and some of them are now commercial products[4–7]. While those proved to be very suitable alternatives for fossil-based building blocks in some applications, there is still the need for further developments, in particular for high performance polymers. One such class is aliphatic polyesters of which poly(ε-caprolactone) (PCL), poly(lactide) (PLA) and poly(glycolide) (PGA) are among the most investigated polymers. Biocompatibility and resorbability make aliphatic polyesters appealing for biomedical applications[8–11].

Another class of aliphatic polyesters that is moving into the focus of researchers is derived from fatty acid building blocks with 15 or more carbon units between the ester bonds. These highly hydrophobic and semicrystalline polymers have properties resembling those of polyethylene, one of the highest volume and most versatile polymers[12]. An increasing number of studies has been reported on fatty acid-based polyesters employing the direct polycondensation of fatty acid derived diols and diesters, acyclic diene metathesis (ADMET) polymerization and thiol-ene chemistry of fatty acid-based α,ω-dienes[5,13,14]. Alternatively ring-opening polymerization (ROP) of macrolactones, potentially derived from ω-hydroxy fatty acids[1,15–19,14] can be employed. Enzymatic ROP has long been the only route to high molecular weight polymer from macrolactones[20–25] but recently developed catalytic routes offer interesting alternatives[26–28].

While significant progress in the synthesis of poly(macrolactone)s (PML) has thus been made, the development of materials lags behind. Only a few literature examples focus on materials development and functionalisation, for example the groups of

Martinelle and Malmström investigated functional poly(pentadecalactone) as precursors for coatings[29–31] while we reported the processing of the same polymer into fibres[32]. To open new application fields for these promising polymers, new routes have to be explored combining processing and chemical modification when necessary[33].

We are interested in the development of advanced materials from PML, for example biomaterials. However, PMLs are highly hydrophobic and lack reactive functional groups, which puts limitations on their biomedical use[11,34]. To enhance biomaterial performance we began to investigate polymers from unsaturated macrolactones such as globalide and ambrettolide as the unsaturation provides a chemical handle for functionalisation[35]. A particularly useful technique for the functionalisation of unsaturated polymers is thiol-ene chemistry due to its high reactions rates, the wide range of accessible thiols with various functional groups, the possibility of photoinitiation and tolerance of air/oxygen and water[36–38]. Previously we communicated the successful side-chain modification of poly(globalide) (PGl) with thiols containing hydroxy groups, amines or carboxylic acid functionalities[39].

In this chapter we compare different strategies to produce stable cross-linked surface functional films from PGl employing a dithiol cross-linker and N-acetylcysteamine (nACA) mono-thiol as a model compound. The strategies vary in the sequence of cross-linking and functionalization with nACA. The optimized strategy was then employed to synthesise amino-functional cross-linked PGl films. The availability of amino groups on the surface of polyester films for conjugation was demonstrated by the attachment of fluorescein isothiocyanate (FITC).

3.2 Results and Discussion

Both post and pre-polymerization modification approaches were investigated (Figure 3.1) with the aim to identify an optimum strategy that produces a high density of amino groups on the surface of the cross-linked PGl film. Initially thermally induced

(AIBN) thiole-ene coupling of nACA to globalide was used to functionalise the monomer (route A, Figure 3.1). nACA was selected as a convenient model compound as it is easily detectable in ATR-IR.
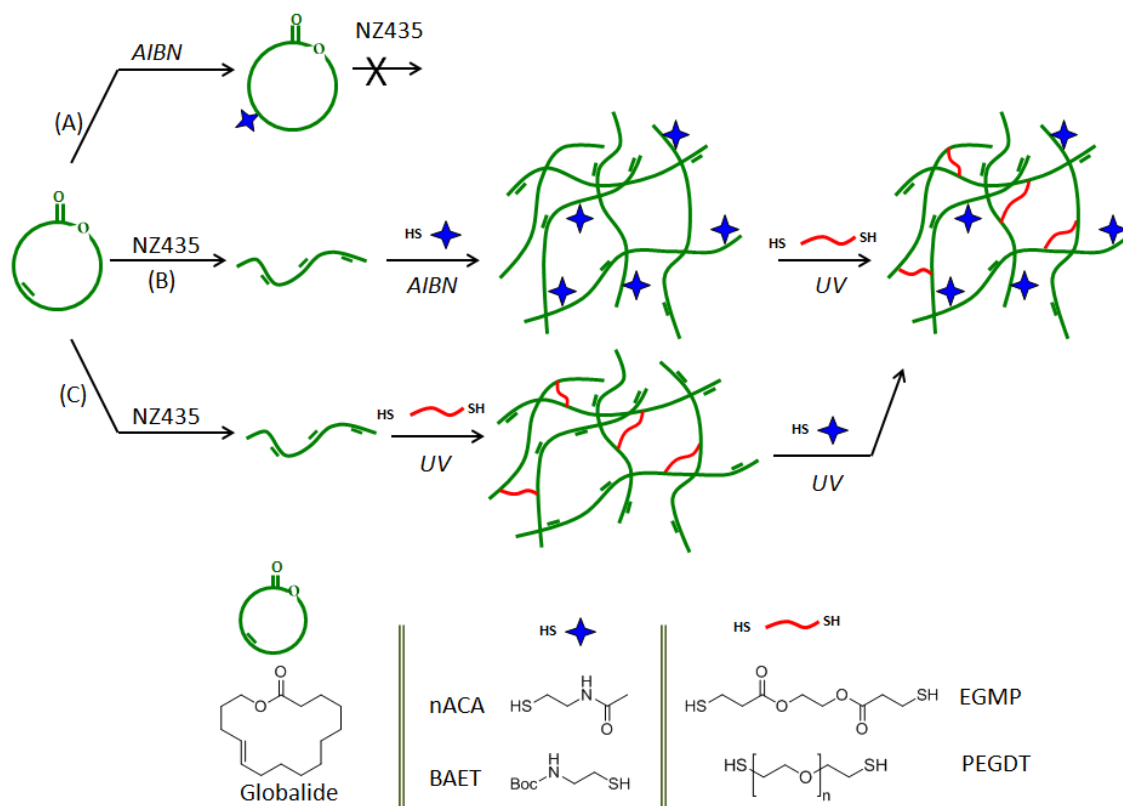
Figure 3.1: Synthetic routes to functional cross-linked films from macrolactone using thiol-ene chemistry. NZ435: Novozyme 435; AIBN: azobisisobutyronitrile; nACA: N-acetylcysteamine; BAET: 2-(Boc-amino) ethanethiol; EGMP: ethylene glycol bis(3-mercapto propionate); and PEGDT: Poly(ethylene glycol) dithiol. Globalide is a mixture of two constitutional isomers with double bonds at the 11 and 12 position. For reasons of clarity only one isomer is shown.

The ^{1}H NMR obtained for nACA functionalised Gl reveals characteristic peaks corresponding to Gl and signals from the nACA, which suggests the success of the reaction. Moreover, a reduction of the Gl double bond peak in the spectrum of the final product was observed upon thiol-ene coupling of nACA to Gl. The thiol-ene

coupling yield was quantified by comparing the integration of these peaks at around 5.4 ppm (a`) with the peaks representative of the methylene group (b) (Figure 3.2) indicating the coupling yield of 55 %. The success of nACA functionalization was also confirmed by the presence of amide bonds at around 1650 and 1550 cm^{-1} in the FTIR spectrum (Figure 3.3).
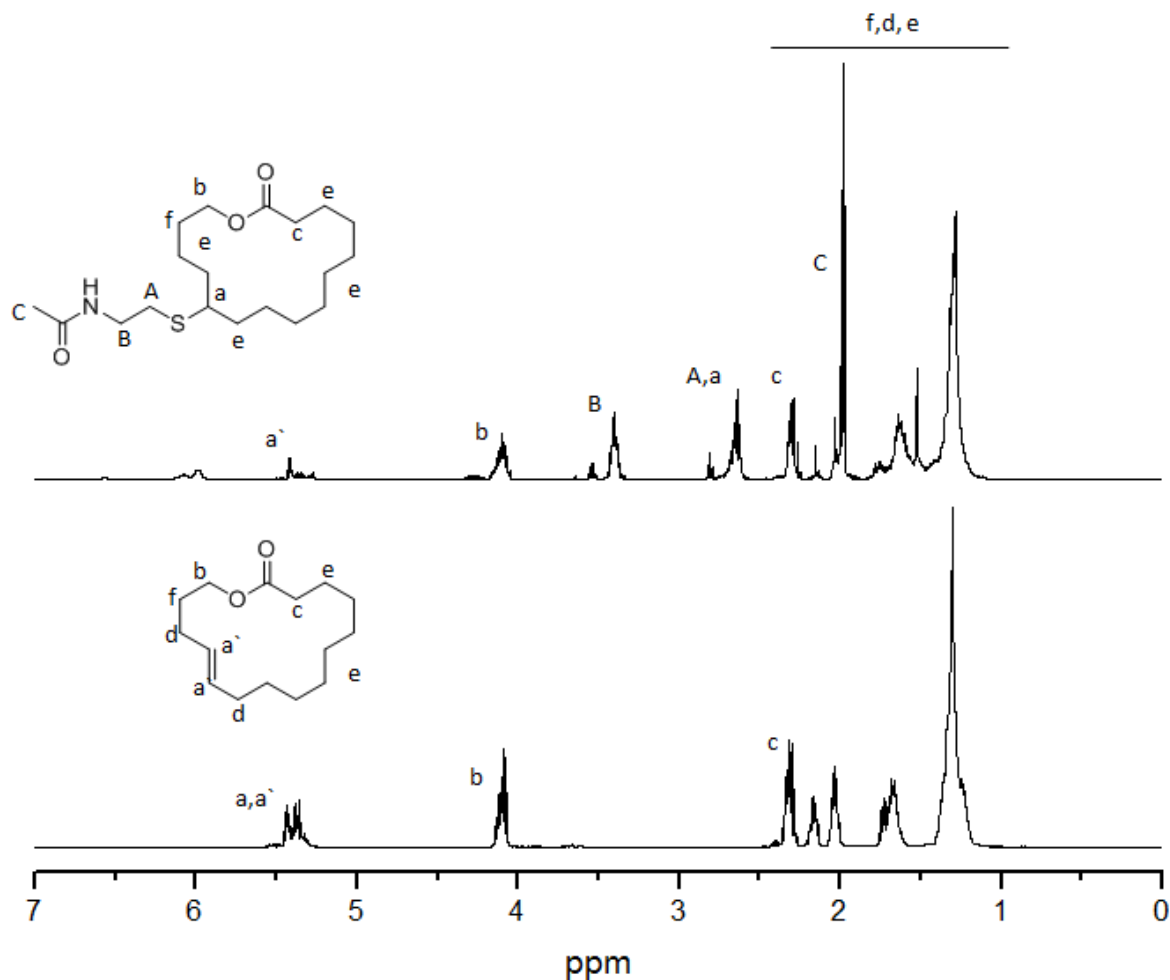
Figure 3.2: ^{1}H NMR spectra of Globalide (Gl) and the thiol-ene coupling product from nACA and Gl (unpurified product)(Route A). Spectra recorded in CDCl$_3$ using a 400 MHz spectrometer.

However, the subsequent polymerisation of the unpurified monomer mixture using immobilized *Candida Antarctica* Lipase B (Novozyme 435, NZ435) produced only low molecular weight polymers in low yields (30 %). While the exact reason was not further investigated, it can be speculated that this is due to the inhibition effect of remaining thiol compound in the reaction mixture[40]
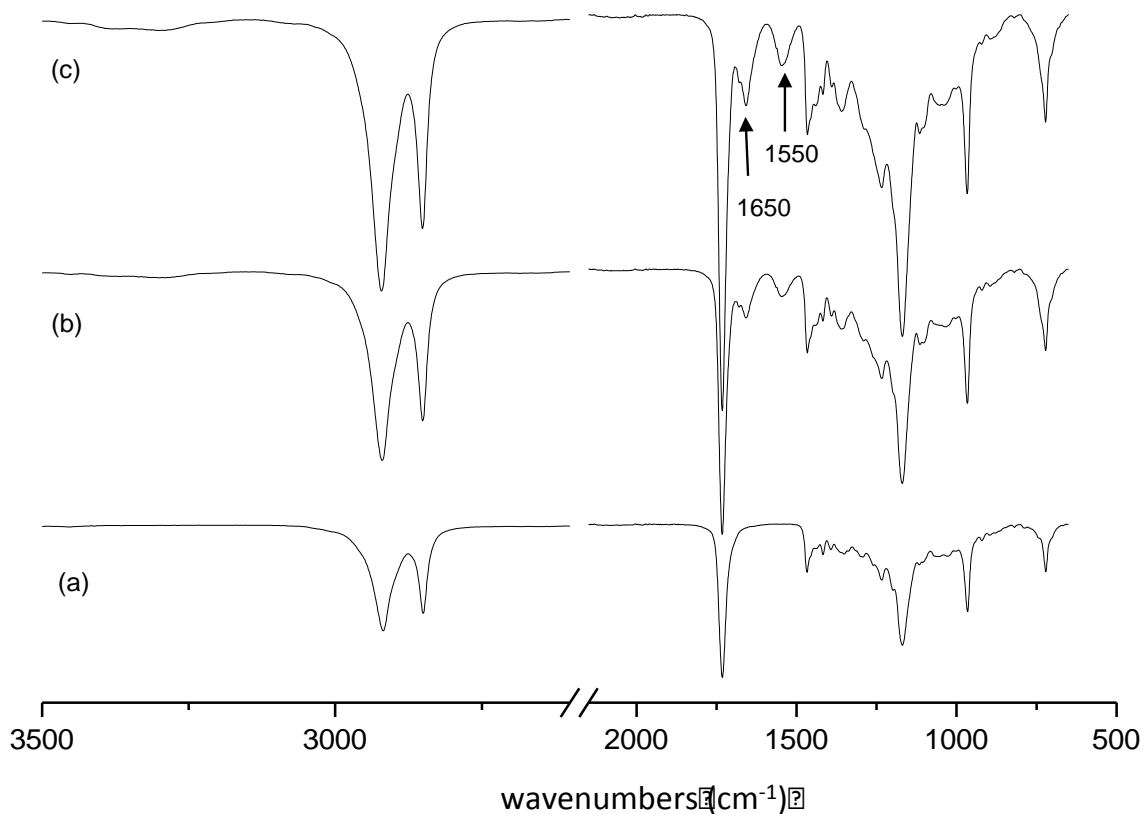
Figure 3.3: ATR-IR spectra of (a) a non-functionalized cross-linked PGl film, (b) nACA functionalized globalide (Route A) and (c) nACA functionalized cross-linked poly(globalide) film (Route B).

Alternatively, globalide was first polymerized by NZ435 (route B, Figure 3.1) using residual traces of water present in the monomer and/or the NZ435 as the nucleophile. Typically molecular weights in the range of 16,000 g/mol (D = 2.5) were obtained. Varying the ratio of SH to double bonds in the thermal AIBN induced polymer analogous thiol-ene coupling with nACA, PGl with 50 % of substitution were

targeted. After precipitation the success of nACA functionalization was confirmed by the presence of amide bonds at around 1650 and 1550 cm^{-1} in the FTIR spectrum (Figure 3.3). Moreover, the percentage of polymer functionalisation was calculated to be 40 % by comparison of the ^{1}H-NMR integrated peak areas corresponding to the double bond protons at 5.4 ppm with those representative of the methylene groups adjacent to the hydroxyl terminal group at around 4 ppm[39]. A good agreement with the targeted values was found. Recently, Claudino et al. have reported the efficient UV-curing of unsaturated PML using thiol cross-linkers[41]. Cross-linking of the 40 % nACA functional PGl was attempted by UV-induced thio-ene reaction with ethylene glycol bis(3-mercapto propionate) (EGMP), an ester containing degradation susceptible cross-linker. Typically, the desired amount of polymer and di-thiol cross-linker was dissolved in THF together with photo initiator at a polymer concentration of 300 mg/mL. The formulations were transferred into Teflon molds and exposed to UV-light using a commercial UV curing equipment. While cross-linking was achieved all obtained films were tacky and of low mechanical integrity (Figure 3.4B) irrespective of the cross-linker to polymer ratio, rendering this route unfeasible. The results suggest an incomplete network formation, which might be due to a too large distance between the double bonds preventing optimal formation of a three-dimensional network.
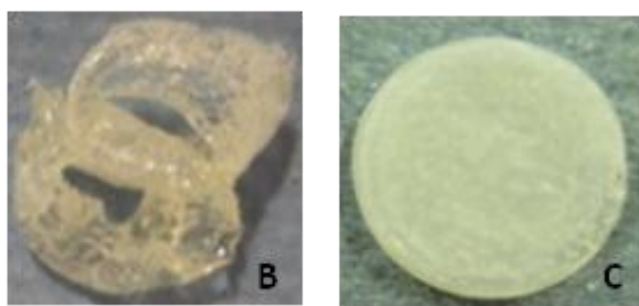
Figure 3.4: Images of films prepared by methods B and C (Figure 3.1).

We hypothesized that this could be overcome by carrying out the geometrically more demanding cross-linking reaction first followed by the nACA post-functionalization of the cross-linked film (route C, Figure 3.1). PGl films were first synthesized by UV induced thiol-ene reaction with EGMP. Films obtained by this method were non-tacky. FT-Raman spectra of PGl displayed a characteristic peak around 1660 cm^{-1} arising from alkene functionality in the polymer backbone. When plotting the peak area ratio of an unaffected peak (1733 cm^{-1}) to this reporter peak against the theoretical double bond conversion due to increasing amount of cross-linker used, a near-linear reduction is observed (Figure 3.5). Interestingly even full double bond conversion can be reached by this method. A second reporter peak can be assigned at 1000 cm^{-1}, characteristic of the C-S bond formed in this process. The peak area ratio of this band to the unaffected aliphatic chain band at 1300 cm^{-1} linearly increases with increasing cross-linker ratio (Figure 3.5). While it has to be noted that the error in determining the peak areas might be in the range of 10 % due to overlapping peaks, plots derived from both, double bond conversion as well as C-S bond formation, provide strong evidence for the successful cross-linking reaction in agreement with expectation.
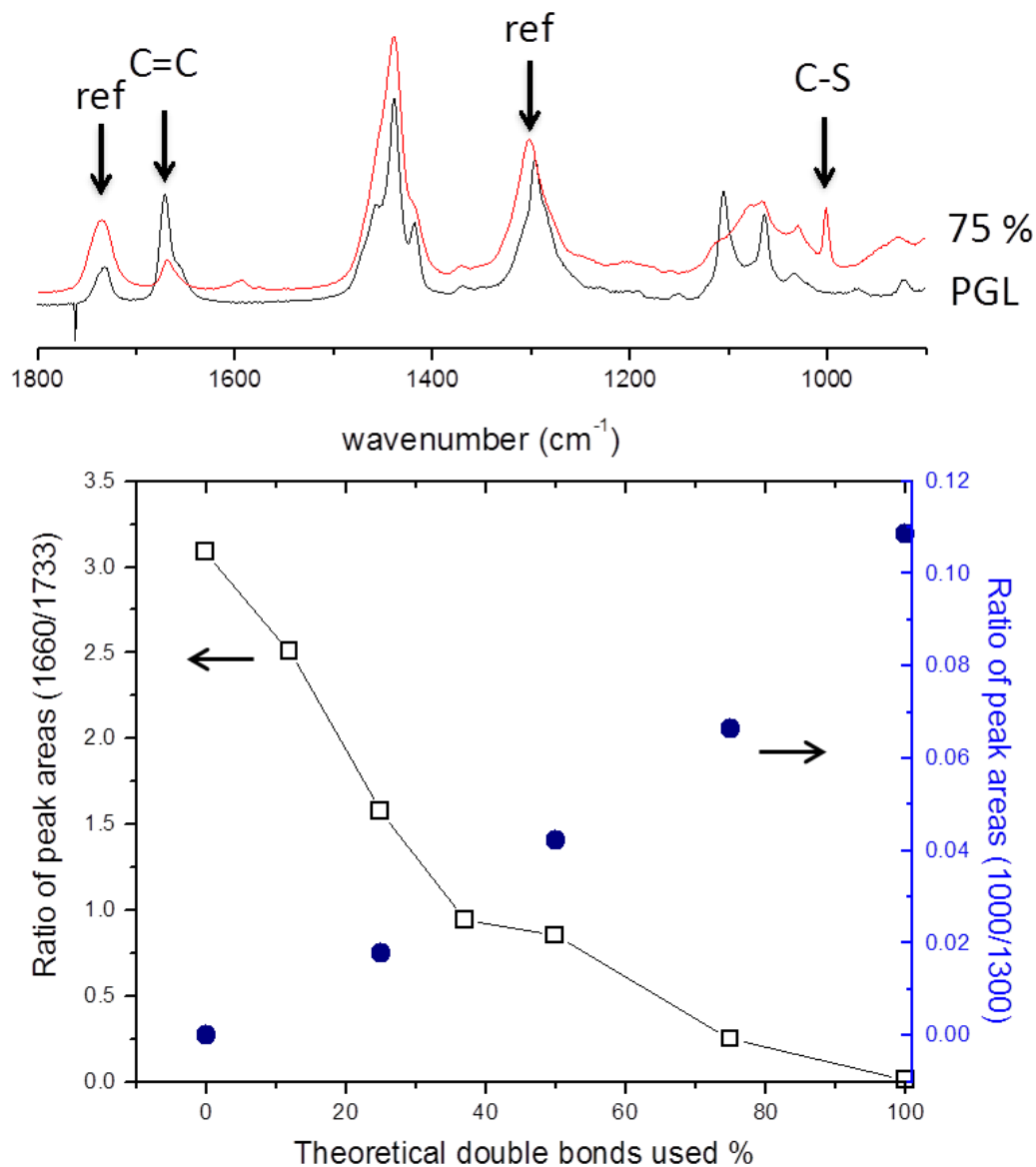
Figure 3.5: Top: FT-Raman spectra of a PGl film and an example of film cross-linked with EGMP (75 % theoretical double bond conversion). Labeled peaks were used to calculate peak area ratios (ref = unaffected reference peak). Bottom: Plot of normalised C-S and double bond peak areas against the theoretical double bond conversion calculated from the mole percent of cross-linker used with respect to polymer double bonds.

In a similar study, PGl films were prepared by UV induced thiol-ene crosslinking with poly(ethylene glycol) dithiol (PEGDT, 1000 g/mol). Characteristic peak of the C-S bond formed at 1000 cm^{-1} and the peak of alkene functionality around 1660 cm^{-1} were followed by FT-Raman spectroscopy as discussed above (Figure 3.6). Increasing cross-linker amount showed a similar reduction of the peak area arising from the alkene functionality. However, it was more difficult to reliably follow the C-S peak for the samples with low amount of cross-linker due to the poor spectral resolution. This might be due to originating from the high molecular weight of PEGDT and low quantities used.
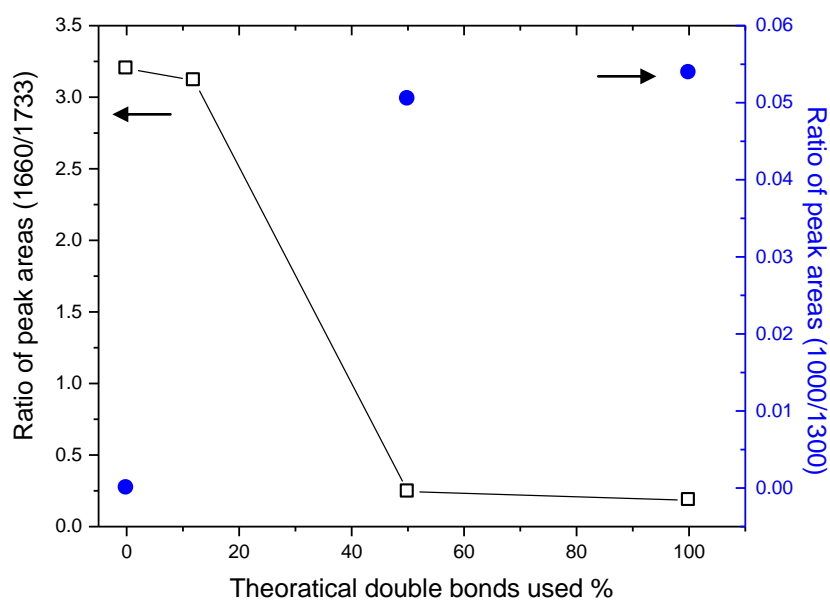
Figure 3.6: Plot of normalised C-S and double bond peak areas against the theoretical double bond conversion calculated from the mole percent of cross-linker (PEG dithiol) used with respect to polymer double bonds.

PGl is a semi-crystalline polymer with a meting point at 48°C (DSC). 100% cross-linked films were fully amorphous and transparent. Films with lower double bond conversion were observed to have melting points below that of the uncrosslinked polymer (Figure 3.7), a phenomenon that has also be observed with cross-linked polyethylene and other polymers[42,43].
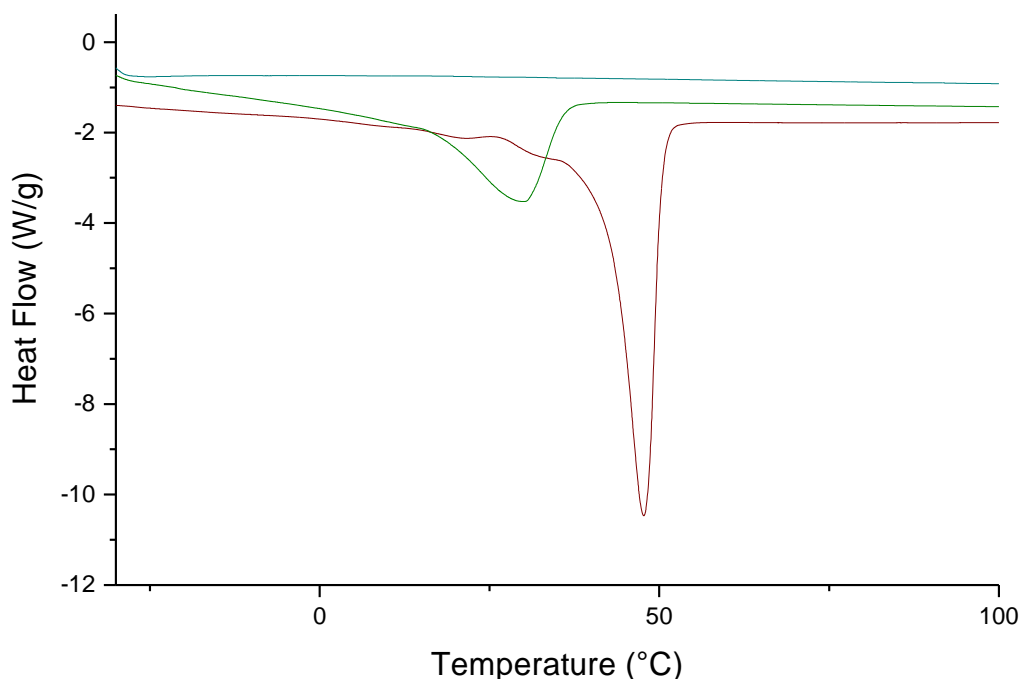
Figure 3.7: DSC thermograms (second heating cycle, heating rate of 10°C/min) of PGl (red) and ethyleneglycol dithiol cross-linked films with theoretically 25% (green) and 100% (blue) double bond conversion.

As biodegradation is a major concern in various biomaterials applications, the PGl cross-linked films equivalent of 25 % and 50 % double bond conversion (theoretically) were subjected to enzymatic degradation. PGl films cross-linked with EGMP were prepared by the method C as described above. A weight loss of 20.8% for PGl films with 25% EGMP was monitored over a 50-day period in the presence of *Pseudonomas Cepacia* Lipase (Lipase PS) while no significant weight loss was detected in absence of the ester-hydrolyzing enzyme over the same period (Figure 3.8). Films cross-linked with 50 % EGMP showed slower degradation with a weight loss of 8% over the same time period. A slower degradation at higher cross-linking density is expected due to the higher network stiffness. Moreover, degradation rate of 50 % EGMP cross-linked films was found to be almost negligible as expected even after 50 days for control experiments (in absence of ester hydrolyzing enzyme) (Figure 3.8).
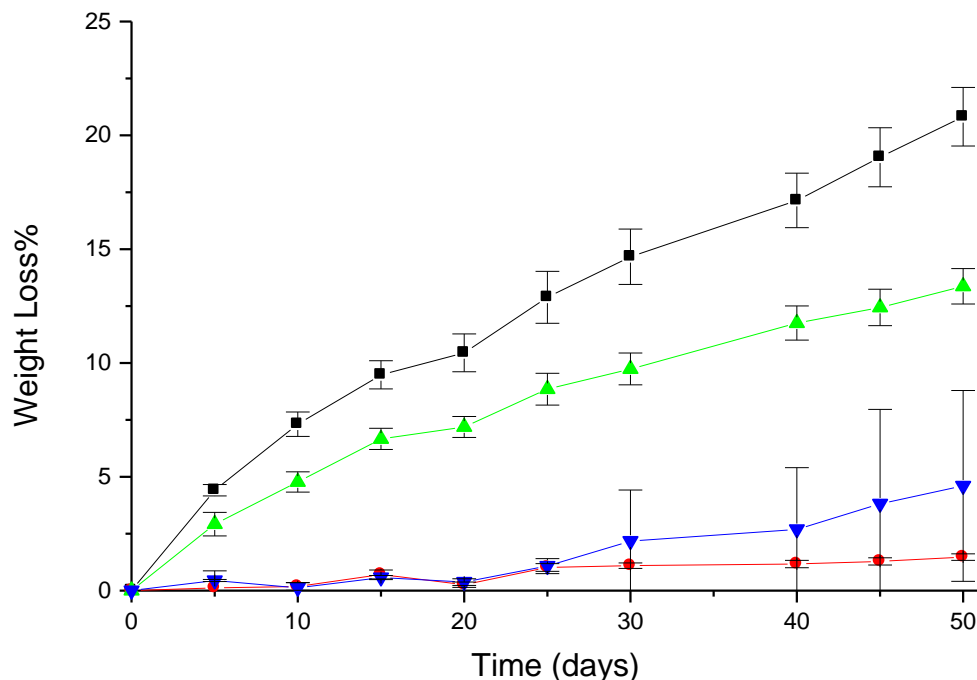
Figure 3.8: Weight loss of cross-linked PGl films with EGMP (25% theoretical double bond conversion) with (■) and without (●) and PEGDT (25% theoretical double bond conversion) with (▲) and without (▼) *Pseudonomas Cepacia* Lipase in PBS buffer at 37°C. (Shaker speed: 60 strokes/minute) Experiments carried out in triplicate.

In a similar study, non-ester bearing cross-linker poly(ethylene glycol) dithiol (PEGDT; Mn: 1000 g/mol), was used to investigate its effect on biodegradation properties of the films. It was hypothesized that this cross-linker introduces a higher hydrophilicty and a more "loose" network due to its higher molecular weight. While targeting 25% and 50% the extent of the cross-linking reaction was found to be lower than expected by FT-Raman studies. This observed deviation from the quantitative photo-induced thiol-ene cross-linking of the films is thought to be related to the reactivity of the thiol group and its lower miscibility with the polyglobalide solution.

Surprisingly it was found that the degradation rate of 25 % PEGDT cross-linked films (note that real cross-linking was lower than theoretical value) was lower in comparison to 25% EGMP cross-linked films (Figure 3.8). It was expected that the hydrophilic character of PEG might assist the diffusion of enzyme solution and enhance the degradation of the material. On the other hand, the rate of degradation of long chain PEG

cross-linked films in absence of enzyme was slightly higher than ester containing short linker suggesting the removal of unbound material by diffusion.
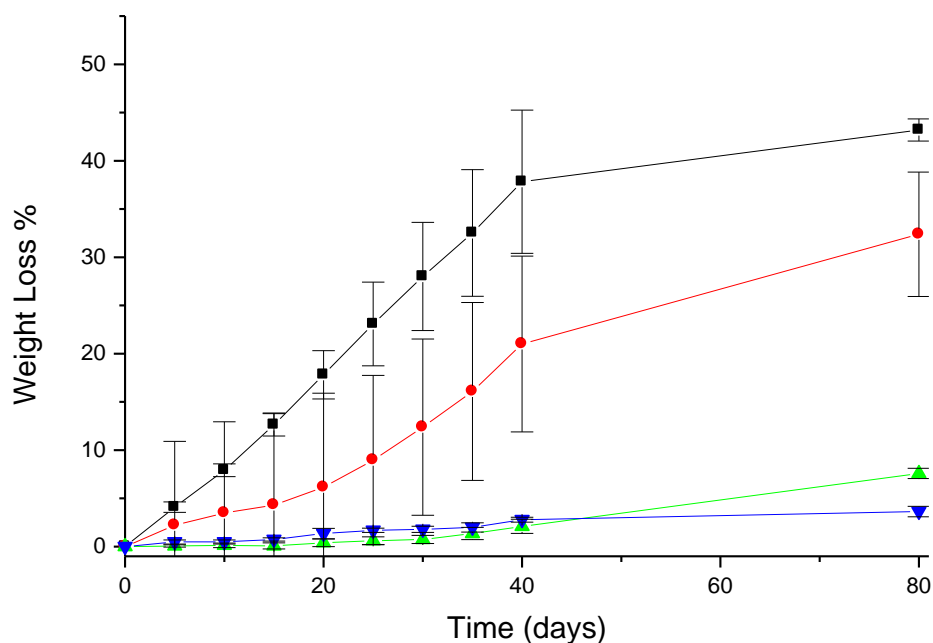
Figure 3.9: Weight loss of cross-linked PGl films with PEGDT (25% theoretical double bond conversion) with (■) and without (●) *Pseudonomas Cepacia* Lipase in PBS, and with PEGDT (50% theoretical double bond conversion) with (▼) and without (▲) *Pseudonomas Cepacia* Lipase in PBS buffer at 37°C. (Shaker speed: 120 strokes/minute) Experiments carried out in triplicate.

In order to investigate if the degradation rate could be increased for the PEGDT samples by better agitation the shaker speed was increased. As seen from Figure 3.9, this indeed increased the general degradation rate as compared to the results shown in Figure 3.8**.** As expected the 50% (theoretical) samples showed slower degradation rate comparing to 25 % samples. Finally, the enzyme concentration (1 mg/4 mL) was increased to observe the effect on film degradation obtained by EGMP and PEGDT cross-linkers but no significant differences in the rates were observed.
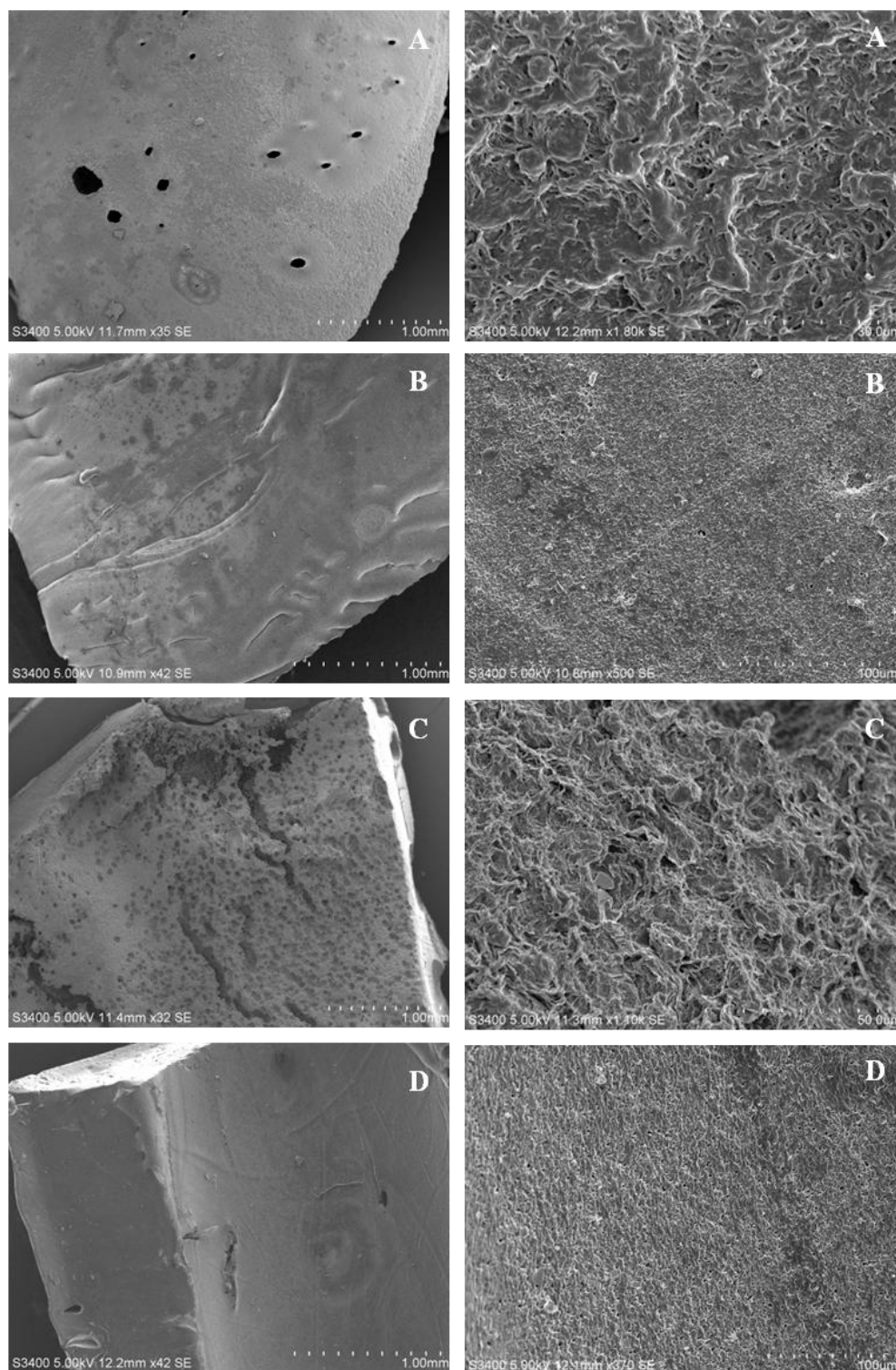
Figure 3.10: SEM images of poly(globalide) films cross-linked with EGMP (theoretical double bond conversion) 25 % (A) and 50% (B) and PEGDT (theoretical double bond conversion) 25% (C) and 50 % (D) after 80 days degradation. (Shaker speed: 120 strokes/minute)

SEM was used to visualize the surface characteristics of degraded films (Figure 3.10, Figure 3.11, Figure 3.12). All of the degraded films showed typical surface erosion. However, it is known that the degradation rate of aliphatic polyesters is affected by diffusion phenomena as well as configuration of polymer chains and crystalline domains[44]. For a full understanding of degradation mechanism and the degradation characteristics, the degradation needs further investigation while varying parameters concerning degradation conditions and, type of enzyme.
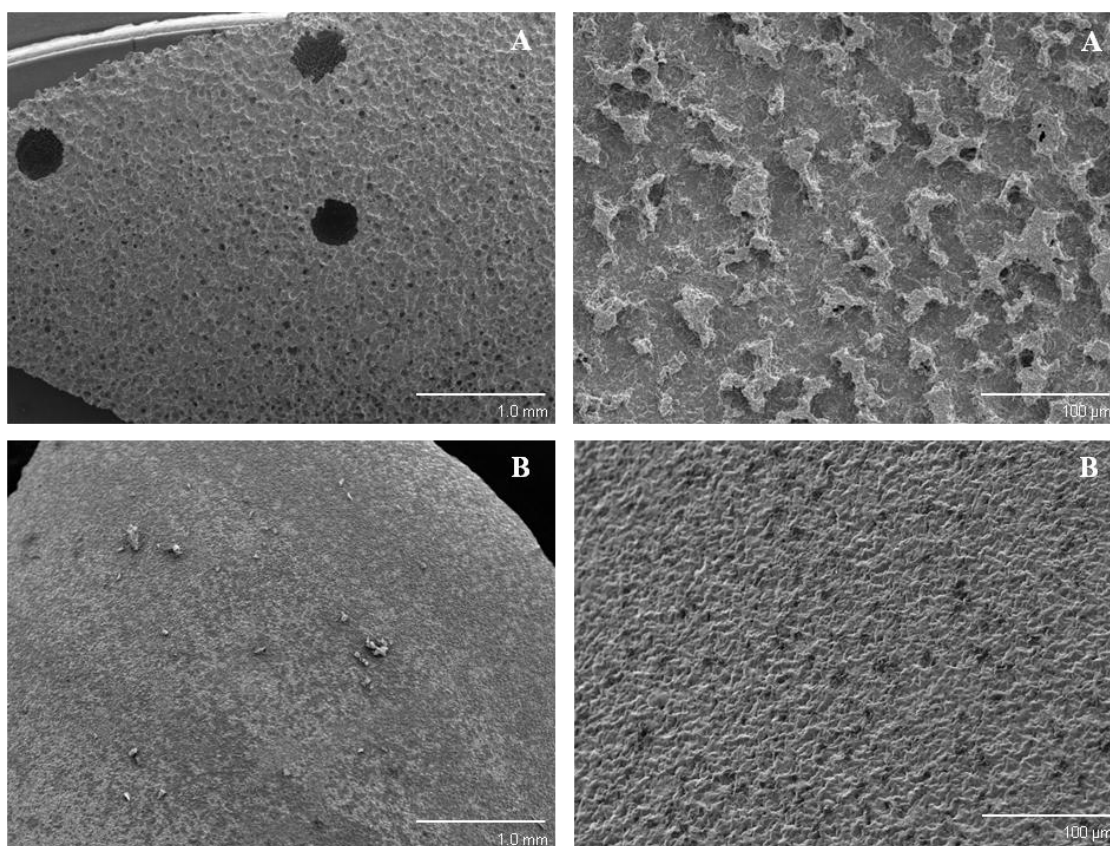
Figure 3.11: SEM images of poly(globalide) films cross-linked with EGMP 25 % (theoretical double bond conversion) (A) and 50 % (theoretical double bond conversion) (B) after 8 weeks of degradation. (Shaker speed: 120 strokes/minute).
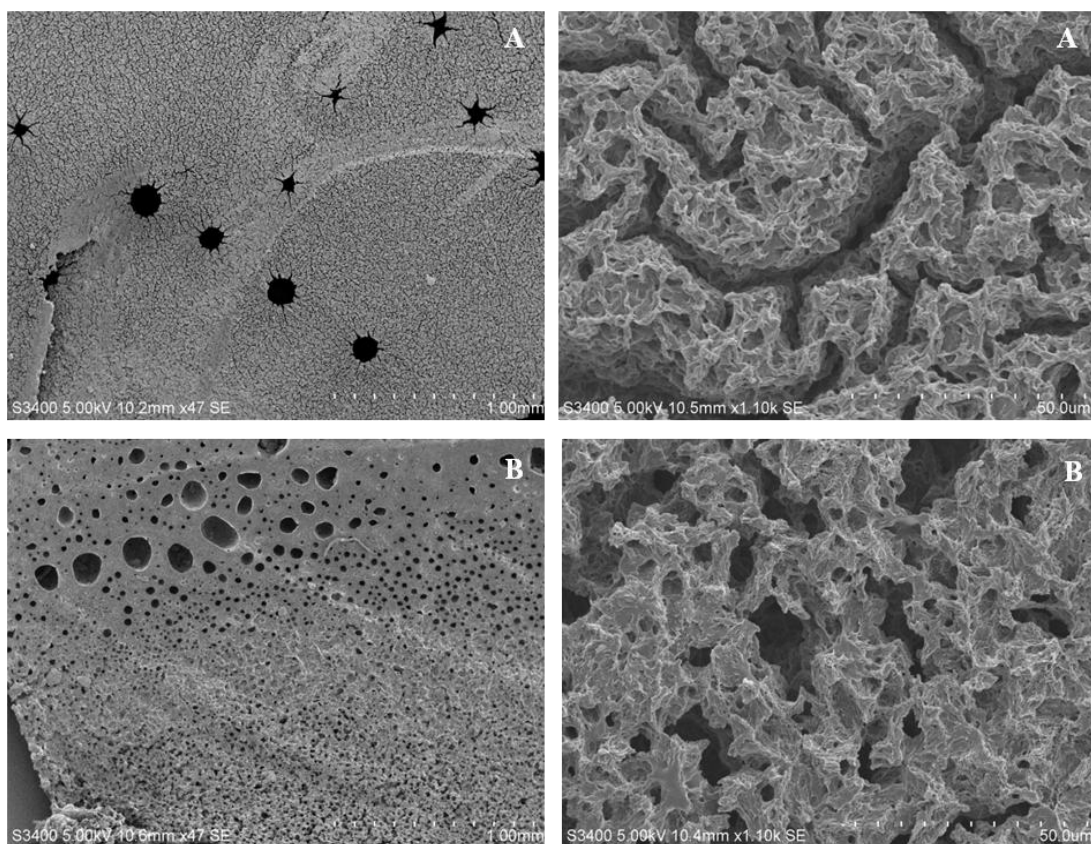
Figure 3.12: SEM images of poly(globalide) films cross-linked with PEGDT 25 % (theoretical double bond conversion) (A) and 50 % (theoretical double bond conversion) (B) after 8 weeks of degradation. (Shaker speed: 120 strokes/minute)

Subsequent surface functionalization of the EGMP cross-linked films by UV induced thiol-ene reactions was investigated. The reaction was carried out by swelling the PGl film with THF containing different amounts of nACA and exposing it to UV light. The cross-linked sample with 25 % double bond conversion was selected for these experiments having theoretically 75 % of unsaturations available.

As only double bonds present on the film surface are accessible for the reaction with nACA the actual double bond conversion is expected to be relatively low in this procedure, which makes its quantification challanging. Nevertheless, after intensive washing, a detectable yet small decrease of alkene peak intensity (1660 cm^{-1}) was observed in FT-Raman spectroscopy. Moreover, it was observed that an excess of thiol in the reaction did not result in a higher double bond conversion as expected for

a surface reaction after the maximum number of double bonds have reacted. Further confirmation of the presence of nACA on the polyester film was obtained from Attenuated Total Reflectance (ATR) FTIR spectroscopy. Typical nACA amide-I and amide-II peaks were observed at 1650 and 1550 cm^{-1}, respectively (Figure 3.13).
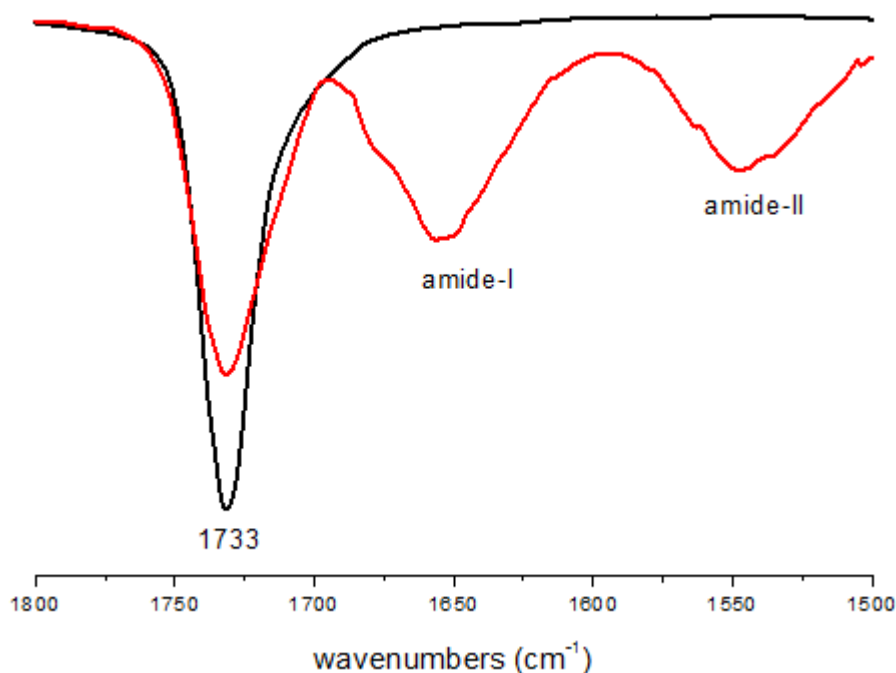
Figure 3.13: ATR-IR spectra of cross-linked (25% theoretical double bond conversion) PGl (top) and nACA functionalized cross-linked PGl film.

The discussed results clearly show that method C (Figure 3.1) is the most feasible route to cross-linked, surface modified PML films. In order to further investigate the introduction of surface functionalities, nACA was replaced by 2-(Boc-amino) ethanthiol (BAET) as the mono-thiol. After deprotection the latter would render the surface amino-functional and suitable for further (bio)conjugation. 2-(Boc-amino) ethanthiol was attached to the surface of a cross-linked PGl following the same procedure as used for the nACA. Deprotection of Boc protected amine groups was achieved by simply stirring the film in trifluoroacetic acid (TFA). ATR FTIR spectroscopy confirmed the quantitative deprotection by the disappearance of typical absorbance bands associated with the Boc group at around 1513 and 1457 cm^{-1}. First evidence for the presence of amino groups was obtained from a positive ninhydrine

test resulting in the typical purple color upon reaction between amine and ninhydrine.

The availability of the surface amino groups for further conjugation was verified by the reaction with fluorescein isothiocyanate isomer (FITC), a widely used fluorophore for amine conjugation [45]. FITC conjugated polyester films appear green and exhibit an absorption maximum at 495 nm and emission maximum at 525 nm. After washing no evidence of free FITC on the PGl films could be found in the ATR FTIR spectrum (absence of isothiocyanate group around 2100 cm^{-1}) signifying that the green fluorescence must be due to covalently attached FITC. Control experiments also confirmed the absence of significant fluorescence without surface amino groups due to the physical adsorption.
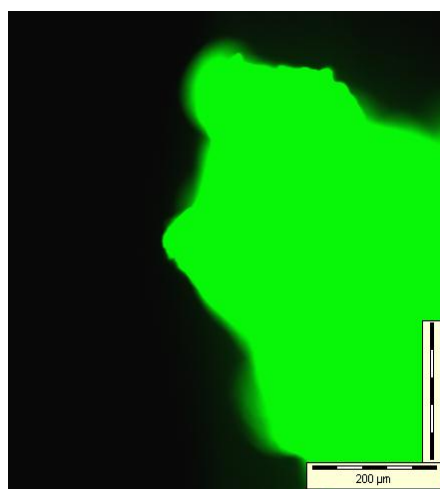
Figure 3.14: Fluorescence optical microscopy images with 66 ms exposure time. FITC coupled amine functional cross-linked PGl. Image was taken at 10x magnification.

3.3 Conclusions

Three approaches were investigated to synthesise functional films from a bio-inspired unsaturated macrolactone. The most feasible method involved the enzymatic polymerization of the monomer, followed by thiol-ene type cross-linking and surface functionalisation of the film. The thus obtained films are bio-degradable and allow

further surface (bio)conjugation as highlighted by model reactions. The presented work thus provides an example of a renewable and degradable material platform with the potential of property enhancement. This opens opportunities for integration into advanced systems for example as functional biomaterials.

3.4 Materials and Methods

3.4.1 Materials

Globalide was provided by Symrise. Novozyme 435 (*Candida Antarctica* Lipase B immobilised on cross-linked polyacrylate beads) was purchased from Novozymes A/S. It was stored in a Schlenk flask over a molecular sieve at 40 °C in a vacuum oven overnight. N-Acetylcysteamine (nACA), 2-(Boc-amino) ethanethiol (BAET), trifluoroacetic acid (TFA), poly (ethylene glycol) dithiol (Mn=1000 g/mol), photoinitiator mixture diphenyl(2,4,6-trimethylbenzoyl) phosphine oxide/2-hydroxy-2-methylpropiophenone were purchased from Sigma-Aldrich and used without further purification. Ethylene glycol bis(3-mercapto propionate) was purchased from Wako. Toluene was dried over aluminium oxide. All other reagents and solvents used were purchased from Sigma-Aldrich and used without further purification.

3.4.2 Methods

Gel Permeation Chromatography (GPC) measurements were performed on an Agilent 1200 series instrument equipped with GPC control software. All measurements were carried out using a Polymer Laboratories Gel 5 μm Mixed-C 300x7.5 mm column at 40 °C. Tetrahydrofuran (THF) was used as the eluent at a flow rate of 1 mL/min. Molecular weights were calculated based on polystyrene standards. ^{1}H NMR spectra were recorded using Bruker Avance 400 MHz spectrometer in CDCl$_3$. Attenuated Total Reflection Fourier Transform Infra Red (ATR-FTIR) spectroscopy was done in the solid state on a Perkin-Elmer Spectrum 100. Fourier transform Raman spectroscopy (FT-Raman) spectra were acquired using a Perkin Elmer 88 Raman station at 2 cm^{-1} resolution (20 scans). A 785 nm laser line 89 was used. An inverted fluorescence microscope (IX81, Olympus

Co., Japan) equipped with an EMCCD camera (DV887-BI, Andor Technology, U.K.) and an MT20 fluorescence illumination unit fitted with a 150 W xenon lamp was used in combination with a FITC filter set to image the green fluorescence of the FITC attached cross-linked poly(macrolactone) films. Differential Scanning Calorimetry (DSC) measurements were performed on a TA Instruments Q200 DSC at a heating rate of 10 °C per minute under nitrogen atmosphere from -50°C to 150°C. Samples were UV cured using a commercial Fusion UV system, LCGE Bench top conveyor with F300S Fusion lamp (120 W/cm) equipped with a 13 mm H-bulb. The samples were exposed to the UV lamp 3 min. at 5 m/min. belt speed. Scanning Electron Microscopy (SEM) was performed on a Hitachi S3400 with samples previously coated with gold using vapor deposition in the case of SEM analysis.

3.4.3 Synthesis of polyglobalide

Globalide (2.1 g), NZ435 (0.44 g) and dried toluene (2.0 g) were added to a reaction flask which was then purged with nitrogen before being heated in an oil bath set at 60 °C. After four hours, dichloromethane (DCM) was added to the reaction mixture to dissolve the product and inhibit enzyme activity. After the removal of Novozymes 435 by filtration, the product was isolated from the solution by precipitation in ice-cold methanol and filtration. The resultant polymer was dried overnight at room temperature under vacuum. Typical yields were around 60% and M_n 16000 g/mol (D=2.5).

3.4.4 Preparation of poly(globalide) films

3.4.4.1 Functionalization of monomer (Method A)

Different ratios of globalide and the nACA were mixed according to the desired percentage of functionality. In a typical example aiming at 50 % functionalisation, 5 g globalide (0.021 mol) and 1.41 g nACA (0.011 mol) were placed into a Schlenk flask containing AIBN (1.52 mmol, 250 mg) and immersed into an oil bath at 80 °C under nitrogen atmosphere for one day. ^{1}H-NMR analysis revealed 30 %

functionalisation. The unpurified monomer mixture was polymerised as described for poly(globalide)(see Figure 3.2).

Globalide: ^{1}H NMR: δ (ppm) 5.58-5.27 (m, CH=CH), 4.17-4.02 (m, $CH_2O(C=O)$), 2.36-2.25 (m, $CH_2(C=O)O$), 2.23-1.96, 1.79-1.57, 1.43-1.15 (m, CH_2)

nACA functionalised GI: ^{1}H NMR: δ (ppm) 5.49-5.20 (m, CH=CH), 4.36-4.02 (m, $CH_2O(C=O)$), 3.47-3.31 (m, $CH_2NH)C=O$), 2.76-2.56 (m, CH_2S and $CHS(CH_2)2$), 2.35-2.23 (m, $CH_2(C=O)O$), 2.20-2.09 (m, $CH_2)C=O$), 2.12-1.92, 1.69-1.54, 1.46-1.14 (m, CH_2)

Table 3.1: Reaction details for thiol-ene coupling of Gl with selected thiol compounds.

	Gl (g)	Thiol (g)	AIBN (mg)	Thiol-ene coupling (%)[a]
Gl-B3MP-1	1	0.7	50	24
Gl-B3MP-2	5	3.4	250	30
Gl-nACA-2	5	2.5	250	55
Gl-nACA-3	5	1.4	250	30
Gl-TG-1	2	0.9	100	18
Gl-MH-1	5	2.8	250	56

[a] Thiol-ene coupling calculated by ^{1}H NMR

3.4.4.2 Post-polymerization functionalization (Method B)

Thiol-ene reactions on poly(globalide) with nACA were carried out following our reported earlier protocol.[39] In a typical example, 0.4 g (0.026 mmol) poly(globalide) and 0.4 mg nACA (3.35 mmol) were placed into a Schlenk flask containing AIBN (0.21 mmol) and immersed into an oil bath at 80 °C under nitrogen atmosphere for one day. The products were precipitated into ice-cold methanol. ^{1}H-NMR analysis revealed 40 % functionalisation.

For the thiol-ene cross-linking, nACA functionalised poly(globalide) (300 mg) was dissolved in 1.0 mL THF and mixed with ethylene glycol bis(3-mercapto propionate). To achieve various cross-link ratios, the required thiol to ene ratios were calculated. For example for an estimated double bond conversion of 25 %, 0.060 mL (0.3 mmol) ethylene glycol bis(3-mercapto propionate) was added. The 0.060 mL (0.3 mmol) of UV initiator mixture (diphenyl(2,4,6-trimethylbenzoyl) phosphine oxide/2-Hydroxy-2-methylpropiophenone dissolved in dichloromethane at a ratio of 1:1 (w/w)) was added to each sample. Within 3 minutes the formulation was casted in disc-shaped teflon molds to form 15 mm diameter films (1 mm deep) and passed under the UV lamp. Afterwards, samples were washed with THF to remove the unreacted cross-linker and initiator and dried under ambient conditions.

3.4.4.3   Functionalization concurrently with cross-linking (Method C)

Poly(globalide) was cross-linked according to the above procedure followed by UV induced thiol-ene reaction of nACA onto the surface in the presence of equal molar of photo initiator mixture in 0.5 mL THF. Varying degrees of substitution were targeted including 12, 25, 37, 50, 75 and 100%. Surface thiol-ene reaction of nACA was performed onto films with 25% degree of substitution. Subsequently, samples were washed with THF to remove the unreacted thiol compounds and initiator and dried under ambient temperature.

3.4.5 Amine functional films

Films were prepared using method C followed by thiol-ene reaction on the surface with 2-(Boc-amino) ethanethiol. Equal moles of photo initiator and 2-(Boc-amino) ethanethiol (0.35 mmol) were mixed with 0.5 mL THF and then transferred onto film surface followed by UV curing. The deprotection of the Boc group was conducted by immersing samples into TFA [46] for one hour followed by neutralizing with excess of KOH solution and washing with DI water.

3.4.6 FITC attachment to amine functional film

25 mg amine functionalised films were immersed into 1 mL DMF containing 5 mL phosphate buffer (pH 9.2) and 10 mg fluorescein isothiocyanate (FITC) over night at room temperature. Samples were washed with fresh DMF several times to remove unreacted FITC.

3.4.7 Degradation of polymers in a pH buffer

All polymers were molded into Teflon templates to form 15 mm diameter films (1mm deep) and UV induced cross-linked with EGMP or PEGDT.

Each polymer film was added to 10 mL of a 0.1 M PBS buffer (pH=7.4) containing 1 mg Pseudonomas cepacia Lipase (Lipase PS). The samples were placed in a shaking water bath at 37°C with 60 strokes per minute or 120 strokes per minute, respectively. Every week films were removed and dried overnight to determine the weight loss. Afterwards buffer was replaced and the new enzyme was added. In terms of exploring the effect of enzyme concentration, 4 mL of a 0.1 M PBS buffer (pH=7.4) containing 1 mg of Pseudonomas cepacia Lipase (Lipase PS) was used with the different batch of samples. The samples were placed in a shaking water bath at 37°C with 60 strokes per minute. Subsequently the same process was applied as explained above. Experiments carried out in triplicate for each batch of samples.

3.5 References

1. M. R. L. Furst, R. Le Goff, D. Quinzler, S. Mecking, C. H. Botting, and D. J. Cole-Hamilton, *Green Chem.*, 2012, **14**, 472–477.

2. R. Mülhaupt, *Macromol. Chem. Phys.*, 2013, **214**, 159–174.

3. U. Biermann, U. Bornscheuer, M. A. R. Meier, J. O. Metzger, and H. J. Schäfer, *Angew. Chem. Int. Ed. Engl.*, 2011, **50**, 3854–3871.

4.   M. Eriksson, K. Hult, E. Malmström, M. Johansson, S. M. Trey, and M. Martinelle, *Polym. Chem.*, 2011, **2**, 714–719.

5.   O. Türünç and M. A. R. Meier, *Macromol. Rapid Commun.*, 2010, **31**, 1822–1826.

6.   M. Firdaus and M. A. R. Meier, *Green Chem.*, 2013, **15**, 370–380.

7.   A. Vishwa Prasad and Z. Yinghuai, *J. Appl. Polym. Sci.*, 2013, **128**, 3411–3416.

8.   R. Jain, N. H. Shah, A. W. Malick, and C. T. Rhodes, *Drug Dev. Ind. Pharm.*, 1998, **24**, 703–727.

9.   A.-C. Albertsson and I. K. Varma, *Biomacromolecules*, 2003, **4**, 1466–1486.

10.   C. K. Williams, *Chem. Soc. Rev.*, 2007, **36**, 1573–1580.

11.   H. Seyednejad, A. H. Ghassemi, C. F. van Nostrum, T. Vermonden, and W. E. Hennink, *J. Control. Release*, 2011, **152**, 168–176.

12.   http://www.essentialchemicalindustry.org/polymers/polyethene.html (13.06.2014)

13.   L. M. De Espinosa and M. A. R. Meier, *Macromol. Rapid Commun.*, 2011, **32**, 1357–1361.

14.   L. Montero de Espinosa and M. A. R. Meier, *Eur. Polym. J.*, 2011, **47**, 837–852.

15.   D. Quinzler and S. Mecking, *Angew. Chem. Int. Ed. Engl.*, 2010, **49**, 4306–4308.

16.   F. Stemp, D. Quinzler, I. Heckler, and S. Mecking, *Macromolecules*, 2011, **44**, 4159–4166.

17.   J. Trzaskowski, D. Quinzler, C. Bährle, and S. Mecking, *Macromol. Rapid Commun.*, 2011, **32**, 1352–1356.

18.   H. Mutlu and M. A. R. Meier, *J. Polym. Sci. Part A Polym. Chem.*, 2010, **48**, 5899–5906.

19.   C. Vilela, A. J. D. Silvestre, and M. A. R. Meier, *Macromol. Chem. Phys.*, 2012, **213**, 2220–2227.

20.   I. van der Meulen, M. de Geus, H. Antheunis, R. Deumens, E. A. J. Joosten, C. E. Koning, and A. Heise, *Biomacromolecules*, 2008, **9**, 3404–3410.

21.   L. Van Der Mee, F. Helmich, R. De Bruijn, J. A. J. M. Vekemans, A. R. A. Palmans, and E. W. Meijer, *Macromolecules*, 2006, **39**, 5021–5027.

22.   C. Vaida, H. Keul, and M. Moeller, *Green Chem.*, 2011, **13**, 889–899.

23.   A. Kumar, K. Garg, and R. A. Gross, *Macromolecules*, 2001, 3527–3533.

24.   A. Kumar, B. Kalra, A. Dekhterman, and R. A. Gross, *Macromolecules*, 2000, 6303–6309.

25.   G. Ceccorulli, M. Scandola, A. Kumar, B. Kalra, and R. A. Gross, *Biomacromolecules*, 2005, **6**, 902–907.

26.   I. van der Meulen, E. Gubbels, S. Huijser, R. Sablong, C. E. Koning, A. Heise, and R. Duchateau, *Macromolecules*, 2011, **44**, 4301–4305.

27.   M. P. F. Pepels, M. Bouyahyi, A. Heise, and R. Duchateau, *Macromolecules*, 2013, **46**, 4324–4334.

28.   M. Bouyahyi, M. P. F. Pepels, A. Heise, and R. Duchateau, *Macromolecules*, 2012, **45**, 3356–3366.

29.   N. Simpson, M. Takwa, K. Hult, M. Johansson, M. Martinelle, and E. Malmström, *Macromolecules*, 2008, **41**, 3613–3619.

30.   M. Takwa, N. Simpson, E. Malmström, K. Hult, and M. Martinelle, *Macromol. Rapid Commun.*, 2006, **27**, 1932–1936.

31.   M. Takwa, Y. Xiao, N. Simpson, E. Malmström, K. Hult, C. E. Koning, A. Heise, and M. Martinelle, *Biomacromolecules*, 2008, **9**, 704–710.

32.   M. de Geus, I. van der Meulen, B. Goderis, K. van Hecke, M. Dorschu, H. van der Werff, C. E. Koning, and A. Heise, *Polym. Chem.*, 2010, **1**, 525–533.

33.   T. Desmet, R. Morent, N. De Geyter, C. Leys, E. Schacht, and P. Dubruel, *Biomacromolecules*, 2009, **10**, 2351–2378.

34.   R. J. Pounder and A. P. Dove, *Polym. Chem.*, 2010, **1**, 260–271.

35.   I. van der Meulen and Y. Li, *Biomacromolecules*, 2011, **12**, 837–843.

36.   C. E. Hoyle and C. N. Bowman, *Angew. Chem. Int. Ed. Engl.*, 2010, **49**, 1540–1573.

37.   A. B. Lowe, *Polym. Chem.*, 2010, **1**, 17–36.

38.   O. Türünç and M. A. R. Meier, *Eur. J. Lipid Sci. Technol.*, 2013, **115**, 41–54.

39.   Z. Ates, P. D. Thornton, and A. Heise, *Polym. Chem.*, 2011, **2**, 309.

40. A. A. Panova and D. L. Kaplan, *Biotechnol. Bioeng.*, 2003, **84**, 103–113.

41. M. Claudino, I. van der Meulen, S. Trey, M. Jonsson, A. Heise, and M. Johansson, *J. Polym. Sci. Part A Polym. Chem.*, 2012, **50**, 16–24.

42. M. Krumova, D. Lopez, R. Benavente, C. Mijangos, and J. M. Perena, *Polymer*, 2000, **41**, 9265–9272.

43. A. Charlesby and M. Ross, *Proc. R. Soc. A Math. Phys. Eng. Sci.*, 1953, **217**, 122–135.

44. M. Vert, *Biomacromolecules*, 2005, **6**, 538–546.

45. F. Audouin, R. Larragy, M. Fox, B. O'Connor, and A. Heise, *Biomacromolecules*, 2012, **13**, 3787–3794.

46. M. Maltese, *J. Org. Chem.*, 2001, **66**, 7615–7625.

Functional Brushes Decorated Poly(globalide) Films for Bioconjugation

Abstract

Formation of hydroxyl functionalized poly(macrolactone) films was achieved by a combination of enzymatic ring opening polymerization (e-ROP) and thiol-ene coupling reactions. Efficient activator regeneration by electron transfer (ARGET) ATRP was employed polymerizing *tert*-butyl acrylate (*t*BA) monomer from ATRP initiator decorated surfaces. A dense coating of polymer brushes was obtained by controlled growth of grafted polymer in the presence of a sacrificial initiator. Deprotection of the *tert*-butyl ester decorated polymer surfaces yielded carboxylic acid groups, a convenient attachment point for biomolecules immobilization. As an example, the successful conjugation of green fluorescent protein (eGFP) and active enzyme chitobiase (Chb) on densely poly(acrylic acid)-functionalized polyester films was demonstrated. Similarly, stimuli-responsive surfaces were generated by modifying poly(globalide) (PGl) films using poly(Gl-g-NIPAM). The straightforward and versatile methodology presented herein exemplifies the design of (bio)functional polyester surfaces by modification of the properties of grafted polymer brushes.

4.1 Introduction

There is a growing interest in new functionalized polyesters which can address the limitations of the current generation of biopolymers, such as slow biodegradation, lack of introducing biomolecules or reduce tissue inflammation at the site of implant[1]. Aliphatic polyesters are widely used in various branches of industry as well as in medical applications, such as for sutures, stents, bone screws, tissue engineering scaffolds, and drug delivery systems[2–4]. These polymers can exhibit tunable physico-chemical characteristic, including hydrophilicity and degradation rate, but often lack functional groups for surface attachment of e.g. peptide ligands or growth factors to improve cell adhesion and enhance cell growth[5–7]. Hence, there are several methods reported for the modification of polymers including surface modification methodologies such as wet chemical methods, plasma treatment, UV irradiation or grafting of polymers[8–11]. Plasma treatment is an effective and widely used technique to modify the surfaces of polymeric biomaterials with reactive sites such as amine or carboxyl groups. Oxygen plasma can be used to render hydrophobic surfaces hydrophilic while hydrophilic surfaces can be rendered hydrophobic with CF_4 plasma[12,13]. Moreover, degradable polymers such as poly(lactic-co-glycolic acid) (PLGA) or fibers from poly(ε-caprolactone) (PCL) can be modified by the choice of proper plasma gas to enhance material properties for desired applications[14–18]. For example, PCL nanofiber meshes were modified by using different plasma gas mixtures including N_2+H_2, NH_3+O_2 and $Ar+O_2$ resulting in extremely hydrophilic surfaces with water contact angle of $0°$[17].

Grafting polymer brushes from the polymeric surfaces can be considered an alternative technique[19]. Polymer brushes are particularly suited for covalent immobilization of biomolecules as they possess a well defined structure, excellent mechanical stability and dense functionalisation[20–23]. In addition, the number of binding sites for biomolecules can be controlled by the polymer chain length[24]. Yuan et al. presented the controlled growth of brushes on initially surface modified PCL substrates, one of the widely studied polyesters for biomedical applications[25]. Improved cell-material interactions were reported with collagen-conjugated PCL substrates which were decorated with functional brushes of poly(methyacrylic acid) (PMMA) via Atom Transfer Radical Polymerization

(ATRP). Stimuli responsive brushes were also reported on the surface of PCL membranes[26]. Poly(sodium 4-styrenesulfonate) (NaSS) brushes on the PCL/PNIPAM (Poly(N-isopropylacrylamide)) porous membranes result in temperature and electrolyte responsive characteristics.

By and large almost all aliphatic polyesters lack intrinsic functionality and must undergo surface functionalisation as outlined above prior to attachment of a bioactive compound. Unsaturated macrolactones (ML) are an interesting class of renewable monomers. It has been shown that high molecular weight polymers can be obtained from ML by enzymatic[27,28] as well as catalytic polymerization[29–31]. Moreover, the double bond presents a perfect anchor point for polymer functionalisation. In previous studies, functional films from poly(macrolactones) (PMLs) by using thiol-ene reactions were reported[32]. Thiol-ene reactions were used to obtain cross-linked films from aliphatic polyglobalide as well as for the surface functionalization of obtained films for further conjugation as shown with FTIC as a model compound (see chapter 3). The drawback of this approach is that the variation of the functionalities depends on the thiol compound used and some showed low reactivity. Moreover, this methods only affords low degree of functionality on the surface due to the low surface area of flat surface and the low surface double bond density[5]. To overcome these drawbacks, we are interested in introducing polymer brushes via surface initiated polymerizations onto thiol-ene cross-linked PML films with the aim to increase the variety of surface functional groups through conventional acrylates/methacrylates as well as the functional group density.

At present, surface initiated polymerization from covalently immobilized initiators has been shown to be a powerful method to achieve a high degree of control over the functionality, density and thickness of grafted materials[33]. Depending on the properties of the polymer to be grafted to the surface, such coatings can be used for a variety of applications such as sensing, nanoactuation and in selective membranes[34]. Grafting can be achieved using a `grafting to` or a `grafting from` technique. In the `grafting from` process, the polymer chains grow from initiating sites on the surface. Consequently, the grafting density becomes higher compared to the `grafting to` method where preformed polymer chains have to be attached onto the surface covalently or physically with

suitable chemistries. In most cases, the 'grafting from' approach is be preferred due to less steric hindrance of diffusing small monomers compared to polymer chains[35].

Surface-initiated controlled radical polymerizations (SI-CRP) also allow preparation of different architectures on the surface while having control over the polymerization. Recently, atom transfer radical polymerization (ATRP) has been extensively studied as a controlled radical polymerization (CRP) process which is compatible with a wide range of monomers and solvents while providing control over their molecular weights, polydispersity and molecular architectures[36]. Surface initiated ATRP (SI-ATRP) is a suitable technique for functionalisation of surfaces since bromoesters, well-known ATRP initiators, can easily be formed by the esterification between 2-bromoisobutyrate and available surface hydroxyl groups[37,38]. As ATRP relies on the equilibrium between active and dormant species, generated by the redox reaction between a solubilized transition metal and alkyl halide, a sacrificial initiator can be used to adjust the concentration of these active molecules in SI-ATRP. The free polymer generated by the free initiator can be analyzed with respect to molecular weight and the characteristics of the grafted polymer can be estimated assuming the bulk polymerization rate is similar to the surface polymerization rate. However, SI-ATRP requires relatively large amount of transition metal catalyst which is mostly copper based. Due to the coloring of the grafted substrate, it requires intensive purification steps to remove the catalyst which increases the costs for industrial production and leads to limitations in medical applications because of toxicological concerns[39].

Hence, Matyjazewski et. al. have developed a new approach which is based on activators regenerated by electron transfer (ARGET-ATRP)[40–42]. Surface initiated ARGET ATRP is frequently used to graft polymers to a variety of surfaces in order to introduce new properties, such as hydrophilicity, stimulus responsivity, anti-bacterial properties[7,43–45]. In ARGET-ATRP, an inactive Cu(II) salt is reduced to an active Cu(I) species by a reducing agent which is added at the start of the polymerization[46]. Air and other radical traps can be eliminated by an excess reducing agent in the polymerization system which *in-situ* converts all Cu(II) into active Cu(I)[47]. Due to ppm level catalyst amounts required

and the tolerance to air/solvent, ARGET-ATRP is a green approach to devise hybrid brushes on different surfaces[48].

Herein, we demonstrate surface initiated ARGET-ATRP from the surface of thiol-ene cross-linked polyester films from macrolactones. Poly(globalide) surfaces were decorated with poly(AA) brushes to enhance their surface hydrophilic properties. Subsequently, NIPAM was chosen as a functional monomer because of its thermo responsive properties. With the increase of functional group density on the polyester surface, it opens opportunities to introduce proteins such as enhanced Green Fluorescent Protein (eGFP) as demonstrated successfully. Moreover, effective immobilization of β-N-acetyl-glucosaminidase (chitobiase) enzyme was achieved onto PGl-g-PAA films. The activity of the immobilized enzyme is demonstrated by the reaction with a chromogenic substrate, 4-nitrophenyl N-acetyl-β-D-glucosaminide.

4.2 Results and Discussion

4.2.1 ARGET ATRP from Poly(Macrolactones)

Grafting of polymeric brushes can easily be performed from different types of surfaces if those are decorated with ATRP initiators[49–51]. Herein, films from unsaturated poly(macrolactones) were used as the substrate which were prepared by UV-induced cross-linking via thiol-ene reactions. The detailed methodology to prepare such PML films was described in chapter 3 (Method C). Moreover, surface functionalisation of PML films was subsequently conducted by UV-induced thiol-ene reactions with 6-mercapto 1-hexanol. The hydroxyl functionalized surface was reacted with α-bromoisobutyryl bromide in the presence of triethylamine to form ATRP initiators on the surface of PML films. Elemental analysis confirmed the presence of Br atoms linked to the surface after the reaction. Results of the hydroxyl functionalized cross-linked films: (w%) C=68.81, H=10.05, N=0.08, Br=0 and ATRP-initiator decorated cross-linked films: (w%) C=62.94, H=9.43, N=0.26 and Br=5.81.
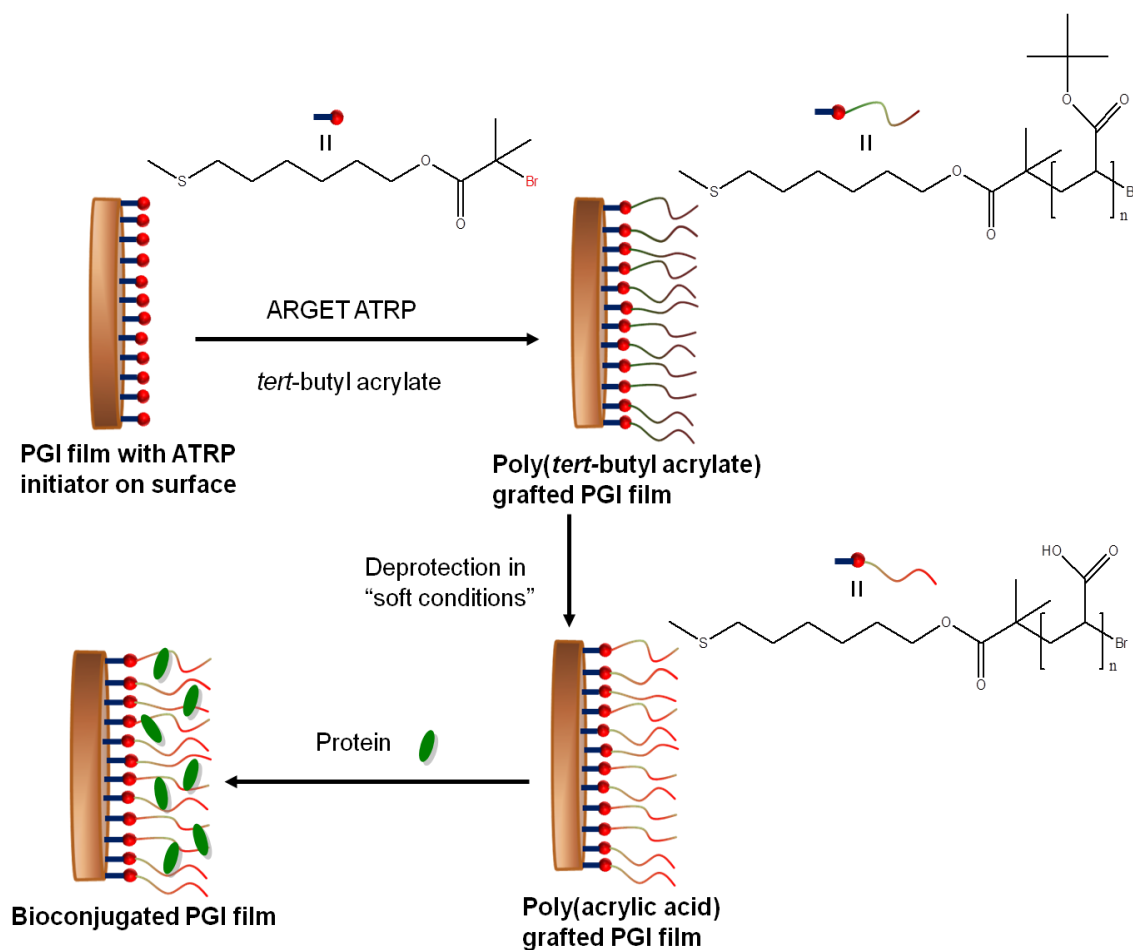
Figure 4.1: Schematic cartoon for the synthesis PAA grafted PGl surfaces followed by bioconjugation.

The grafting of tBA from initiatior functionalized PGl was conducted via ARGET-ATRP in the presence of $CuBr_2$, ligand (TPMA), monomer, anisole and tin (II) 2-ethylhexanote as reducing agent under nitrogen atmosphere. Initial ATRP reactions were conducted by using [EBiB]/[CuBr$_2$]/[TPMA]/[Tin(II)]=1/0.1/1/1 and [CuBr$_2$]/[tBA]=91 ppm at 60°C. The polymerizations were conducted in the presence and absence of sacrificial initiator ethyl 2-bromoisobutyrate using the same experimental conditions. Sacrificial initiator can be utilized to adjust the concentration of initiator and monomer-to-initiator ratio since ATRP depends on a dynamic equilibrium between active and dormant species[52]. The free polymer can easily be analyzed in terms of molecular weight and polydispersity

by assuming that the bulk polymerization occurs at the same rate as the surface polymerization. However, this correlation is strongly dependent on the surface morphology and diffusion processes[53–55]. Despite these limitations, analysis of unbound polymers can provide an estimation of the characteristics of the grafted polymers[35].

After intensive washing to remove the free P*t*BA chains, samples were analyzed by ATR-IR and TGA to confirm the success of surface initiated ARGET ATRP. As the characteristic ester carbonyl peak at 1726 cm^{-1} in the spectrum of P*t*BA overlapped the ester peak of PGl, the peak of the methyl bending at around 1366 cm^{-1} was most relevant to confirm the surface grafted P*t*BA (Figure 4.2).
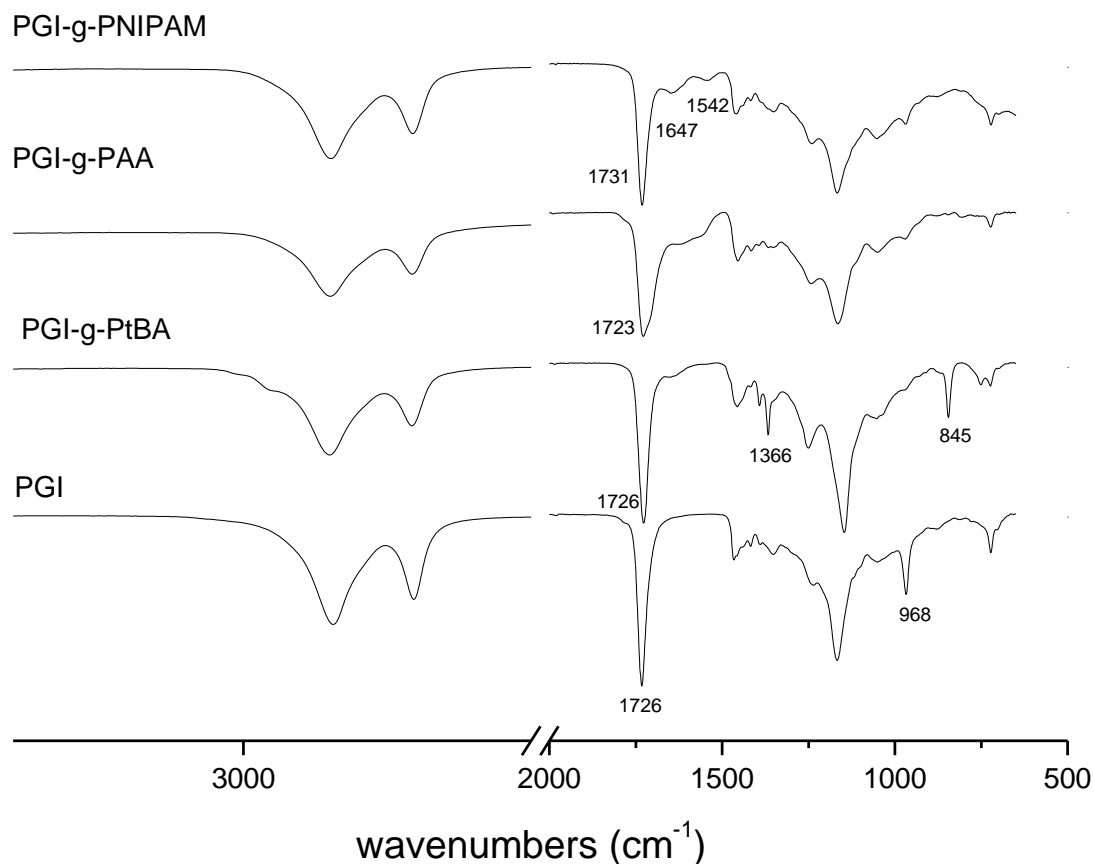
Figure 4.2: ATR-IR spectra of P*t*BA, PAA and PNIPAM grafted PGl films.

The *tert*-butyl groups of P*t*BA are known to undergo a thermal decomposition at around 200 °C to yield isobutylene[56]. As poly(globalide) undergoes thermal decomposition above 400°C, TGA offers the opportunity to determine the amount of grafted P*t*BA polymer on the PGl surface. Figure 4.3 shows the TGA results of PGl-g-P*t*BA1 (with sacrificial initiatior (SI), EBiB) and PGl-g-P*t*BA2 (without SI) demonstrating the two significant decomposition stages. The first stage between 220 and 280°C was assigned to the weight loss of the *tert*-butyl group and the second stage from 300 to 550°C arises from the weight loss of the remaining polymer backbone and PGl. The weight fractions of P*t*BA on PGl surfaces were estimated from the TGA results. In the presence of sacrificial initiator, 72 wt% of grafting was successfully achieved while the same polymerization conducted in the absence of sacrificial initiator yielded 63 wt% of grafting. In all cases, very similar grafting percentage was observed which indicates similar amounts of grafted polymer irrespective of the presence of SI. Polymerization with and without sacrificial initiator were repeated three times producing similar TGA results confirming the reproducibility of the reaction. On the other hand, several control experiments were conducted confirming the success of the grafting. Bare PGl films were stirred for a day in anisole in the presence of Poly(*t*BA) with a molecular weight of 20,000 g/mol and *t*BA monomer, respectively. Secondly, ATRP was conducted by using the following ratio [Poly(*t*BA)]/[EBiB]/[CuBr$_2$]/[TPMA]/[Tin(II)]=1/0.1/1/1 in anisole at 60°C under nitrogen atmosphere in the presence of PGl films without surface initiator. All of the samples were intensively washed until complete removal of free Poly(*t*BA) or *t*BA monomer. Based on TGA and IR results, no evidence of P*t*BA was found in the PGl samples. These experiments clearly indicate the efficiency of the washing process and establish the grafting of Poly(*t*BA) onto PGl surfaces rather than adsorption on the surface or by film swelling.
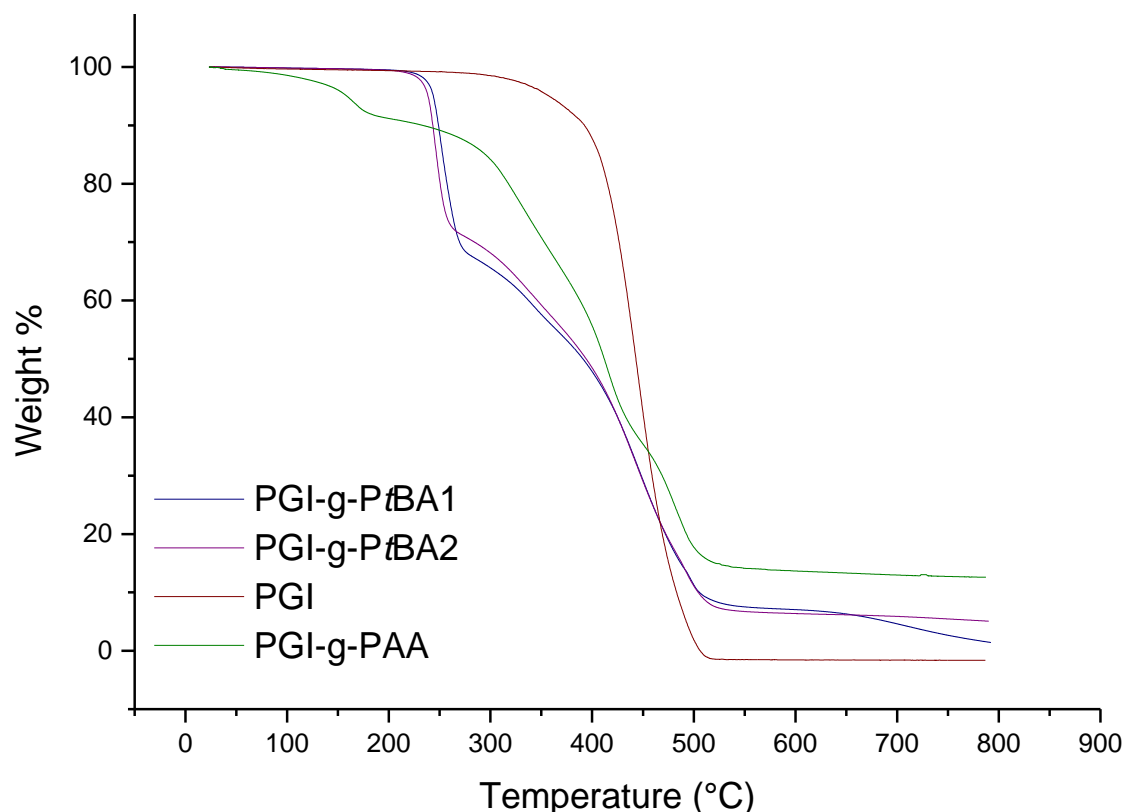
Figure 4.3: Thermograms of poly(globalide) (PGl), P*t*BA grafted PGl before (PGl-g-P*t*BA1 and PGl-g-P*t*BA2) and after deprotection of P*t*BA (PGl-g-PAA) under N$_2$ atmosphere. PGl-g-P*t*BA1 sample is prepared in the presence of SI and PGl-g-P*t*BA2 in the absence of SI (Table 4.1).

To highlight the versatility of this approach a second monomer, i.e. NIPAM was grafted. Poly(NIPAM) is an extensively used thermoresponsive polymer in many biomedical applications owing to its unique lower critical solution temperature (LCST) at ~32°C. Because of the phase change occurring at this temperature it was studied in release systems such as protein, drug or cell[57,44,58]. A similar procedure as for tBA was used for the ATRP of NIPAM from PGl surfaces with the ratio of [CuBr$_2$]/[TPMA]/[Tin(II)]=0.1/1/1 and [CuBr$_2$]/[NIPAM]=91 ppm at 60°C. After intensive washing of the films to remove free Poly(NIPAM), IR spectra of the obtained films exhibit characteristic poly(NIPAM) bands such as amide bands at around 1647 and 1542 cm^{-1} besides an N-H stretching band at around 3292cm^{-1} (Figure 4.2). In order to estimate the amount of the grafted polymer, elemental analysis was carried using the

poly(NIPAM) nitrogen as a quantifiable reporter. Poly(NIPAM) grafted cross-linked PGl films gave the following results (w%) C:70.94, H:10.66, and N:2.03. In comparison, 6-MH decorated cross-linked PGl films had a composition of (w%) C:68.8, H:10.05, N:0.08. The detected amount of nitrogen was normalized to the amount of carbon found in the films and the weight % of grafted poly(NIPAM) was calculated by using the formula below.

wt% grafted polymer=100x[(wt%(N)/wt%(C) in PGl-NIPAM) – (wt%(N)/wt%(C) in hydroxyl functionalized cross-linked PGI)] / [wt%(N)/wt%(C) per unit NIPAM]

wt%(N)/wt%(C) per unit NIPAM=19.44 %

In the absence of sacrificial initiator, the amount of grafted PNIPAM was calculated to be 15.09 ±1.5%. Generally, the percentage of grafted PNIPAM on the surface was significant lower compared to poly(*t*BA). Teodorescu and Matyjaszewski have reported the inactivation of the catalyst by complexation of the formed polyacrylamides[59]. Due to the high complexation ability of polyacrylamides, the formed polymer may competitively bind to copper. Removing the active catalyst from its ligated complex may reduce the reaction kinetic or even stop the polymerization. Studies reported later by the same and other authors indicated that these side reactions can be suppressed by the selection of ATRP starting compounds such as solvent[60–62] but this was not further explored here.

4.2.2 Surface Properties and Protein Immobilization

The *tert*-butyl group is one of the most commonly used protecting groups for carboxyl groups. This is because various carboxylic acid and alcohols can easily be converted into *tert*-butyl esters and deprotection is usually straightforward and quantitative. The deprotection of *tert*-butyl protected poly(acrylic acid) was reported earlier in literature by using hydrolysis under acidic conditions or by thermal decomposition[63,64]. Acidic hydrolysis was not a suitable deprotection method for our system as it unselectively hydrolysed the *tert*-butyl group as well as the ester functionalities of the PGl. Moreover, deprotection by thermal decomposition resulted in undesired discolouration of the

samples due to the decomposition byproducts. Wu and co-workers performed the mild deprotection of *tert*-butyl groups by using a $ZnBr_2$ biphasic system[65]. Formation of the complex between $ZnBr_2$ and the substrate was reported as the rate limiting step in deprotection rather than water hydrolysis. The cleavage rate was confirmed to be stable at a 5:1 ratio of $ZnBr_2$ to the substrate while >75% of deprotection was achieved. Adopting this methodology, the deprotection of grafted poly(*tert*-butyl acrylate) was achieved in a mild $ZnBr_2$/water biphasic system. Following this treatment the broad absorbance band of hydroxyl group of the acid functionality from 3200 to 3600 cm^{-1} was clearly seen in the FTIR spectra (Figure 4.2). Moreover, the doublet band at around 1355 cm^{-1} corresponding to the stretching of the tert-butyl groups disappeared after deprotection. Additionally, the efficiency of the deprotection was calculated as 80% by the difference of the weight loss of the *t*BA group obtained by TGA before and after deprotection with $ZnBr_2$ biphasic system (Figure 4.1).
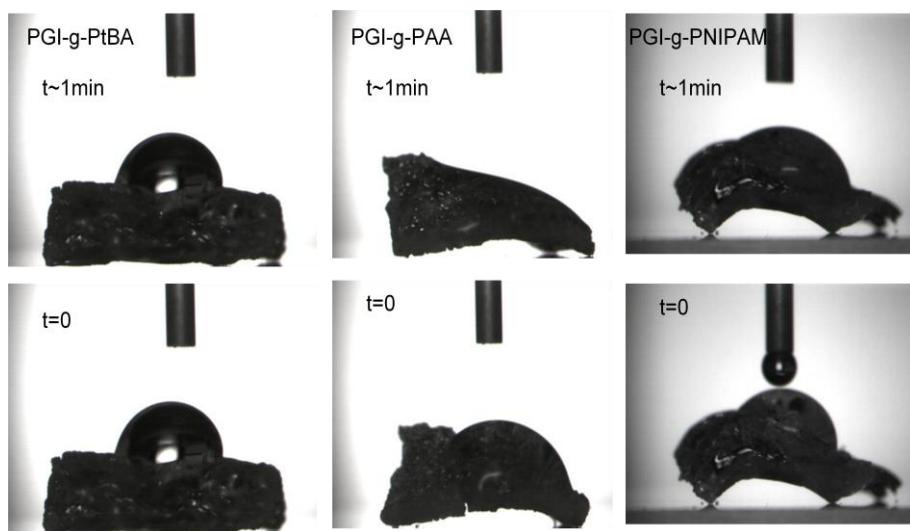
Figure 4.4: Change of hydrophilicity of P(*t*BA), PAA and PNIPAM grafted PGl films visualized by placing a drop of water onto the film.

Contact angle experiments were conducted to visualize the change of surface properties in terms of increasing hydrophilicity after deprotection. While it was not possible to

record exact contact angles due to the physical limitations (roughness) of films after grafting a clear trend could be observed. PGl-g-P*t*BA samples were not absorbing water droplets even after one minute as expected. In contrast, since the deprotection introduces PAA to the PGl surfaces, the water droplet was absorbed within a minute. An increased hydrophilicity was also observed for PNIPAM grafted surfaces, although not as pronounced as shown in Figure 4.4.

Immobilization of biomolecules, such as proteins, enzymes or antibodies as recognition elements or interface mediators has great importance for the application of biomaterials owing to their specific affinity for their targets. Moreover, the immobilization of biomolecules on solid substrates also plays a key role in biosensors and biotechnology applications[66]. Owing to their robust and versatile characteristics functional polymer brushes have been utilized extensively for the immobilization of biomolecules[67,45]. Herein, our key interest is the immobilization of biomolecules onto the polymeric brushes decorated PGl cross-linked films which might be adapted for the immobilization of various biomolecules. A model protein and an enzyme have been chosen to conceptually investigate the covalent immobilization through carboxylic acid groups of PAA decorated PGl films.
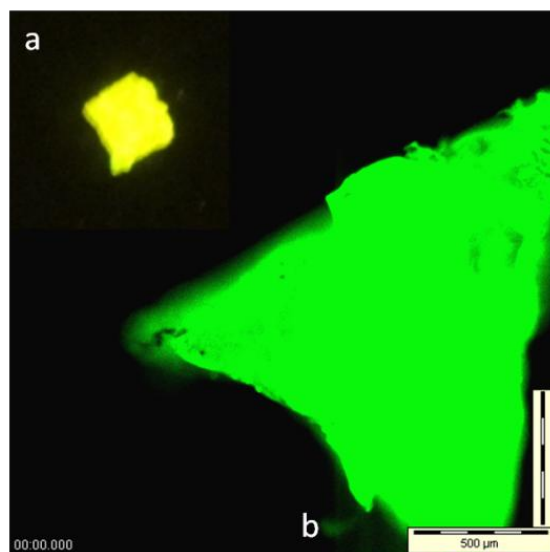
Figure 4.5: Fluorescence optical microscopy image of functional PGl-g-PAA after conjugation with eGFP exposed to a blue light source (a, top left) and PGl-g-PAA after conjugation of eGFP (b, bottom right).

Initially, enhanced green fluorescent protein, eGFP[68], existing as a homodimer with two identical subunits of a total molecular weight of 53.7 kDa was chosen for the bioconjugation to the PGl-g-PAA surfaces. Protein immobilization was performed by using common EDC/sulfo-NHS coupling chemistry between amino groups of ε-lysine residue of eGFP and carboxyl groups of grafted PAA in carbonate solution at pH 8.6. The esterification reaction between the –COOH groups of the polymer and the –NH$_2$ groups of the biomolecules is a well-known covalent coupling reaction[66]. The –COOH groups can be easily activated by EDC/NHS to form succinimide esters under mild pH and temperature conditions which can react spontaneously with the amine groups of the biomolecules[66]. The success of eGFP immobilization was visualized by blue-light exposure and fluorescence optical microscopy images (Figure 4.5).

A significant increase of fluorescence intensity was observed for eGFP conjugated PGl-g-PAA samples. On the other hand, cross-linked PGl films without grafted PAA were exposed to the same experimental conditions but no fluorescence intensity was observed for these materials. This clearly demonstrates the potential of the PGl-g-PAA materials for the immobilization of various proteins by using the described surface chemistry.

4.2.3 Chitobiase Assay

To further explore the feasibility of the immobilization approach with an active biomolecule an enzyme was covalently attached to the PGl-g-PAA film. Immobilized enzymes are constantly receiving attention for uses in many areas such as pharmaceutical, agricultural, chemical and food industries since it decreases the production cost and the generation of waste[69,70]. Enzyme immobilization on solid surfaces is one of the most appropriate methods to improve enzyme activity and stability under demanding conditions over extended periods of time. Enzyme immobilization methods basically include adsorption, covalent bonding, cross-linking, graft co-polymerization and entrapment[69,70].
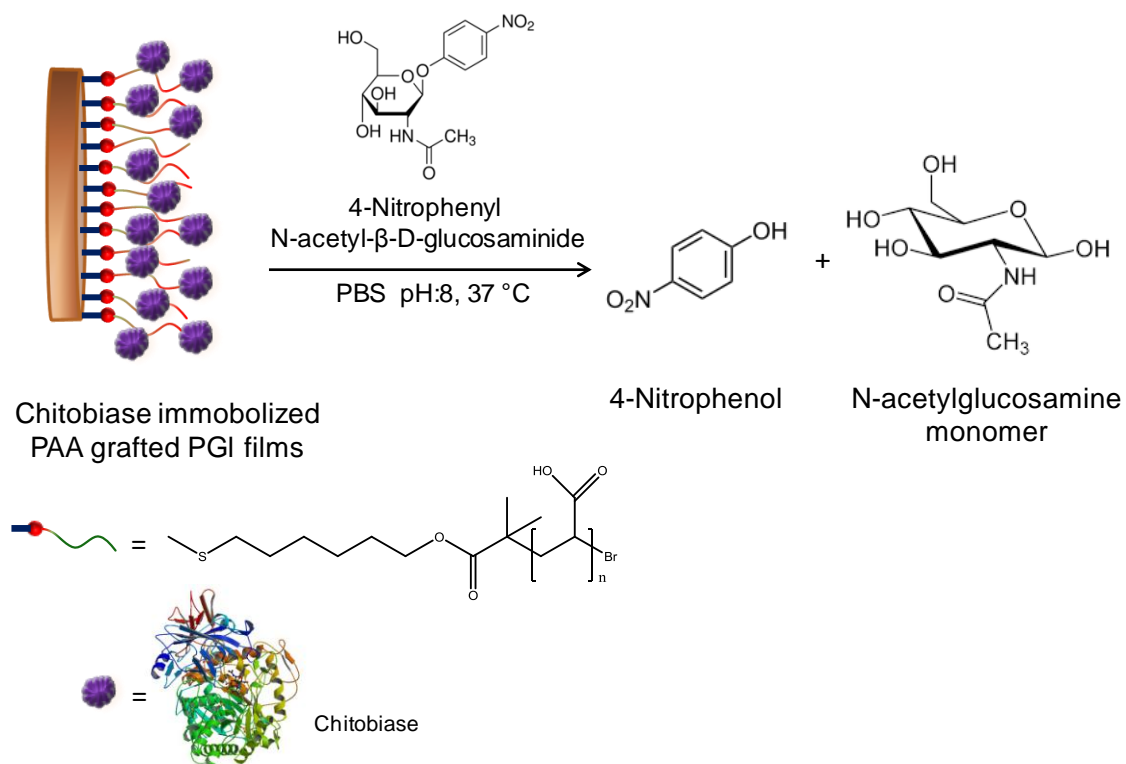
Figure 4.6: Schematic cartoons for the reaction of immobilized chitobiase on the surface of PGl-g-PAA films and PNP-GlcNAc

The chitobiase used in this study is a bacterial glycosyl hydrolase from *Photorhabdus luminescens*. Its substrate is chitobiose, a dimer of N-acetylglucosamine and a breakdown product of chitin. Chitin is the second most naturally abundant biopolymer in the world and is hydrolysed through the synergistic action of chitinases and chitobiases. The hydrolysis of chitin yields commercially important products such as chito-oligosaccharides and N-acetylglucosamine monomers. The hydrolysis of chitin waste is also a major industry. Enzymatic hydrolysis of chitin is the most efficient and environmentally friendly method of chitin breakdown, in comparison with chemical and physical methods. Therefore there is a constant demand for easy to produce, fast-performing, reliable chitinolytic enzymes such as chitobiases. The bacterial chitobiase in this study was recombinantly produced, ensuring a uniform constant supply of enzyme. Advantages of immobilising enzymes over using them in solution include increased stability of the enzyme, the ability to re-use the enzyme until its catalytic activity has

been exhausted, the capacity to use the enzyme in large reactors and the absence of enzyme in the final product solution. One major disadvantage may be a loss of catalytic activity due to immobilisation.
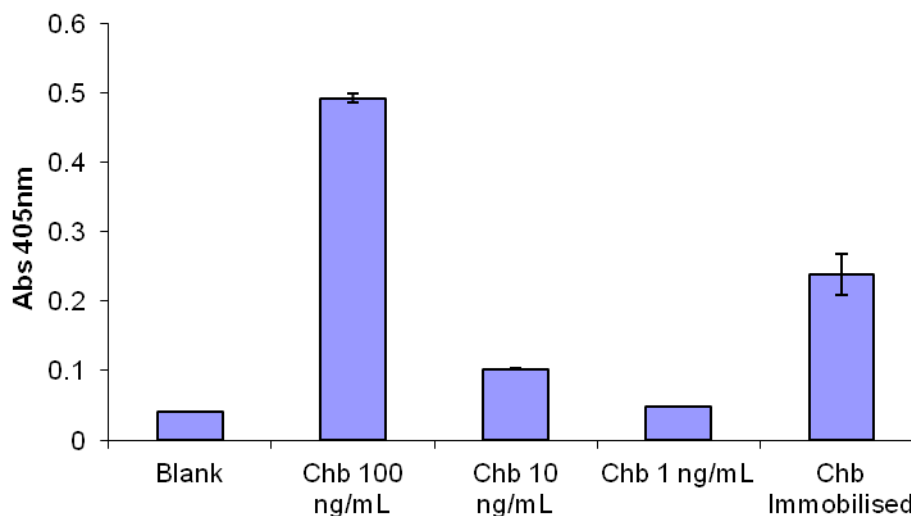
Figure 4.7: Activity assay of free and immobilized chitobiase (Chb) enzyme on N-acetylglucosamine hydrolysis.

Enzyme immobilization was achieved by using the same methodology as proposed for eGFP conjugation. Amino groups of chitobiase and carboxyl groups of grafted PAA were coupled through EDC/sulfo-NHS chemistry in sodium phosphate pH 8.0. For this assay, 4-nitrophenyl N-acetyl-β-D-glucosaminide (PNP-GlcNAc) was selected as an artificial chromogenic substrate, which can be broken down by the chitobiase enzyme producing UV detectable 4-nitophenyl to determine the activity of the enzyme (Figure 4.6). The substrate consists of a 4-nitrophenyl group attached to an N-acetylglucosamine substrate. In nature, the substrate of chitobiase is chitobiose, a dimer of N-acetylglucosamine residues. The chitobiase cleaves the bond between the N-acetylglucosamine residues to release monomers of N-acetylglucosamine. In this assay, the chitobiase cleaves the bond between the 4-nitrophenyl and the N-acetylglucosamine monomer. The reaction is stopped through the addition of a strong base, such as 1 M sodium carbonate. Firstly, this inhibits the enzymatic activity and consequently stops the

reaction. Secondly, it ensures that all the nitrophenyl is deprotonated to nitrophenol (which is yellow in colour). Therefore, activity of the chitobiase enzyme on the synthetic substrate was analysed through the monitoring of the production of the coloured nitrophenol compound, whose absorbance was read at 405 nm as shown in Figure 4.7. Solutions of chitobiase (non-immobilised) were used as controls at concentrations of 100, 10 and 1 ng/mL in phosphate buffered saline solution. The blank was also phosphate buffered saline solution. The absorbance readings obtained from the immobilization proved that the chitobiase enzyme was still active, retaining its ability to catalyze the hydrolysis of the N-acetylglucosamine substrate after immobilization onto PGI-g-PAA films. However, from these data it is not possible to calculate an exact amount of immobilized enzyme as that depends on unknown factors such as enzyme configuration, substrate parameters such as surface area, hydrophilicity as well as assay parameters such as the solubility, concentration and the pH[71]. On the other hand, the comparison between the activity of immobilized enzyme and non-immobilized enzyme clearly showed the enzyme was still active, retaining the ability to catalyze the hydrolysis of the N-acetylglucosamine substrate after immobilization.

4.3 Conclusions

Functionalisation of PGl surfaces with a high density of desired functional groups for bio-conjugation was achieved by a simple polymer grafting method. Combining enzymatic ROP with thiol-ene cross-linking and surface functionalisation allowed the introduction of anchor groups for ATRP initiators. The successful surface initiated ARGET ATRP methodology was demonstrated for the polymerization of NIPAM and *t*BA. Deprotection of the latter permited the increase of surface functional group density and the control of surface properties. The possibility for further bioconjugation was highlighted by the immobilisation of proteins or enzymes as shown with eGFP and Chitobiase enzyme.

4.4 Materials and Methods

4.4.1 Materials

Globalide was provided by Symrise. Novozyme 435 (*Candida Antarctica* Lipase B immobilised on cross-linked polyacrylate beads) was purchased from Novozymes A/S. *Tert*-Butyl acrylate (*t*BA, Aldrich 98%) was passed through a column of basic alumina to remove inhibitor prior to reaction. Ethylene glycol bis(3-mercapto propionate) was purchased from Wako. N-isopropylacrylamide (NIPAM, Aldrich 97%) was purified by recrystallization from hexane prior to use. All other reagents and solvents used were purchased from Sigma-Aldrich and used without further purification.

4.4.2 Methods

Gel Permeation Chromatography (GPC) measurements were performed using an Agilent 1200 series instrument equipped with GPC control software. All measurements were carried out using a Polymer Laboratories Gel 5 μm Mixed-C 300 x 7.5 mm column, at 40 °C with DAD and RID detection. Tetrahydrofuran (THF) was used as the eluent at a flow rate of 1 mL/min. The molecular weights of all polymers were calculated based on polystyrene standards.

GPC analysis was also carried out using an Agilent 1100 series instrument fitted with PSS GRAM analytical columns (300 and 100 Å, 10μ) using DMF (0.1M LiBr) as eluent equipped with a Wyatt Optilab rEX refractive index detector (thermostat set at 40 °C) and a Wyatt DAWN HELEOS-II multi-angle light scattering detector (MALS). Molecular weights and dispersities were calculated from the MALS signal by ASTRA software (Wyatt) using a dn/dc value of 0.0731 mL/g for PNIPAM in DMF[72].

Attenuated Total Reflection Fourier Transform Infra Red (ATR-FTIR) spectroscopy was done in the solid state on a Perkin-Elmer Spectrum 100 spectrophotometer.

An inverted fluorescence microscope (IX81, Olympus Co., Japan) equipped with an EMCCD camera (DV887-BI, Andor Technology, U.K.) and an MT20 fluorescence

illumination unit fitted with a 150 W xenon lamp was used in combination with a FITC filter set to image the green fluorescence of the FITC attached crosslinked poly(macrolactone) films. The fluorescent images were acquired using Cell-R software (Olympus Soft Imaging Solutions, GmbH, Germany).

Thermogravimetric analysis (TGA) was performed using TGA Q50 (TA instruments) using a temperature ramp of 20 °C/min to 800 °C under a nitrogen atmosphere. The amount of grafted PtBA was estimated on the basis of the weight loss between 220 and 300 °C from thermal elimination of the *tert*-butyl group.

The samples were UV-cured using a Fusion UV system, LCGE Bench top conveyor with a F300S Fusion lamp (120 W/cm) equipped with a 13mm H-bulb. The samples were exposed to the UV lamp for 3 min with a 5 m/min belt speed.

4.4.3   Synthesis of Polyglobalide via Enzymatic Ring Opening Polymerization

A suspension of Globalide (2.1 g) and NZ435 (0.44 g) in toluene (2.0 g) was purged with nitrogen, then heated in an oil bath set at 60 °C. After four hours, dichloromethane (DCM) was added to the reaction mixture to dissolve the product and inhibit enzyme activity. The product was isolated from the solution by precipitation in ice-cold methanol and filtration. The resulting polymer was dried overnight at room temperature under vacuum. Typical yields were around 60% and M_n 16000 g/mol (Đ=2.5).

4.4.4   Preparation of Functional films

Cross-linked Poly(globalide) films were prepared with an estimated double bond conversion of 25%. To poly(globalide) (300 mg, 0.02 mmol) dissolved in THF (1 mL) was added ethylene glycol bis(3-mercaptopropionate) (0.060 mL, 0.3 mmol). The UV initiator mixture, (diphenyl(2,4,6-trimethylbenzoyl) phosphine oxide / 2-Hydroxy-2-methylpropiophenone (0.060 mL, 0.3 mmol) dissolved in dichloromethane at a ratio of 1:1 (w/w) was added to each sample. Within 3 minutes the formulation was cast into

disc-shaped teflon molds to form 15 mm diameter films (1 mm deep) and passed under the UV lamp (for 3 min). Subsequently, THF (1 mL) containing 6-mercapto 1-hexanol (0.12 mL, 0.88 mmol) and equimolar photoinitiator was transferred onto the film surfaces and UV cured for further 3min. Samples were then washed with THF to remove unreacted cross-linker and initiator, and dried under ambient conditions.

Hydroxyl-decorated films (PGI-OH) were converted into ATRP initiator by immersing 100 mg films into a solution of triethylamine (0.28 mL, 2 mmol) in dry DMF (4 mL). Next, the solution was cooled to 0 °C, α-bromoisobutyryl bromide (0.25 mL, 2 mmol) was added dropwise and the reaction allowed standing overnight. Subsequently, samples were washed with THF and ethanol to remove residual reactants and byproducts. The ATRP-initiator decorated films were dried under vacuum at room temperature.

4.4.5   ARGET ATRP of Surface Decorated Cross-linked Films

Initiator decorated films were placed into a Schlenk flask containing 4 mL anisole, 4 mL (27 mmol) tBA, 0.56 mg (0.0025 mmol) $CuBr_2$, 7.2 mg (0.024 mmol) tris(2-pyridylmethyl)amine (TPMA) and 4.88 mg ethyl 2-bromoisobutyrate (EBiB; 0.025 mmol). The Schlenk flask was sealed and purged with nitrogen for 30 min. Following, 10 mg (0.025 mmol) tin(II) 2-ethylhexanoate in 0.5 mL of anisole was introduced to the solution and the reaction flask placed into an oil bath at 60°C. After the mixture was allowed to stand for 24 hour, the reaction flask was exposed to air. The poly(tBA) grafted films were transferred into a beaker and washed with anisole, THF and ethanol following each other. Samples were dried under vacuum at room temperature for further analysis.

In the case of reaction realized with a sacrificial initiator (SI), the free polymer was diluted with anisole and transferred into dialysis membrane (MWCO 1000g/mol). Dialysis was performed against methanol for a week and molecular weights of free polymers were determined by GPC analysis. ARGET ATRP of NIPAM from the surface was performed with the similar method as described for tBA.

Table 4.1: Experimental conditions for ARGET ATRP of *t*BA from the ATRP initiator decorated PGl films.

Sample	PGl-Br (mg)	Monomer (g)	EBiB (mg)	CuBr$_2$ (mg)	Ligand (mg)	Tin(II) (mg)	Anisole (mL)	Reaction time[*] (hours)	Mn (g/mol)[a]
PGl-g-tBA1	45	3.5	4.88	0.56	7.2	10	4	24	11000
PGl-g-tBA2	45	3.5	-	0.56	7.2	10	4	24	
PGl-g-tBA3	20	1.75	-	0.28	3.6	5	2	12	
PGl-g-tBA4	20	1.75	1.22	0.28	3.6	5	2	24	7200
PGl-g-tBA5	20	1.75	-	0.28	3.6	5	2	48	
PGl-g-tBA6	25	1.75	2.44	0.28	3.6	5	2	24	5400
PGl-g-NIPAM1	30	1.5	-	0.56	7.2	10	4	48	
PGl-g-NIPAM2	30	1.5	4.88	0.56	7.2	10	4	48	4400

[a] Molecular weights were calculated by GPC measurements based on polystyrene standards.

[*]All experiments conducted at 60 °C.

4.4.6 Conversion of PGl-g-P*t*BA to PGl-g-PAA

Mild deprotection of *tert*-butyl ester groups was conducted using $ZnBr_2$ as a Lewis acid catalyst, based on the procedure of Wu et al.[65] PGI-g-P*t*BA sample (30 mg) was added to a stirred suspension of $ZnBr_2$ (0.47 g, 0.002 mol) in dichloromethane (DCM, 5 mL) and the reaction allowed to continue overnight at room temperature. The solution was then quenched by addition of DI water, (50 mL) stirring for a further 4h at room temperature. Samples of PGI-g-PAA were removed and washed with DCM and then dried under vacuum overnight at room temperature.

4.5 Immobilization of Fluorescent Protein (eGFP) onto PGl-g-PAA films

PGl-g-PAA (3.8 mg) was mixed with N-hydroxysulfosuccinimide sodium salt (0.5 mg, $2.30x10^{-3}$ mmol) and 1-ethyl-3-(3-dimethylaminopropyl) carbodiimide hydrochloride (EDC) (1 mg, $6.44x10^{-3}$ mmol) in 2 mL of sodium carbonate buffer (CBS; 20mM, pH=8.6). Afterwards, eGFP (1.3 mL) in CBS (1.9 mg protein per 1 mL CBS (20mM, pH=8.6)) was added and the solution was stirred overnight at room temperature. The decorated film was then washed with the same buffer solution to remove unbound protein. After washing with DI water to remove the traces of buffer, and drying under vacuum at room temperature overnight, the decorated film was isolated in a pure form.

4.5.1 Immobilization of Chitobiase Enzyme

5.5 mg PGl-g-PAA sample was mixed with 0.5 mg ($2.30x10^{-3}$ mmol) *N*-hydroxysulfosuccinimide sodium salt and 1 mg ($6.44x10^{-3}$ mmol) of 1-ethyl-3-(3-dimethylaminopropyl) carbodiimide hydrochloride (EDC) in 2 mL of sodium phosphate buffer (PBS; 50 mM, pH=8.0). Afterwards, 1.0 mL chitobiase in PBS (80 µg per 1 mL PBS) was added and the solution was stirred overnight at room temperature. Sample was

then washed with the same buffer solution to get rid of the non-immobilised enzyme, following with DI water and dried under vacuum at room temperature overnight.

4.5.2 Chitobiase assay

350 μL 1mM PNP-GlcNAc substrate (in 50 mM Sodium Phospate buffer pH 8.0) were transferred into each eppendorf. Following, the appropriate concentration of chitobiase enzyme (either 1 μg/mL 100ng/mL 10ng/mL or 1ng/mL) was also added which is made up in 50mM sodium phosphate buffer of the immobilised enzyme on the polymer film. After the reaction left at 37 °C for 45 minutes, 100 μL sample was removed and transferred into 96-well plates from each reaction. 100 μL 1M sodium carbonate solution was added to each well to stop the reaction. The absorbance was recorded at 405 nm. Samples were prepared as triplicates.

4.6 References

1. H. Seyednejad, A. H. Ghassemi, C. F. van Nostrum, T. Vermonden, and W. E. Hennink, *J. Control. Release*, 2011, **152**, 168–176.

2. S. B. Idris, K. Arvidson, P. Plikk, S. Ibrahim, A. Finne-Wistrand, A.-C. Albertsson, A. I. Bolstad, and K. Mustafa, *J. Biomed. Mater. Res. A*, 2010, **94**, 631–639.

3. P. Mainil-Varlet, C. Hauke, V. Maquet, G. Printzen, S. Arens, T. Schaffner, R. Jérme, S. Perren, and U. Schlegel, *J. Biomed. Mater. Res.*, 2001, **54**, 335–343.

4. C. Jérôme, A. Aqil, S. Voccia, D.-E. Labaye, V. Maquet, S. Gautier, O. F. Bertrand, and R. Jérôme, *J. Biomed. Mater. Res. A*, 2006, **76**, 521–529.

5. F. J. Xu, Z. H. Wang, and W. T. Yang, *Biomaterials*, 2010, **31**, 3139–3147.

6. A. Tamura, M. Nishi, J. Kobayashi, K. Nagase, H. Yajima, M. Yamato, and T. Okano, *Biomacromolecules*, 2012, **13**, 1765–1773.

7. Y. Q. Yang, X. D. Guo, W. J. Lin, L. J. Zhang, C. Y. Zhang, and Y. Qian, *Soft Matter*, 2012, **8**, 454–464.

8.	J.-S. Kong, D.-J. Lee, and H.-D. Kim, *J. Appl. Polym. Sci.*, 2001, **82**, 1677–1690.

9.	A. Cammarano, G. Luca, and E. Amendola, *Cent. Eur. J. Chem.*, 2012, **11**, 35–45.

10.	J. M. Goddard and J. H. Hotchkiss, *Prog. Polym. Sci.*, 2007, **32**, 698–725.

11.	S. Yoshida, K. Hagiwara, T. Hasebe, and A. Hotta, *Surf. Coatings Technol.*, 2013, **233**, 99–107.

12.	M. B. O. Riekerink, J. G. A. Terlingen, G. H. M. Engbers, and J. Feijen, *Langmuir*, 1999, **15**, 4847–4856.

13.	D. M. Svirachev and N. A. Tabaliov, *Bulg. J. Phys.*, 2005, **32**, 22–33.

14.	M. P. Prabhakaran, J. Venugopal, C. K. Chan, and S. Ramakrishna, *Nanotechnology*, 2008, **19**, 455102–455110.

15.	A. Martins, E. D. Pinho, S. Faria, I. Pashkuleva, A. P. Marques, R. L. Reis, and N. M. Neves, *Small*, 2009, **5**, 1195–1206.

16.	S. J. Kim, D. H. Jang, W. H. Park, and B.-M. Min, *Polymer*, 2010, **51**, 1320–1327.

17.	D. Yan, J. Jones, X. Y. Yuan, X. H. Xu, J. Sheng, J. C.-M. Lee, G. Q. Ma, and Q. S. Yu, *J. Biomed. Mater. Res. A*, 2013, **101**, 963–972.

18.	H. Park and K. Y. Lee, *Macromol. Res.*, 2007, **15**, 238–243.

19.	S. Edmondson, V. L. Osborne, and W. T. S. Huck, *Chem. Soc. Rev.*, 2004, **33**, 14–22.

20.	Y. K. Jhon, S. Arifuzzaman, A. E. Özçam, D. J. Kiserow, and J. Genzer, *Langmuir*, 2012, **28**, 872–882.

21.	P. Ye, H. Dong, M. Zhong, and K. Matyjaszewski, *Macromolecules*, 2011, **44**, 2253–2260.

22.	J. Choi, H. Dong, K. Matyjaszewski, and M. R. Bockstaller, *J. Am. Chem. Soc.*, 2010, **132**, 12537–12539.

23.	Z. B. Zhang, X. L. Zhu, F. J. Xu, K. G. Neoh, and E. T. Kang, *J. Memb. Sci.*, 2009, **342**, 300–306.

24.	S. Ohno and K. Matyjaszewski, *J. Polym. Sci. Part A Polym. Chem.*, 2006, **44**, 5454–5467.

25. S. Yuan, G. Xiong, X. Wang, S. Zhang, and C. Choong, *J. Mater. Chem.*, 2012, **22**, 13039–13049.

26. T. Cai, M. Li, K.-G. Neoh, and E.-T. Kang, *J. Mater. Chem.*, 2012, **22**, 16248–16258.

27. M. de Geus, I. van der Meulen, B. Goderis, K. van Hecke, M. Dorschu, H. van der Werff, C. E. Koning, and A. Heise, *Polym. Chem.*, 2010, **1**, 525–533.

28. I. van der Meulen, M. de Geus, H. Antheunis, R. Deumens, E. A. J. Joosten, C. E. Koning, and A. Heise, *Biomacromolecules*, 2008, **9**, 3404–3410.

29. I. van der Meulen, E. Gubbels, S. Huijser, R. Sablong, C. E. Koning, A. Heise, and R. Duchateau, *Macromolecules*, 2011, **44**, 4301–4305.

30. M. Bouyahyi, M. P. F. Pepels, A. Heise, and R. Duchateau, *Macromolecules*, 2012, **45**, 3356–3366.

31. M. Bouyahyi and R. Duchateau, *Macromolecules*, 2014, **47**, 517–524.

32. Z. Ates and A. Heise, *Polym. Chem.*, 2014, **5**, 2936–2941.

33. C. M. Hui, J. Pietrasik, M. Schmitt, C. Mahoney, J. Choi, M. R. Bockstaller, and K. Matyjaszewski, *Chem. Mater.*, 2013, **26**, 745–762.

34. F. J. Xu, K. G. Neoh, and E. T. Kang, *Prog. Polym. Sci.*, 2009, **34**, 719–761.

35. S. Hansson, V. Trouillet, T. Tischer, A. S. Goldmann, A. Carlmark, C. Barner-Kowollik, and E. Malmström, *Biomacromolecules*, 2013, 64–74.

36. V. Coessens, T. Pintauer, and K. Matyjaszewski, *Prog. Polym. Sci.*, 2001, **26**, 337–377.

37. A. Carlmark and E. E. Malmström, *Biomacromolecules*, 2003, **4**, 1740–1745.

38. F. J. Xu, J. P. Zhao, E. T. Kang, K. G. Neoh, and J. Li, *Langmuir*, 2007, **23**, 8585–8592.

39. N. V Tsarevsky and K. Matyjaszewski, *Chem. Rev.*, 2007, **107**, 2270–2299.

40. W. Jakubowski and K. Matyjaszewski, *Angew. Chemie*, 2006, **45**, 4482–4486.

41. K. Tanaka and K. Matyjaszewski, *Macromol. Symp.*, 2008, **261**, 1–9.

42. W. Jakubowski and K. Matyjaszewski, *Macromolecules*, 2005, 4139–4146.

43. S. Hansson, E. Ostmark, A. Carlmark, and E. Malmström, *ACS Appl. Mater. Interfaces*, 2009, **1**, 2651–2659.

44. H. Lee, J. Pietrasik, S. S. Sheiko, and K. Matyjaszewski, *Prog. Polym. Sci.*, 2010, **35**, 24–44.

45. F. Audouin, R. Larragy, M. Fox, B. O'Connor, and A. Heise, *Biomacromolecules*, 2012, **13**, 3787–3794.

46. Y. Wang, M. Zhong, Y. Zhang, A. J. D. Magenau, and K. Matyjaszewski, *Macromolecules*, 2012, **45**, 8929–8932.

47. K. Matyjaszewski, H. Dong, W. Jakubowski, J. Pietrasik, and A. Kusumo, *Langmuir*, 2007, **23**, 4528–4531.

48. R. Nicolaÿ, Y. Kwak, and K. Matyjaszewski, *Angew. Chem. Int. Ed. Engl.*, 2010, **49**, 541–544.

49. S. Hansson, E. Ostmark, A. Carlmark, and E. Malmström, *ACS Appl. Mater. Interfaces*, 2009, **1**, 2651–2659.

50. C. Huang, T. Tassone, K. Woodberry, D. Sunday, and D. L. Green, *Langmuir*, 2009, **25**, 13351–13360.

51. Y. Liu, V. Klep, B. Zdyrko, and I. Luzinov, *Langmuir*, 2004, **20**, 6710–6718.

52. T. von Werne and T. E. Patten, *J. Am. Chem. Soc.*, 2001, **123**, 7497–7505.

53. J. Kim, W. Huang, M. D. Miller, G. L. Baker, and M. L. Bruening, *J. Polym. Sci. Part A Polym. Chem.*, 2002, **41**, 24–29.

54. E. Marutani, S. Yamamoto, T. Ninjbadgar, Y. Tsujii, T. Fukuda, and M. Takano, *Polymer*, 2004, **45**, 2231–2235.

55. C. B. Gorman, R. J. Petrie, J. Genzer, and N. Carolina, *Macromolecules*, 2008, **41**, 4856–4865.

56. R. J. Schaefgek and I. M. Sarasohn, *J. Polym. Sci.*, 1962, **58**, 1049–1061.

57. C. Porsch, S. Hansson, N. Nordgren, and E. Malmström, *Polym. Chem.*, 2011, **2**, 1114–1123.

58. M. A. Cooperstein and H. E. Canavan, *Langmuir*, 2010, **26**, 7695–7707.

59. M. Teodorescu and K. Matyjaszewski, *Macromolecules*, 1999, **32**, 4826–4831.

60. D. Neugebauer and K. Matyjaszewski, *Macromolecules*, 2003, **36**, 2598–2603.

61.   M. Teodorescu and K. Matyjaszewski, *Macromol. Rapid Commun.*, 2000, **21**, 190–194.

62.   Y. Xia, X. Yin, N. A. D. Burke, and H. D. H. Stover, *Macromolecules*, 2005, **38**, 5937–5943.

63.   T. Johnson and R. C. Sheppard, *J. Chem. Soc. Chem. Commun.*, 1991, 1653–1655.

64.   J. R. Spencer, N. G. J. Delaet, A. Toy-Palmer, V. V. Antonenko, and M. Goodman, *J. Org. Chem.*, 1993, **58**, 1635–1638.

65.   Y. Wu, D. C. Limburg, D. E. Wilkinson, M. J. Vaal, and G. S. Hamilton, *Tetrahedron Lett.*, 2000, **41**, 2847–2849.

66.   H. Jiang and F.-J. Xu, *Chem. Soc. Rev.*, 2013, **42**, 3394–3426.

67.   F. J. Xu, Q. J. Cai, Y. L. Li, E. T. Kang, and K. G. Neoh, *Biomacromolecules*, 2005, **6**, 1012–1020.

68.   F. Yang, L. G. Moss, and G. N. Phillips, *Nat. Biotechnol.*, 1996, **14**, 1246–1251.

69.   S. Datta, L. R. Christena, and Y. R. S. Rajaram, *3 Biotech*, 2012, **3**, 1–9.

70.   W. Tischer and F. Wedekind, in *Topics in Current Chemistry*, 1999, vol. 200, pp. 96–126.

71.   H. Shibata and T. Yagi, *Clin. Chim. Acta*, 1996, **251**, 53–64.

72.   F. Audouin and A. Heise, *Eur. Polym. J.*, 2013, **49**, 1073–1079.

Porous Scaffolds and Microspheres from Poly(macrolactone)s

Abstract

3D scaffolds were formed by using particulate leaching technique from linear poly(globalide) under UV irradiation. Pore sizes and distribution were examined by SEM. Moreover, poly(globalide) microspheres were prepared by straightforward oil-in-water emulsion system. However, methodologies to produce scaffolds as well as microspheres need to be further improved to fulfil intended application requirements.

5.1 Introduction

Design and fabrication of scaffolds plays a major role in the biomaterial world, for example, for tissue engineering applications. A scaffold is essential to restore function or regenerate tissues. Such materials are classified as three-dimension (3D) porous solid biomaterials which perform some/or all of the following functions: promoting cell-biomaterial interactions, cell adhesion, permitting sufficient transport of gases or nutrients, biodegrade at a controllable rate that approximates the rate of tissue regeneration, and not provoking toxicity[1]. The criteria for selecting materials as biomaterials are based on their chemistry, solubility, shape and structure, hydrophilicity/hydrophobicity, lubricity, surface energy, and degradation[1–3]. The 3D scaffolds provide a pathway for cells to attach and form an extracellular matrix and can also carry growth factors or bimolecular signals. In an ideal situation, *in vivo* degradation of scaffolds should occur in an appropriate time in order to be replaced by the target tissue in the desired application[4]. For example, 3D scaffolds have been used for tissue engineering of nerve, skin, bone and cartilage[4–7].

Polymeric scaffolds are attracting considerable attention owing to their unique properties that include having suitable surface chemistry for cell attachment, having appropriate mechanical properties and degradation profile, biocompatibility (where neither the polymer nor the degradation products should cause an unwanted response), and possibilities to introduce high porosity with interconnected pores for cell growth and transportation[1,7,8]. Several methodologies have been employed to design 3D polymeric scaffolds. These methodologies include freeze-drying[9,10], particulate leaching[11], gas foaming[12], phase separation[9,10,13], 3D printing techniques[14], as well as combinations of these techniques[15]. The particulate leaching is one of the most widely used methods which is based on solubility differences[1]. Salt, sugar or wax are known as porogens and used to create the pores or channels. In this method, a polymer solution is transferred into a mould which is filled with the desired porogen particles. After the evaporation of the solvent, the porogen particles are leached away using the proper solvent to form the pores of the scaffold. The pore size can be controlled by tuning the amount of porogen added, the size and the shape of the porogen.
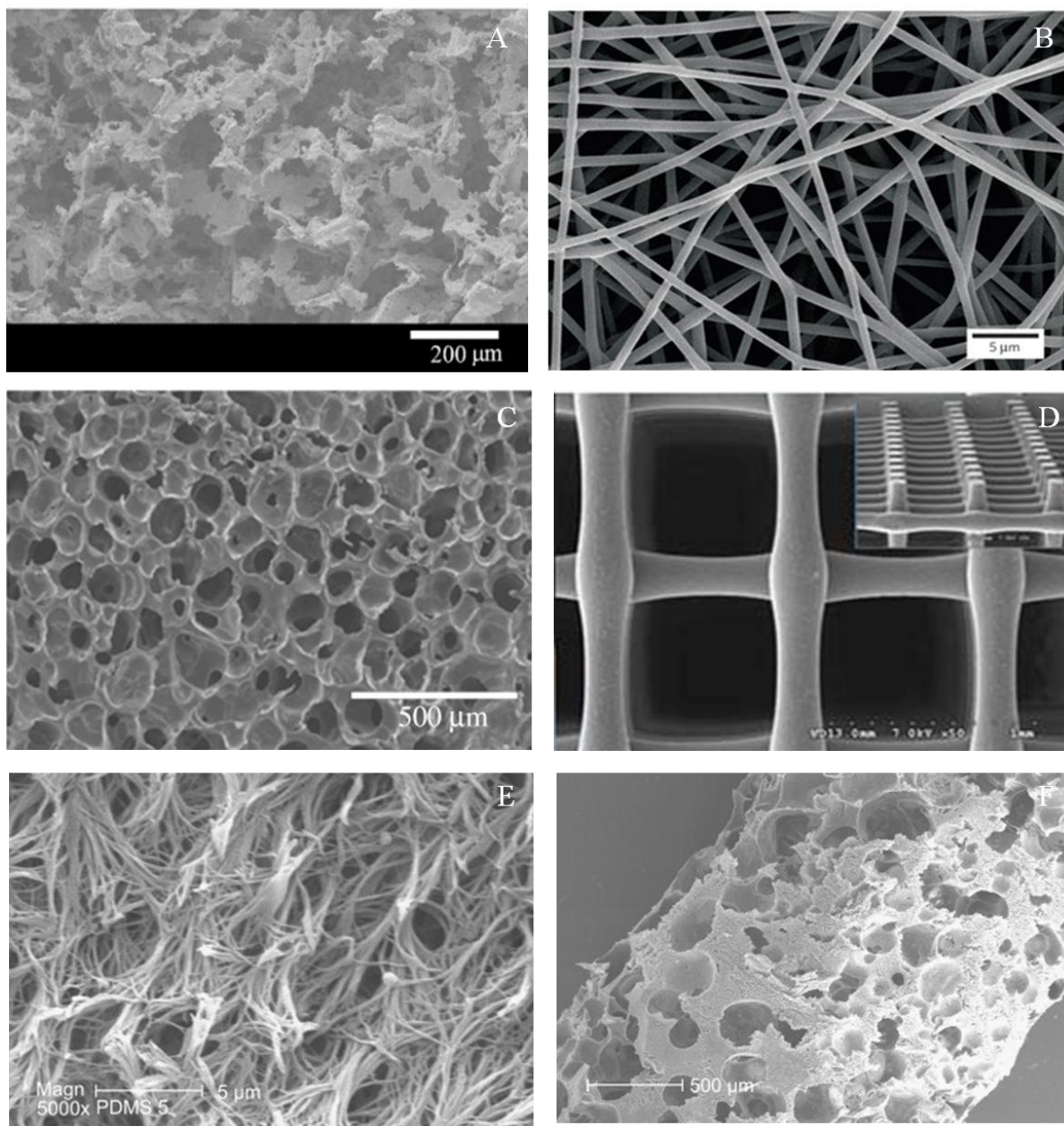
Figure 5.1: SEM images of scaffolds from (A) PCL–PHB ($C_{gel} = 5\%$)[16] via NaCI leaching, (B) PLGA/sP(EO-stat-PO)[17] via electrospinning, (C) PLA scaffolds[18] via supercritical carbondioxide, (D) PCL[19] via rapid prototyping (RP) technique, and (E&F) poly(L-lactide) nanofibrous scaffolds[20].

Moreover, incorporation of bioactive agents can be achieved by phase separation while forming the porous structures. Phase separation requires a temperature change that separates the polymeric solution in two phases, where one phase has low polymer concentration and other has a high polymer concentration[13]. The liquid-liquid phase is separated by lowering the temperature whereby two solid phases are formed and the solvent is removed by extraction, evaporation and sublimation to give porous scaffolds. On the other hand, the freeze drying methodology is based upon the principle of sublimation. The desired concentration of polymer solution is frozen and solvent is removed by lyophilization under the high vacuum creating the scaffold with high porosity and inter-connectivity[21]. However, new methodologies have been developed to provide more control over the pore shape and inter-pore connections. Rapid prototyping (RP) is one of these advanced techniques for scaffold production[14]. Layer manufacturing method is used to design 3D objects controlled by computers. Corresponding to each cross section a RP machine lays down a layer of material starting from the bottom and moving up a layer at a time to create the scaffolds. RP is an efficient way for generating the scaffolds with the desired properties as well as highly reproducible architecture and compositional variations. Moreover, high pressure carbon dioxide gas can be used to design highly porous scaffolds by organic solvent free methodology[4,12,18]. The porosity and pore structure of the scaffolds depends on the amount of the gas dissolved in the polymer. The mentioned techniques can also be combined to design porous scaffolds depending on the desired properties. For example, a polymer/porogen solution is exposed to high pressure until saturated with carbon dioxide. This is followed by the foaming process and the porogen is removed producing a highly interconnected pore structure[22].

On the other hand, biodegradable polymer particles, such as microspheres, microcapsules, and nanoparticles, have been widely studied due to their biocompatibility and biodegradability[23–26]. PGA, PLA and copolymers of these are widely used to design spherical carriers for drug delivery applications due to their rapid degradation compared to other polyesters[27–29]. Moreover, microspheres of natural polymers were also studied such as collagen, protein and elastin[27]. For example, growth factor releasing collagen microspheres were reported by Huang et al.[30].

These particles can be fabricated by using several methodologies such as solvent evaporation, suspension/emulsion polymerization, and sedimentation polymerization[26]. Solvent evaporation is one of the commonly used, simple and straightforward techniques. Double emulsion is often used when a drug or other molecules needs to be encapsulated[31,25].
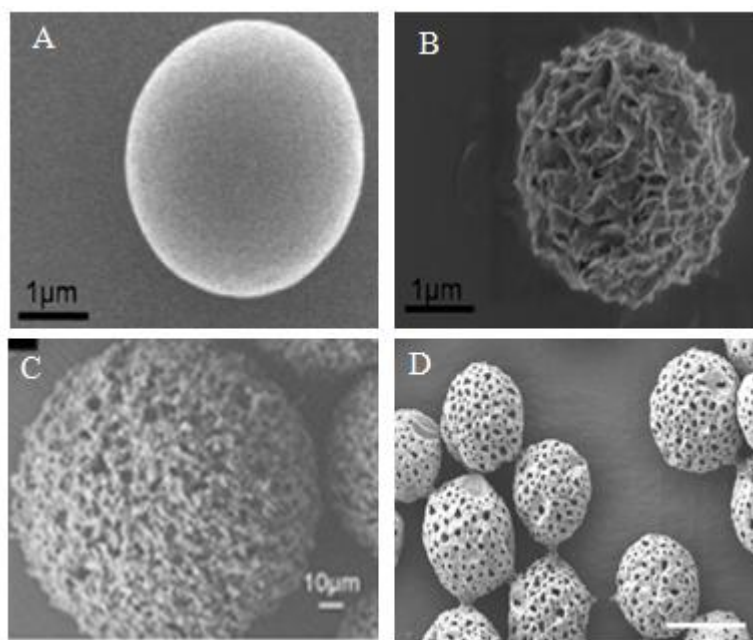
Figure 5.2: SEM images of (A) PLG microsphere[32], (B) mineral-coated PLG microsphere after incubation in mSBF for 7 days[32], (C) HA-*g*-PDLLA hybrid microspheres after alkaline treatment of 20 min[33], and (D) PLA porous microspheres before self-healing[34].

Herein, we focus on designing 3D materials from poly(macrolactones) which can be used in various biomedical applications. PGl scaffolds were prepared by using particulate leaching with different porogens to have control over the pore size, distribution and connectivity. Moreover, PGl microspheres were prepared in oil/water (o/w) emulsion systems to investigate the possible application of such PMLs as biodegradable particles.

5.2 Results and Discussion

5.2.1 Porous Scaffolds

3D porous materials were prepared by using a porogen/particulate leaching technique with sugar (sucrose, glucose monohydrate), and salt (sodium chloride) used as porogens. Ring-opening polymerisation of globalide was catalyzed by NZ435 and homopolymer was synthesized as described in chapter 2. Initially, sucrose at various concentration (ranging from 1:0.5 to 1:5 (w:w; PGl:sucrose) was used as porogen and added to poly(globalide) solution in THF. Samples were crosslinked by UV induced thiol-ene coupling reaction while aiming for 25% cross-linking (theoretical) by using EGMP as cross-linker. Curing was performed by using longer exposure times (6-10 min) due to the low penetration through the sample volume. After intensive washing to remove the porogen, SEM was used to analyze the pore size and pore distribution of the resulting scaffolds.

The best results were obtained for the 1:2 PGl:sucrose ratio (Figure 5.3 A&B). However, not all of the pores were interconnected. Pores were also irregularly shaped and with large size distribution which is most probably due to aggregation and the irregular shape of sugar particles (Figure 5.3 C). Moreover, all samples were inhomogeneous in terms of pore distribution due to the inevitable sedimentation of the porogen during processing. Lower ratios of sucrose resulted in less porous materials (Figure 5.3 F) as expected but the the effect of sedimentation was more pronounced compared to samples with higher ratios. As the concentration of sucrose was increased (above the ratio of 1:5, Sucrose:PGl), disintegration of the network occurred which might be caused by inefficient cross-linking due to the high quantity of particles in the suspended mixture.
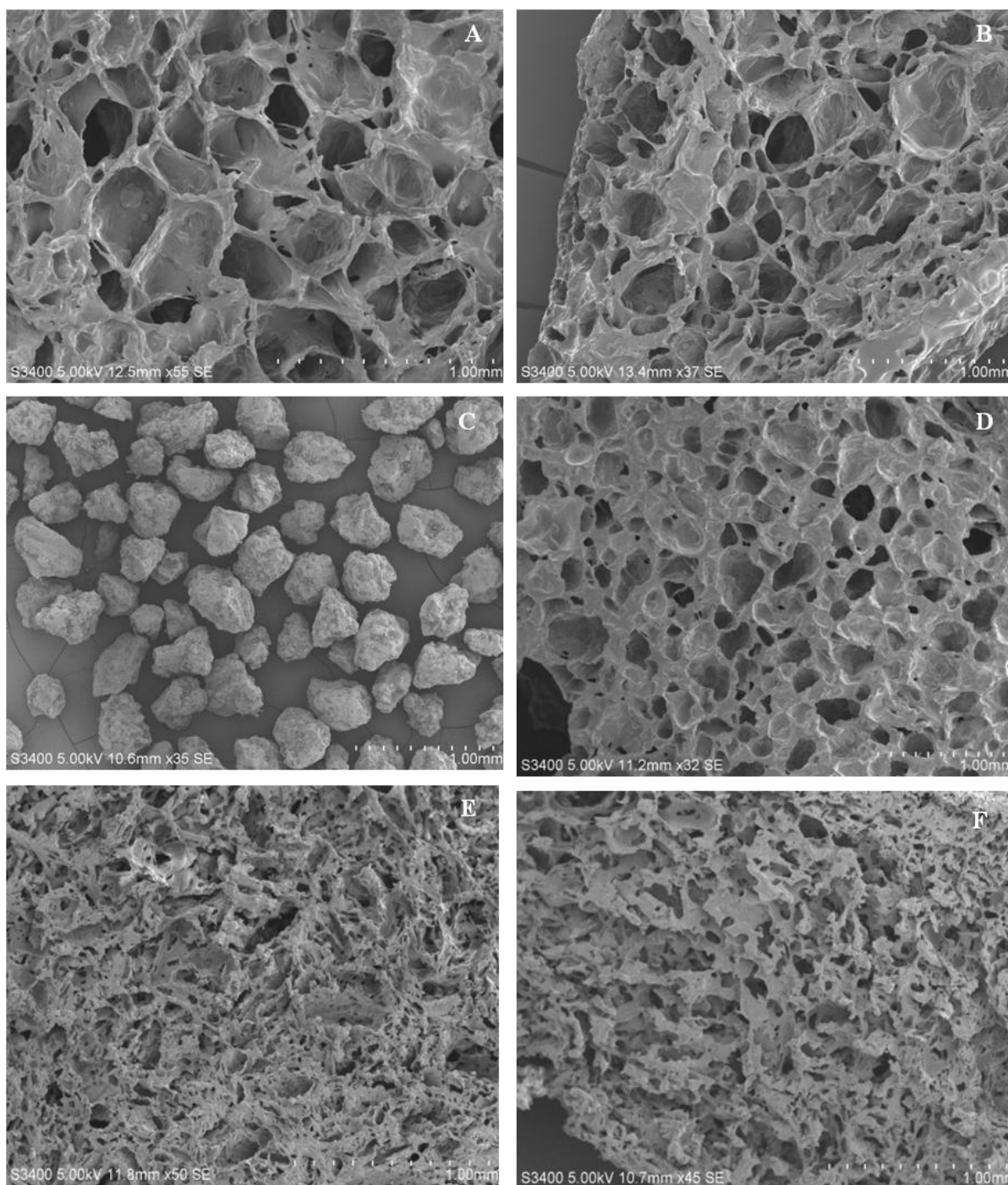
Figure 5.3: SEM images of (A, B) 1:2 (w/w) PGl:Sucrose (C) sucrose particles, (D) 1:2 (w/w) PGl:Sucrose, (E) 1:4 (w/w) PGl:GMH, and (F) 1:3 (w/w) PGl:GMH ratio used for porous poly(globalide) networks. Each sample was 25% cross-linked (theoratically).

Glucose monohydrate (GMH) was examined as porogen to investigate the effect of different porogens on the size and connectivity of pores (Figure 5.3 E&D) with the PGl:GMH ratios of 1:2, 1:3 and 1:4. The resulting materials were porous but pores were of irregular shape and not connected to each other. Furthermore, the scaffolds were brittle and handling these samples was difficult as they easily broke into small fragments.

On the other hand, addition of sucrose at a ratio higher than 1:5 (w/w) also resulted in disintegration of the scaffold. This might be caused by a nonuniform distribution of particles within the polymer solution locally reducing the cross-linking efficiency but further investigation and optimisation are needed to draw reliable conlcusions.

5.1.1 Microspheres

Biodegradable polymers in the form of microspheres are useful in drug delivery applications as they can be ingested or injected as well as modified to meet the desired release profile. Such microspheres can be prepared by oil-in-water emulsion systems, a simple straightforward methodology[35]. The characteristics of the final microspheres are influenced by several parameters such as the rate of the solvent removal, temperature, concentration and the solubility of the polymer, solvent, nature of the emulsifier, volume ratio of the dispersed and the continuous phases, and the stirring speed of the system[36].

Herein, an oil-in-water (O/W) emulsion system was used to fabricate PGl microspheres (Figure 5.4). O/W emulsions were formed by adding the polymer solution to an aqueous medium containing stabilizers such as poly(vinyl alcohol) (PVA)[37] under continuous stirring at an appropriate temperature (Figure 5.4). The evaporation of the organic solvent from the emulsion droplets afforded the formation of microspheres. The obtained particles were washed and collected by centrifuging. In order to obtain an optimized size distribution and morphology of microspheres, the experimental parameters were explored systematically as described in section 5.1.3.
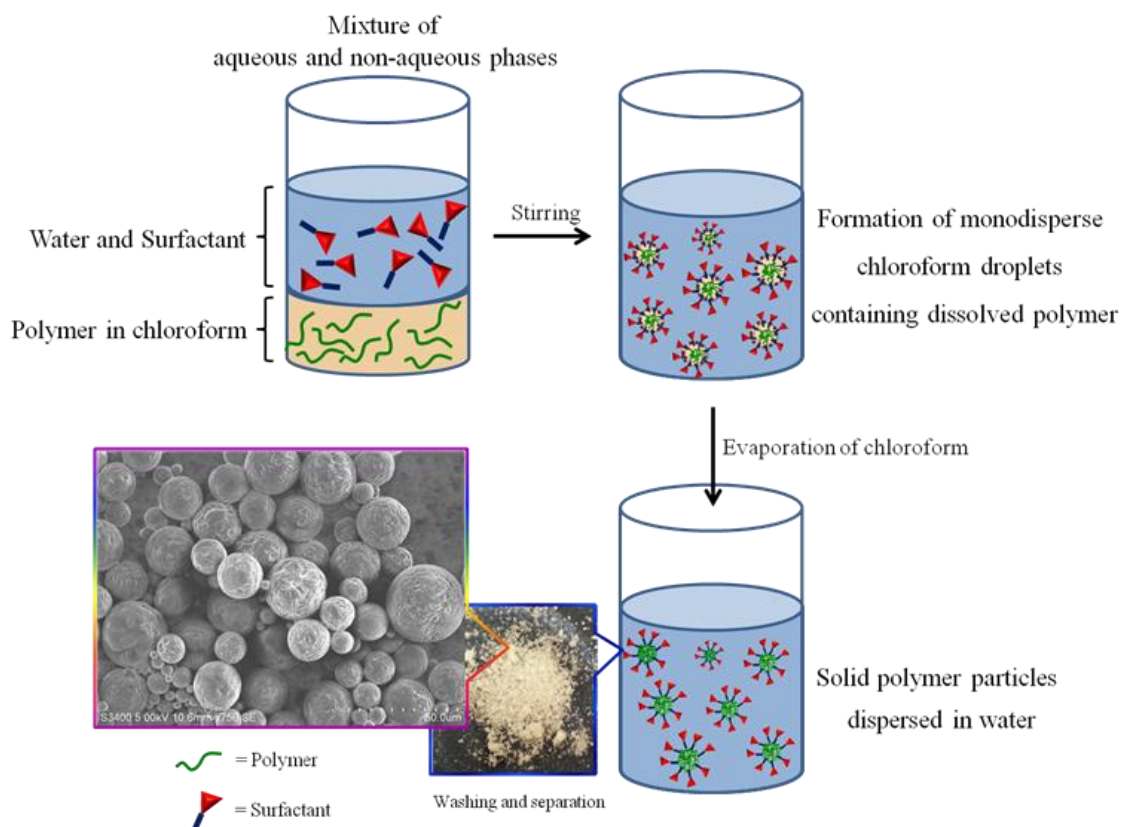
Figure 5.4: Schematic cartoons of oil-in-water system used for polymer microsphere production. The emulsion consists of water-immiscible organic phase and aqueous phase containing polymer and stabilizer. Shear forces form dispersed droplets dissolved polymer. Subsequently, the organic solvent is evaporated from the system resulting in solid particles.

Figure 5.5 shows SEM images of microspheres obtained by this technique at two different polymer concentrations and stirring speed using PVA as a surfactant. In both cases spherical particles in the 10 μm range were produced. From the SEM images it is observed that the surface morphologies were different depending on the concentration and the temperature of the experiment. Samples prepared at 40 °C showed higher surface roughness comparing to the ones prepared at room temperature. Increased surfaces roughness of microspheres can be the result of the increased rate of solvent removal from o/w system by increased temperature as seen in Figure 5.5. Moreover, varying the concentration of surfactant and polymer did not result in a significant difference of

obtained microsphere morphology. On the other hand, the size distribution of the obtained particles was quite broad from batch to batch. It was therefore difficult to conclude what the effect of experimental parameters on the size distribution of the obtained particles with this proposed O/W emulsion system is.
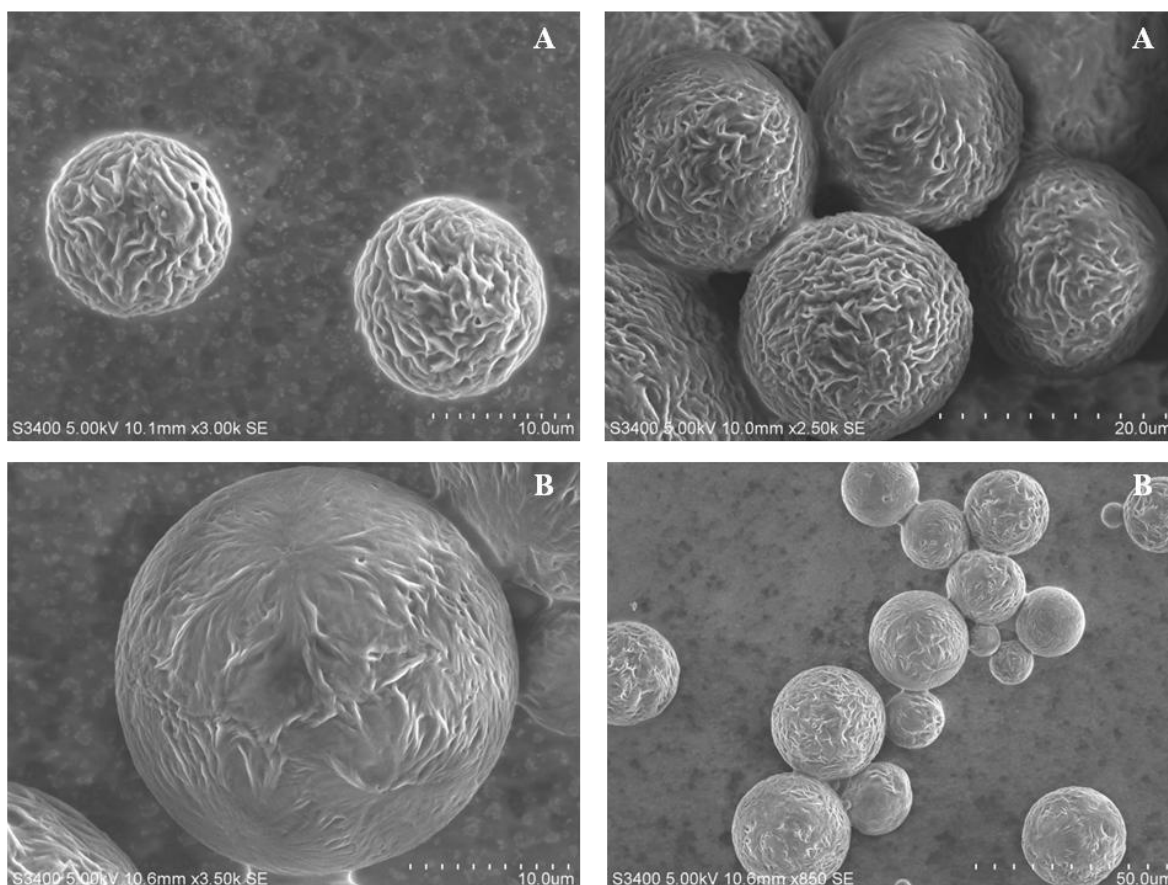
Figure 5.5: SEM images of PGl microspheres prepared by (A) 0.1 g PGl (900 rpm at 40°C) and (B) 0.15 g PGl (500 rpm at RT) in 0.2 % PVA o/w emulsion system.

As the physicochemical properties and the concentration of the emulsifier strongly influence the size and shape of the microspheres[36] Tween 20 was tested as an alternative nonionic surfactant. Tween 20 is a polyoxyethylene sorbitol ester, with a calculated molecular weight of 1,225 dalton, assuming 20 ethylene oxide units, 1 sorbitol, and 1 lauric acid as the primary fatty acid[38]. In most cases, the hydrophile-lipophile balance (HLB) number is used to define the affinity of a surfactant for water or oil phase where

the HLB number is the ratio of hydrophilic and lipophilic groups of amphiphilic surfactant. The HLB numbers of both Tween 20 (16) and PVA (18) are very similar so that they mainly differ in their chemical structures[39].
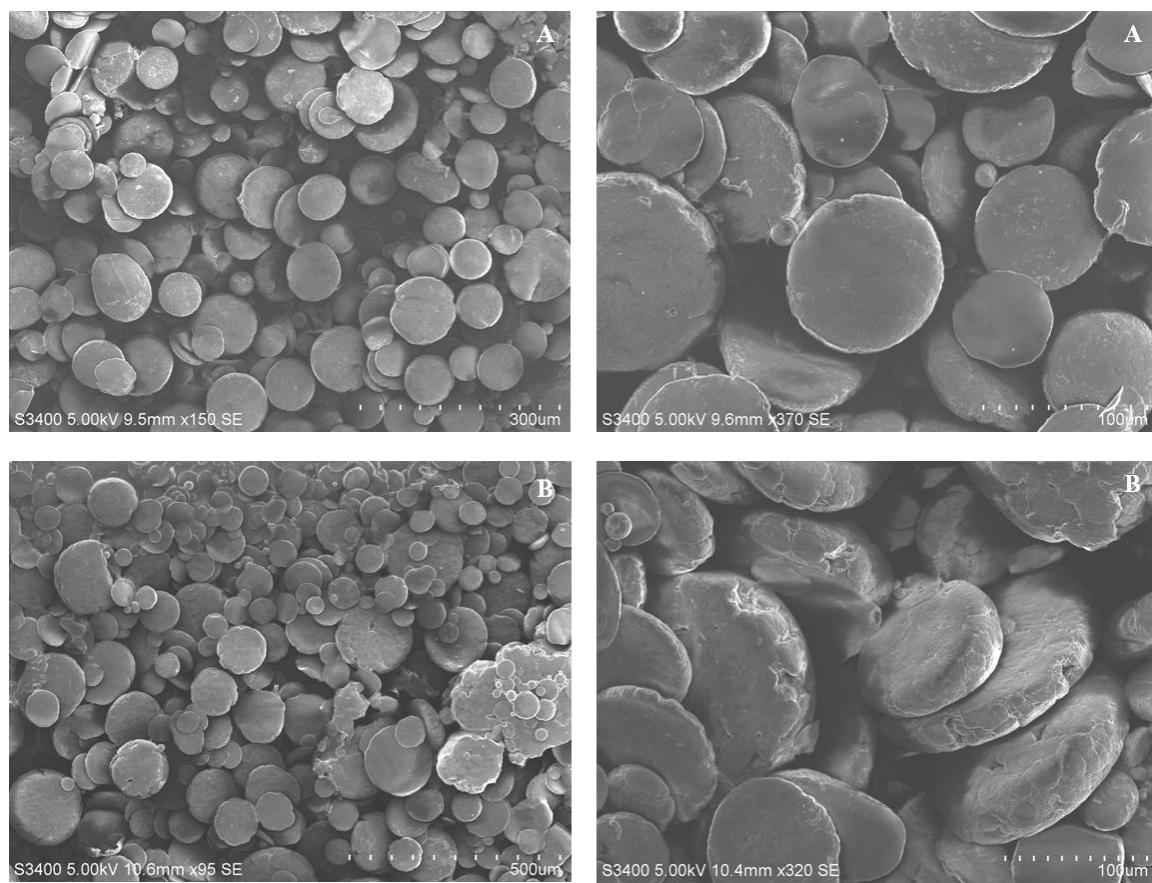
Figure 5.6: SEM images of PGl particles prepared by (a) 0.1 g PGl (750 rpm at RT) in 0.2 % PVA and (b) 0.15 g PGl (750 rpm at RT) in 0.4 % PVA o/w emulsion system.

The particles obtained by using Tween 20 as surfactant resulted in smoother surfaces while forming aggregates in most cases. These results emphasise the delicate nature of the proposed system to fabricate PGl microspheres even if both surfactants have similar HLB numbers. Notably, Xu et al. reported that the effect of emulsifier is determined not only by HLB value, but also by the chemical configuration of the emulsifier[39]. It can be

speculated that the chemical configuration of the chosen surfactants might strongly affect the particle shape and surface morphology in the O/W system.

It must be noted that in some of the batches, particles with a pancake/plate-like shape were obtained as seen in Figure 5.6. The parameters of these O/W systems were not different to those that afforded microspheres as shown in Figure 5.5. It can be speculated that such results might be due to the sensitive equilibrium between oil and water phases, too. In general, the balance between the turbulent forces and interfacial tension and viscosity forces can be decisive in determining the sizes of particles[40].

Moreover, temperature, type and concentration of surfactant will also affect the interfacial tension of the oil/water system. The stability of the droplets might easily be damaged by one or more of such mentioned parameters related to the interfacial forces. Owing to the importance of the control over the shape and size of the microspheres and reproducibility between batches, the proposed systems need to be further investigated and optimized to further develop applications for these materials. If reproducible PGl microspheres could be achieved, possible surface modification employing the methodology described in previous chapters could be used to tailor the surface properties for selected applications.

5.2 Conclusions

Porous PGl materials were successfully produced using particulate leaching methodology. Most promising results were obtained with sugar as porogen at a ratio of 1:4 PGl:sucrose. Moreover, PGl microspheres were fabricated by using different o/w emulsion systems. While both methodologies produced the targeted three-dimensional morphologies further optimization is required for both systems to develop reproducible materials and potential applications.

5.3 Experimental

5.3.1 Materials

Globalide was provided by Symrise. Novozyme 435 (*Candida Antarctica* Lipase B immobilised on cross-linked polyacrylate beads) was purchased from Novozymes A/S. Ethylene glycol bis(3-mercapto propionate) was purchased from Wako. Glucose monohydrate, Sucrose, Poly(vinyl alcohol) (PVA, Mw= 13.000-23.000 g/mol, 87-89% hydrolyzed), and Tween 20 were purchased from Sigma-Aldrich. All other reagents and solvents used were purchased from Sigma-Aldrich and used without further purification.

5.1.1 Methods

Scanning Electron Microscopy (SEM) was performed on a Hitachi S3400 with samples previously coated with gold using vapor deposition in the case of SEM analysis.

Samples were UV cured using a commercial Fusion UV system, LCGE Bench top conveyor with F300S Fusion lamb (120 W/cm) equipped with a 13 mm H-bulb. The samples were exposed to the UV lamb at 5 m/min. belt speed.

5.1.2 General procedure for porous materials

Poly(globalide) was synthesized by using the same procedure as described in chapter 2. Porous structures were prepared by dissolving 0.3 g of PGl in a minimal amount of THF or DCM (1 mL). The chosen porogen (e.g. sucrose) was added to the dissolved PGl solution after addition of cross-linker (ethylene glycol bis(3-mercapto propionate)) and the UV initiator mixture, (diphenyl(2,4,6-trimethylbenzoyl) phosphine oxide / 2-hydroxy-2-methylpropiophenone (equimolar of cross-linker) dissolved in dichloromethane at a ratio of 1:1 (w/w). After irradiation with Fusion UV system, samples were washed with THF for 6 hours followed by the porogen leaching step carried out in DI water for 4 days.

5.1.3 General procedure for microsphere production

In a typical experiment, 0.2 w % of PVA was dissolved in 10 ml DI water. 0.1 g PGl was dissolved in 1 mL of DCM and added to PVA solution while stirring the solution. Particles were separated by centrifugation after 4 hours of stirring and dried for SEM analysis.

In order to obtain narrow size distribution of microspheres, the quantity of PGl used and tween 20 or PVA were explored at the following ratios 0.2, 0.4, 0.6, 1.2 % while varying the stirring rate. The experiments were conducted at room temperature; those that afforded microspheres were repeated at 40 °C.

5.2 References

1.   R. Ravichandran, S. Sundarrajan, J. R. Venugopal, S. Mukherjee, and S. Ramakrishna, *Macromol. Biosci.*, 2012, **12**, 286–311.

2.   P. A. Gunatillake and R. Adhikari, *Eur. Cell. Mater.*, 2003, **5**, 1–16.

3.   T. Tyson, S. Målberg, V. Wåtz, A. Finne-Wistrand, and A.-C. Albertsson, *Macromol. Biosci.*, 2011, **11**, 1432–1442.

4.   C. M. Agrawal and R. B. Ray, *J. Biomed. Mater. Res.*, 2001, **55**, 141–150.

5.   G. Vunjak-Novakovic and L. Freed, *Adv. Drug Deliv. Rev.*, 1998, **33**, 15–30.

6.   F. J. Rodríguez, N. Gómez, G. Perego, and X. Navarro, *Biomaterials*, 1999, **20**, 1489–1500.

7.   J. R. Fuchs, B. A. Nasseri, and J. P. Vacanti, *Ann. Thorac. Surg.*, 2001, **72**, 577–591.

8.   P. X. Ma and J. W. Choi, *Tissue Eng.*, 2001, **7**, 23–33.

9.   C. Schugens, V. Maquet, C. Grandfils, R. Jerome, and P. Teyssie, *Polymer*, 1996, **37**, 1027–1038.

10.   R. Zhang and P. X. Ma, *J. Biomed. Mater. Res.*, 1999, **45**, 285–293.

11.   G. Chen, T. Ushida, and T. Tateishi, *Biomaterials*, 2001, **22**, 2563–2567.

12.   D. J. Mooney, D. F. Baldwin, N. P. Suh, J. P. Vacanti, and R. Langer, *Biomaterials*, 1996, **17**, 1417–1422.

13.   Y. S. Nam and T. G. Park, *J. Biomed. Mater. Res.*, 1999, **47**, 8–17.

14.   B. Leukers, H. Gülkan, S. H. Irsen, S. Milz, C. Tille, M. Schieker, and H. Seitz, *J. Mater. Sci. Mater. Med.*, 2005, **16**, 1121–1124.

15.   L. D. Harris, B. S. Kim, and D. J. Mooney, *J. Biomed. Mater. Res.*, 1998, **42**, 396–402.

16.   Y.-C. Kuo and C.-T. Wang, *Colloids Surf. B. Biointerfaces*, 2012, **100**, 9–15.

17.   D. Grafahrend, K.-H. Heffels, M. V Beer, P. Gasteier, M. Möller, G. Boehm, P. D. Dalton, and J. Groll, *Nat. Mater.*, 2011, **10**, 67–73.

18.   J. J. A. Barry, M. M. C. G. Silva, V. K. Popov, K. M. Shakesheff, and S. M. Howdle, *Philos. Trans. A. Math. Phys. Eng. Sci.*, 2006, **364**, 249–261.

19.   S. H. Park, D. S. Park, J. W. Shin, Y. G. Kang, H. K. Kim, T. R. Yoon, and J.-W. Shin, *J. Mater. Sci. Mater. Med.*, 2012, **23**, 2671–2678.

20.   P. Wang, J. Hu, and P. X. Ma, *Biomaterials*, 2009, **30**, 2735–2740.

21.   M. G. Haugh, C. M. Murphy, and F. J. O'Brien, *Tissue Eng. Part C. Methods*, 2010, **16**, 887–894.

22.   Y.-C. Huang, D. Kaigler, K. G. Rice, P. H. Krebsbach, and D. J. Mooney, *J. Bone Miner. Res.*, 2005, **20**, 848–857.

23.   T. Moritera, Y. Ogura, Y. Honda, R. Wada, S. H. Hyon, and Y. Ikada, *Invest. Ophthalmol. Vis. Sci.*, 1991, **32**, 1785–1790.

24.   J. H. Park, M. Ye, and K. Park, *Molecules*, 2005, **10**, 146–161.

25.   S. Freiberg and X. X. Zhu, *Int. J. Pharm.*, 2004, **282**, 1–18.

26.   K. Saralidze, L. H. Koole, and M. L. W. Knetsch, *Materials (Basel).*, 2010, **3**, 3537–3564.

27.   B. D. Ulery, L. S. Nair, and C. T. Laurencin, *J. Polym. Sci. B. Polym. Phys.*, 2011, **49**, 832–864.

28.   M. Ye, S. Kim, and K. Park, *J. Control. Release*, 2010, **146**, 241–260.

29. S. Jhunjhunwala, G. Raimondi, A. W. Thomson, and S. R. Little, *J. Control. Release*, 2009, **133**, 191–197.

30. S. Huang, Y. Xu, C. Wu, D. Sha, and X. Fu, *Biomaterials*, 2010, **31**, 5520–5525.

31. K. S. Soppimath, T. M. Aminabhavi, a R. Kulkarni, and W. E. Rudzinski, *J. Control. Release*, 2001, **70**, 1–20.

32. L. Jongpaiboonkit, T. Franklin-Ford, and W. L. Murphy, *ACS Appl. Mater. Interfaces*, 2009, **1**, 1504–1511.

33. K. Du, X. Shi, and Z. Gan, *Langmuir*, 2013, **29**, 15293–15301.

34. X.-M. Na, F. Gao, L.-Y. Zhang, Z.-G. Su, and G.-H. Ma, *ACS Macro Lett.*, 2012, **1**, 697–700.

35. Y. Xiao, D. Cummins, A. R. A. Palmans, C. E. Koning, and A. Heise, *Soft Matter*, 2008, **4**, 593–599.

36. R. Jain, N. H. Shah, A. W. Malick, and C. T. Rhodes, *Drug Dev. Ind. Pharm.*, 1998, **24**, 703–727.

37. M. Sokolsky-Papkov, K. Agashi, A. Olaye, K. Shakesheff, and A. J. Domb, *Adv. Drug Deliv. Rev.*, 2007, **59**, 187–206.

38. http://www.sigmaaldrich.com/content/dam/sigma-aldrich/docs/Sigma/Product_Information_Sheet/1/p5927pis.pdf (23/01/2014)

39. Q. Xu, A. Crossley, and J. A. N. Czernuszka, *J. Pharm. Sci.*, 2009, **98**, 2377–2389.

40. A. R. Bachtsi, C. J. Boutris, and C. Kiparissides, *J. Appl. Polym. Sci.*, 1996, **60**, 9–20.

Conclusions

In this thesis, macrolactones were used to design functional materials due to the high demand for the natural raw materials obtained by green approaches. At the outset, a simple and novel methodology for the modification of poly(globalide), synthesized via e-ROP, was revealed by thiol-ene coupling reactions. The proposed methodology offers single-step side-chain functionalisation of unsaturated aliphatic polyesters as post-polymerization modification with plentiful functional group bearing thiol compounds. Primary alcohol, amine and carboxylic acid functionalities were successfully introduced as side-chain functionalities of linear poly(globalide) as discussed in chapter 2. The thiol-ene coupling efficiency was found to vary with the reactivity and miscibility of the individual thiol compound. Such functional groups can undergo further modifications such as polycondensation via hydroxyl groups or protein coupling mediated by amine groups.

Next, the proposed thiol-ene coupling methodology was extended to produce functional films from poly(globalide). Systematic study of UV-induced thiol-ene cross-linking was investigated by exploring different approaches to introduce controlled functionalities on to the entire network while controlling desired physico-mechanical properties of the obtained materials. In addition, two different dithiol crosslinkers, bearing an ester group and a PEG chain, were chosen to increase the hydrophilicity or biodegradation. Moreover, the double bond conversion and C-S bond formation was followed by FT-Raman measurements which indicated the miscibility and activity of the thiol was found to be effective for cross-linking efficiency. As a consequence, the functionalisation of pre-prepared cross-linked films shown ease of application where the surface was decorated with amine groups. Moreover, availability of such functional groups was shown by successful FITC conjugation with the surface amine groups. The results in chapter 3 provide an example of a renewable and degradable material platform with the potential for property enhancement.

Furthermore, hydroxyl functionalized PML films were equipped by the methodology proposed in chapter 3 in order to obtain ATRP initiator decorated surfaces. Dense coating of polymeric brushes was growth from the surface of ATRP initiator decorated PML films by surface initiated ARGET-ATRP of t-BA and NIPAM, respectively. Next, the successful eGFP conjugation was demonstrated on the poly(acrylic acid) functionalized polyester films after t-BA deprotection. Moreover, the efficiency of improved surface functionalisation was proved by the immobilization of chitobiase enzyme via EDC/sulfo-NHS coupling chemistry on the PGI films decorated with poly(acrylic acid) brushes. The chitobiase enzyme activity on the substrate confirmed the success of the immobilization onto polymer brushes. Besides, a model study was presented by grafting poly(NIPAM) brushes on the surfaces of polyester films showing possible stimuli responsive films. The methodology here presented allows designing functional polyester surfaces while combining properties of polyester and grafted polymer brushes for desired applications.

Last of all, 3D materials from poly(macrolactones) were prepared in the form of scaffolds and microspheres. Sugar leaching afforded porous scaffolds which needs to be further improved because of low interconnectivity between the pores. Besides, a straightforward O/W emulsion system was used to produce PGl microspheres with different surface characteristics. This methodology also needs to be further investigated for the full understanding of the proposed system. On the other hand, enzymatic degradation was found to be higher for films with low amount of ester bearing cross-linker with comparison to PEGDT used samples. It was also observed that the network stiffness affected degradation process, although a systematic degradation study is still needed for full understanding of the proposed system.

The fabrication of such 3D materials with the desired functionality by combining proposed methodologies in previous chapters can increase the number of possible applications with enhanced material properties.

List of Publications

- Ates, Z., Audouin, F., Harrington, A., O'Connor, B., Heise, A., `Functional Brushes Decorated Poly(globalide) Films by ARGET-ATRP for Bioconjugation`, Macromolecular Bioscience (accepted manuscript)

- Ates Z. and Heise A. `Functional films from unsaturated poly(macrolactones) by thiol–ene cross-linking and functionalisation` Polymer Chemistry, 2014,5, 2936-2941

- Ates, Z., Thornton, P.D., and Heise A., `Side-chain functionalisation of unsaturated polyesters from ring-opening polymerisation of macrolactones by thiol–ene click chemistry` Polymer Chemistry, 2011, 2, 309.

- Ziółkowski B., Ates Z., Gallagher S., Fraser K.J., Heise A., Byrne R., Diamond D., `Mechanical Properties and UV Curing Behavior of Poly(N-Isopropylacrylamide) in Phosphonium-Based Ionic Liquids` Macromol. Chem. Phys. 2013, 214, 787.

Conferences

- European Polymer Congress 2013, Pisa Italy, June 2013, `Functional films from unsaturated poly(macrolactones) via thiol-ene click combined with surface initiated ARGET-ATRP` Zeliha Ates, Fabrice Audouin and Andreas Heise (Oral presentation)

- MACRO Group UK International Conference of Polymer Synthesis and UK PFC International Conference of Colloids 2012, Warwick UK, July 2012, `Functional Films from Unsaturated Polyesters from Macrolactones via Thiol-ene Click Chemistry` Zeliha Ates, Paul D. Thornton and Andreas Heise (Poster presentation)

- European Polymer Congress 2011, Granada Spain, June 2011, `Functionalisation of Unsaturated Polyesters from Enzymatic Ring-Opening Polymerisation of Macrolactones by Thiol–ene Click Chemistry` Zeliha Ates, Inge van der Maulen, Paul D. Thornton and Andreas Heise (Oral presentation)

- IUPAC World Polymer Congress, UK, 2010, `Block Copolymers from Renewable Macrolactones` Zeliha Ates and Andreas Heise (Poster presentation)

- MACRO Group UK Young Research Meeting 2010, Nottingham UK, April 2010 `Block copolymers from renewable macrolactones` Zeliha Ates, Andreas Heise (Poster presentation)